

Copyright is owned by the Author of the thesis. Permission is given for a copy to be downloaded by an individual for the purpose of research and private study only. The thesis may not be reproduced elsewhere without the permission of the Author.

# **Proximal sensing techniques to monitor pasture quality and quantity on dairy farms**

**A thesis presented in partial fulfilment of the  
requirements for the degree of**

**Doctor of Philosophy**

**in**

**Soil Science**

**at Massey University, Manawatu,**

**New Zealand**



**Pullanagari Rajasheker Reddy**

**2011**



## Abstract

Regular and timely measurements of pasture quality and quantity allow dairy farmers to make effective decisions ensuring an adequate supply of nutrients to animals, efficient utilization of pasture, manipulation of stocking rates, management grazing intervals, and optimisation of input resources (e.g. nitrogen fertilisers) which results in more economic, environmentally aware, sustainable grazing systems.

The objectives of this research were to investigate the potential of proximal sensing tools to estimate pasture quality parameters (crude protein, CP; acid detergent fibre, ADF; neutral detergent fibre, NDF; ash, dietary cation-anion difference, DCAD; lignin, lipid, metabolisable energy, ME and organic matter digestibility, OMD) in mixed pastures. Three proximal sensors, ASD FieldSpec<sup>®</sup> Pro FR spectroradiometer (hyperspectral), Cropscan<sup>™</sup> (multispectral) and Crop Circle<sup>™</sup> (multispectral), were employed in this study.

In the hyperspectral study, the spectral reflectance measurements of pasture samples were acquired using an ASD FieldSpec<sup>®</sup> Pro FR spectroradiometer which has a spectral range of 350-2500 nm and attached with canopy pasture probe (CAPP) to ensure ambient light conditions. The acquired spectral data were pre-processed by various procedures: spectral averaging, smoothing and derivative transformation, then partial least squares regression was applied to regress against the corresponding measured values. The regression model was validated with an external dataset to evaluate the reliability and robustness of the model. The performance of both calibration and validation models were more or less similar. The validation model predicted the pasture quality parameters CP, ADF, NDF, ash, DCAD, lignin, ME and OMD with reasonable accuracy ( $0.65 \leq R^2 \leq 0.83$ ;  $1.70 \leq RPD \leq 2.48$ ;  $0.64 \leq NSE \leq 0.83$ ) and the lipid was predicted with lower accuracy ( $R^2=0.55$ ;  $RPD=1.44$ ;  $NSE=0.50$ ).

Cropscan relies on sunlight for its energy source and measures reflectance in 16 broad wavebands; it was evaluated for its potential to assess pasture quality parameters that are collected in one season. The relationship between spectral reflectance measured using the Cropscan and pasture quality parameters were established using single wavebands, new vegetation indices and stepwise multiple linear regression (SMLR) and the models were

validated with an external dataset. Of all the models, the new non-linear new combination of RDVI index models were performed satisfactory results ( $0.65 \leq R^2 \leq 0.85$ ) for predicting CP, DCAD, ME and OMD. CP, ash, DCAD, lipid, ME and OMD were estimated with moderate accuracy ( $0.60 \leq R^2 \leq 0.80$ ) using the SMLR model. The Cropscan instrument was also used to test the potential for predicting pasture quality in different seasons (autumn, spring and summer). Improved accuracy was observed with season-specific models as compared to the combined season dataset models.

A three channel active optical sensor, Crop Circle™ was used to estimate herbage biomass and standing crude protein (SCP) using various indices. The results showed that the three channel based pasture index proved a reliable index for estimating biomass ( $R^2 = 0.69$ ;  $RMSE = 518 \text{ kg ha}^{-1}$ ) and SCP ( $R^2 = 0.77$ ;  $RMSE = 110 \text{ kg ha}^{-1}$ ) with moderate accuracy. Based on the calibration of PI, spatial analysis was assessed for biomass in ten dairy fields. In spatial analysis, semivariograms revealed the spatial dependency for biomass was moderate to strong and varied between the fields.

This study indicates that proximal sensors have considerable potential for real-time *in situ* assessment of pasture quality and quantity in mixed pastures. The results indicate that spectral resolution and number of wavelengths used in the sensor are crucial for determining pasture quality with high accuracy which would allow future research to develop proximal sensors with an optimal number of wavelengths and spectral resolution.

## Acknowledgements

I am deeply indebted to, chief supervisor, Professor Ian Yule for his continuous support and encouragement during this study. His creative and stimulating ideas allowed me to think as an independent researcher. My sincere thanks also go to co-supervisor's: Mike P. Tuohy who taught me the fundamentals of remote sensing and Prof. Mike J. Hedley whose valuable suggestions helped me in all the time of research.

I would like to acknowledge Pastoral 21 Feed Programme and Foundation of Arable Research (FAR) for financial support for this study and also to Massey University for providing scholarships: Colin Homes, DG Bowler, Helen E Akers, Peter During and Sports Turf.

My special thanks go to Dr. Robyn Dynes from AgResearch who provided valuable and critical comments on the manuscripts which have been submitted to various journals. I am also grateful to Dr. Carolyn Hedley from Land Care for her thoughtful ideas and kind suggestions towards improving the quality of thesis.

I would like to express my gratitude to staff from AgResearch, Grant Rennie, Linda Yates, Brian DeVantier, Ray Moss and Westlea Clarke-Hill; and Dairy NZ, Laura Rossi for being involved in field work at various places of New Zealand. My thanks also to the staff of Soil & Earth Sciences for their assistance, Dr. Ranvir Singh, Liza Haarhoff, Bob Toes and Lance Currie.

My immense pleasure to Mathew Irwin, genuine kiwi, for his kind assistance and fun throughout study. In addition, I extend my gratitude to Michel Killick for his help during the field work. During the journey of PhD, in New Zealand, I had great fun and joy with friends, namely, Palash, Anand, Jatin, Ina Draganova, Venu, Thariq, Stefanie and Pip.

Especially, I would like to express my heartfelt thanks to my family whose patient love enabled me to complete this work successfully.



## Table of Contents

ABSTRACT .....	I
ACKNOWLEDGEMENTS .....	III
TABLE OF CONTENTS .....	IV
LIST OF TABLES .....	VIII
LIST OF FIGURES .....	X
ACRONYMS .....	XII
<b>CHAPTER 1.....</b>	<b>1</b>
<b>GENERAL INTRODUCTION .....</b>	<b>1</b>
1.1.    GENERAL BACKGROUND .....	2
1.2.    RESEARCH OBJECTIVES.....	5
1.3.    THE STUDY AREAS.....	6
1.4.    THESIS OUTLINE.....	8
<b>CHAPTER 2.....</b>	<b>10</b>
<b>LITERATURE REVIEW .....</b>	<b>10</b>
2.1.    GENERAL BACKGROUND OF REMOTE SENSING .....	11
2.2.    REMOTE SENSING OF VEGETATION .....	18
2.3.    COMPUTATION OF SPECTRAL DATA .....	21
2.3.1. <i>Empirical based approaches</i> .....	22
2.3.1.1.    Univariate Statistical Methods .....	22
2.3.1.1.1. <b>Multispectral Indices</b> .....	24
2.3.1.1.2. <b>Hyperspectral Indices</b> .....	25
2.3.1.2.    Multivariate Regression methods.....	26
2.3.1.2.1. <b>Step wise multiple linear regression (SMLR)</b> .....	27
2.3.1.2.2. <b>Partial Least Squares Regression (PLSR)</b> .....	28
2.3.1.3.    Red Edge Position (REP).....	29
2.3.1.3.1. <b>Linear Interpolation</b> .....	29
2.3.1.3.2. <b>Linear Extrapolation</b> .....	30
2.3.1.3.3. <b>Polynomial fitting technique</b> .....	31
2.3.1.3.4. <b>Lagrangian Technique</b> .....	31
2.3.1.3.5. <b>Inverted Gaussian (IG) fitting technique</b> .....	32
2.3.1.4.    Artificial intelligence (AI) .....	33



2.3.1.4.1.	Artificial Neural Networks .....	33
2.3.1.4.2.	Support Vector Machine (SVM) .....	34
2.3.2.	Physically based approach .....	34
2.3.3.	Integrated Approaches .....	35
2.4.	SUMMARY.....	36

## **CHAPTER 3 ..... 39**

### **IN-FIELD HYPERSPECTRAL PROXIMAL SENSING FOR ESTIMATING QUALITY PARAMETERS OF MIXED PASTURE..... 39**

ABSTRACT .....	40
3.1. INTRODUCTION .....	40
3.2. MATERIALS AND METHODS .....	42
3.2.1. Study area .....	42
3.2.2. Spectral measurements .....	42
3.2.3. Sampling .....	44
3.2.4. Chemical Analysis.....	45
3.2.5. Data processing and statistical analysis .....	45
3.2.5.1. Data manipulations .....	45
3.2.5.2. Data Analysis.....	46
3.2.6. Quantifying Model Accuracy.....	47
3.3. RESULTS .....	50
3.3.1. Summary statistics of NIRS data .....	50
3.3.2. Correlation among the pasture quality parameters .....	52
3.3.3. Principal component analysis.....	52
3.3.4. PLSR models for calibration and validation datasets.....	53
3.3.5. Important wavebands explaining the variance of pasture quality components.....	54
3.4. DISCUSSION.....	57
3.5. CONCLUSION .....	61

## **CHAPTER 4 ..... 62**

### **MULTISPECTRAL RADIOMETRY TO ESTIMATE PASTURE QUALITY COMPONENTS ..... 62**

ABSTRACT .....	63
----------------	----

4.1.	INTRODUCTION .....	63
4.2.	MATERIALS AND METHODS .....	66
4.2.1.	<i>Reflectance readings</i> .....	67
4.2.2.	<i>Data analysis</i> .....	68
4.3.	RESULTS .....	69
4.3.1.	<i>Summary of reflectance spectrum and pasture quality components data</i> .....	69
4.3.2.	<i>Single band relationships for pasture quality estimation</i> .....	71
4.3.3.	<i>Combinations of broad-band vegetative indices relationships with pasture quality components</i> .....	74
4.3.4.	<i>Stepwise multiple linear regression (SMLR) for pasture quality assessment</i> .....	76
4.4.	DISCUSSION .....	77
4.5.	CONCLUSION .....	81
<b>CHAPTER 5.....</b>		<b>83</b>
<b>PROXIMAL SENSING OF THE SEASONAL VARIABILITY OF PASTURE NUTRITIVE VALUE USING MULTISPECTRAL RADIOMETRY .....</b>		<b>83</b>
	ABSTRACT .....	83
5.1.	INTRODUCTION .....	83
5.2.	MATERIALS AND METHODS .....	85
5.2.1.	<i>Study Area and sampling</i> .....	85
5.2.2.	<i>Data analysis</i> .....	86
5.3.	RESULTS .....	88
5.2.1.	<i>Relationship between pasture nutritive value parameters and spectral reflectance</i> .....	88
5.2.2.	<i>Seasonal-specific models between pasture nutritive value parameters and spectral reflectance</i> .....	92
5.4.	DISCUSSION .....	95
5.5.	CONCLUSION .....	97
<b>CHAPTER 6.....</b>		<b>99</b>
<b>ESTIMATION OF PASTURE BIOMASS, STANDING CRUDE PROTEIN AND SPATIAL ANALYSIS OF HERBAGE BIOMASS USING AN ACTIVE OPTICAL SENSOR .....</b>		<b>99</b>
	ABSTRACT .....	100

6.1.	INTRODUCTION .....	100
6.2.	MATERIALS AND METHODS .....	103
6.2.1	<i>Canopy Reflectance</i> .....	103
6.2.2	<i>Data analysis</i> .....	104
6.2.1.1.	Development and validation of calibration models.....	104
6.2.1.2.	Spatial analysis of herbage biomass on commercial dairy fields .....	105
6.3.	RESULTS .....	107
6.4.	DISCUSSION.....	112
6.5.	CONCLUSION .....	113
<b>CHAPTER 7 .....</b>		<b>115</b>
<b>OVERALL SUMMARY, DISCUSSION AND RECOMMENDATIONS FOR FUTURE WORK.....</b>		<b>115</b>
7.1.	OVERALL SUMMARY.....	116
7.1.1.	<i>Hyperspectral sensor study</i> .....	116
7.1.2.	<i>Multispectral sensors study</i> .....	118
7.2.	RECOMMENDATIONS FOR FUTURE WORK.....	120
<b>REFERENCES.....</b>		<b>122</b>
<b>AUTHOR'S PUBLICATIONS .....</b>		<b>143</b>

## List of Tables

Table 2.1 Selected multispectral sensors and their characteristics.....	15
Table 2.2 Current and future hyperspectral sensors and their characteristics .....	17
Table 2.3 Various vegetation indices listed in literature .....	23
Table 3.1 The experimental site locations .....	43
Table 3.2 Descriptive statistics of the pasture quality parameters of calibration ( $n=107$ ) and validation sets ( $n=107$ ) measured by NIRS .....	50
Table 3.3 Intercorrelation coefficients of measured pasture quality parameters .....	51
Table 3.4 PLSR results between first derivative reflectance and pasture quality concentrations for cross-validated calibration and validation datasets .....	56
Table 4.1 Descriptive statistics of pasture quality components .....	70
Table 4.2 Coefficient of determination ( $r^2$ ) between canopy reflectance at 16 individual wavelengths and pasture quality components.....	72
Table 4.3 Best performing RDVI indices (top two-band combinations) with high coefficient of determination ( $r^2$ ) values for selected pasture quality components .....	75
Table 4.4 Coefficients of determination ( $r^2$ ) between crop reflectance of best regressors and pasture quality components using stepwise linear regression to select important wavelengths .....	76
Table 5.1 Descriptive statistics (mean, minimum, maximum, standard deviation; SD, coefficient of variation %; CV) of pasture nutritive value parameters for the calibration dataset ( $n=210$ ) and calibration model results measured at four sites during three seasons (autumn, spring and summer) in 2009-2010 in Waikato, Tarnaki, Manawatu and Catebury regions, New Zealand.....	90

Table 5.2 Descriptive statistics (mean, minimum, maximum, standard deviation; SD, coefficient of variation %; CV) of pasture nutritive value parameters for the validation dataset (n=210) measured at four sites during three seasons (autumn, spring and summer) in 2009-2010 in Waikato, Taranaki, Manawatu and Canterbury regions, New Zealand ....	90
Table 5.3 Descriptive statistics (mean, minimum, maximum, standard deviation; SD, coefficient of variation %; CV) of pasture nutritive value parameters measured at four sites for individual seasons (autumn, spring and summer) in 2009-2010 in Waikato, Taranaki, Manawatu and Canterbury regions, New Zealand. ....	92
Table 5.4 Calibration and cross-validation of spectral and pasture nutritive value data using partial least squares regression (PLSR) at four sites during three seasons (autumn, spring and summer) in 2009-2010 in Waikato, Taranaki, Manawatu and Canterbury regions, New Zealand. ....	94
Table 6.1 The selected vegetation indices. ....	105
Table 6.2 Descriptive statistics of pasture biomass and standing crude protein for the calibration dataset (n=200). ....	107
Table 6.3 Regression equations for predicting biomass and standing crude protein from various indices. ....	108
Table 6.4 Summary of variogram parameters (nugget, partial sill and range), model type and root mean square error (RMSE) of pasture biomass at 10 fields .....	110

## List of Figures

Figure 1.1 Study farms located across New Zealand; 1) Ruakura dairy farm, AgResearch 2) Tokanui dairy farm, AgResearch 3) Scot dairy farm, AgResearch 4) Dairy No. 1, Massey University dairy farm 5) Dairy No. 4, Massey University dairy farm 6) Aorangi dairy farm, AgResearch 7) WESTPAC dairy farm, DairyNZ 8) Brian dairy farm 9) Lincoln University dairy farm 10) Synlait dairy farm 11) Mackie dairy farm 12) Greendale dairy farm 13) Pang Born dairy farm 14) Ward dairy farm .....	7
Figure 2.1 Electromagnetic spectrum (NASA, 1998).....	11
Figure 2.2 Spectral signatures for various feature types (Lillesand <i>et al.</i> , 2004) .....	13
Figure 2.3 Interaction between energy source, leaf structure and spectral sensor (Lillesand <i>et al.</i> , 2004); the diagram of the leaf structure adapted from <a href="https://dbscience3.wikispaces.com/Drew">https://dbscience3.wikispaces.com/Drew</a> .....	18
Figure 2.4 Spectral signatures of green and dry vegetation (NASA, 1994) .....	20
Figure 2.5 The various computational approaches for analysing spectral data.....	21
Figure 3.1 (a) Mean reflectance (b) Mean and standard deviation of first derivative reflectance of acquired pasture samples ( $n=214$ ) .....	44
Figure 3.2 Score plot of first and second principal components from the PCA.....	52
Figure 3.3 Variable importance in projection (VIP) plot showing the importance of each waveband in developing a model of pasture quality attributes across the electromagnetic spectrum; X-axis represents wavelength (nm) and Y-axis represents VIP-scores.....	54
Fig. 4.1 Canopy spectral mean reflectance ( $n=151$ ) and coefficient of variation values at 16 wavelengths .....	70

Figure 4.2 The 2-D correlograms showing the amount of variation in pasture quality components explained ( $r^2$ values colour bar) by spectral reflectance acquired in the field and expressed as RDVI indices calculated from 16 discrete wavelengths .....	74
Figure 4.3 The amount of variation in pasture quality components explained ( $r^2$ ) by spectral reflectance acquired in the field using four different predictive modelling techniques.....	79
Figure 5.1 (a) The relative proportion of variation explained by the six principal components in the principal component analysis (PCA) (b) The score plot of third and fourth principal components with respective seasons (autumn, spring and summer) in 2009-2010. ....	89
Figure 5.2 Relationship between near infrared spectroscopy (NIRS) measured pasture nutritive values and values predicted by multispectral radiometer of validation (n = 210) dataset of total (autumn ●, spring ● and summer * datasets) dataset using partial least squares regression (PLSR) method .....	91
Figure 5.3 Average pasture canopy reflectance (lines) and coefficient of variation (%) (bars) during autumn, spring and summer seasons in 2009-2010 at the three sites (Waikato, Taranaki, Manawatu and Canterbury) across New Zealand. ....	93
Figure 6.1 Typical shape of a spherical variogram model.....	107
Figure 6.2 Relationship between measured and predicted herbage biomass in the validation dataset (n=207) using vegetation indices .....	109
Figure 6.3 Semivariograms of herbage biomass of 10 fields.....	111

## Acronyms

AI	artificial intelligence
ANN	artificial neural networks
AOAC	association of official analytical chemists
ASD	analytical spectral devices – ASD Inc.
ADF	acid detergent fibre
AVIRIS	airborne visible infrared imaging spectrometer
CAPP	canopy pasture probe
CCRS	canada centre for remote sensing
CV	coefficient of variation
DCAD	dietary cation-anion difference
DM	dry matter
EM	electromagnetic
FDR	first derivative reflectance
FOV	field of view
GIS	geographic information system
GPS	global positioning system
IR	infrared
LAI	leaf area index
LIBERTY	leaf incorporating biochemistry exhibiting reflectance and transmittance yields
LV	latent variable
ME	metabolisable energy
MIR	mid infrared
NASA	national aeronautics and space administration
NDF	neutral detergent fibre
NDVI	normalised difference vegetation index
NIR	near infrared region
NSE	nash-sutcliffe efficiency
NV	nutritive value



NIRS	near infrared reflectance spectroscopy
OMD	organic matter digestibility
PCA	principal component analysis
PCR	principle component regression
PLSR	partial least squares regression
PRESS	predicted residual error sum of square
$R^2$	coefficient of determination
RDVI	renormalized difference vegetation index
REP	red edge position
RMSE	root mean square error
RMSECV	root mean square error of cross-validation
RMSEP	root mean square error of prediction
RPD	ratio prediction to deviation
SD	standard deviation
SAIL	scattering by arbitrarily inclined leaves
SAR	synthetic aperture radar
SAVI	soil adjusted vegetation index
SMLR	stepwise multiple linear regression
SWIR	shortwave infrared
SVM	support vector machines
SVR	support vector regression
USDA	united states department of agriculture
UV	ultra violet
VI	vegetation indices
VIP	variable importance for the projection
Vis/VIS	visible
Vis-NIRS	visible near infrared spectroscopy

## **CHAPTER 1**

# **General Introduction**



### 1.1. General Background

New Zealand is the world's largest exporter of dairy products, which makes its dairy sector a key contributor to the country's economy. This dairy sector accounts for 2.8% of the Gross Domestic Product (GDP) and it had a 26% share (NZ \$ 10.4 billion) of New Zealand's total exports in 2009 (Fonterra, 2010). Additionally, this sector has indirect (fertiliser, agriculture services and transport) and induced (dairy farmer's spending etc.) effects on the New Zealand economy.

New Zealand milk production relies heavily on highly productive and rotationally grazed pasture as its main source of feed, due to the low price received for milk within the international market. The underlying reasons for this pasture dependency are the prevailing temperate climate and sustained pasture growth throughout the year. Concentrates are rarely fed because they are generally uneconomic in New Zealand's climate but, as the price of milk rises the interest in feeding grain or concentrate is also increasing. Grass will continue to dominate cow's diet and it is therefore important to have knowledge of the quality and quantity of feed consumed. These low cost pasture-based systems, coupled with economically beneficial technologies such as genetic improvement, out-door housing and skilled labour and flexibility in grazing and milking systems, makes New Zealand's dairy industry more competitive over other world competitors (Holmes *et al.*, 2007).

In a successful grass-based dairy farming system, the maintenance of high quality and efficient use of pasture (within economic constraints) are essential, since the level of milk production is directly related to pasture quantity and quality (FAO, 2010). Therefore, these elements are critical determinants in grassland management. New Zealand has adopted mixed pasture, dominated by rye grass (*Lolium perenne* L.) and white clover (*Trifolium repens* L.), in order to supply nutrients to their animals. However, the growth rate of these species is greatly influenced by climatic factors, grazing management and animal interference. In order to achieve the desired level of pasture production, particularly during the critical stages, nitrogen fertilisers are applied, in order to boost the growth rate. However, although clover fixes nitrogen from the atmosphere, it is not always adequate for intensive growth and production. Following the intensification of farms with dairy cattle,

the use of nitrogen fertilisers has increased markedly from 47,000 tonnes in 1990 to 277,000 tonnes in 2009 (FertResearch, 2009).

The achievement of continuous intensive growth together with sustainability within dairy farming is a great challenge due to various economic and environmental factors. The cost of input resources, particularly fertiliser, is increasing relative to the milk price: and this price fluctuates over time. Moreover, the environmental constraints associated with inefficient and intensive use of resources is leading to elevated levels of greenhouse gases (GHG) in the atmosphere and nitrates in drainage waters. The agriculture sectors, particularly dairy systems, contribute a major share towards New Zealand's total GHG emissions. Although these emissions were lower than the global average for dairy GHG emissions (Melyukhina, 2011), New Zealand committed to reducing its GHG levels, when it signed the Kyoto protocol. Furthermore, New Zealand will be the first country in the world to enact an emission trading scheme (ETS) for agriculture. This enactment will be effective from 2015 (MfE, 2008) and it will impact on production costs, due to the addition of a carbon tax. The other major environmental constraint is water pollution. Feeding N rich pastures leads to high levels of N excretion through urine and dung patches and this results in nitrate leaching, which pollutes surface and ground water system.

In order to maintain sustainable and profitable management, the prerequisites are to feed adequate amounts of quality feed and to utilise that feed efficiently. For example, milk production and animal performance is heavily influenced by pasture quality. In addition, environmental problems can be reduced. A study conducted by the United Nations Food and Agriculture Organisation (FAO, 2010), which assessed GHG emissions from the global dairy sector, clearly stated that the amounts of GHG (particularly methane and nitrous oxide) are strongly influenced by the quantity, quality and composition of feed. It recommended the manipulation of dietary feeds to improve animal productivity, feed and N use efficiency. In order to follow this recommendation, tools are needed for estimating the biomass and quality of feed. To date, there is a range of pasture measurement techniques (direct and indirect) available. Although direct measurements such as mowing and quadrat sampling techniques are accurate, they involve invasive sampling and tedious procedures. In case of indirect measurements, a variety of tools such as a rising plate meter (Thomson

*et al.*, 2001); the C-Dax Pasturemeter™ (Yule *et al.*, 2005); electrical capacitance probes (Sanderson *et al.*, 2001); and pendulum sensors, are available. Some of these tools are used only occasionally by farmers, partly due to lack of accuracy in measurements and their dependence on environmental conditions, in addition to the limited availability of information and required operating skills. Moreover, although the C-Dax Pasturemeter™ has established itself within the New Zealand market, it will only provide information on pasture quantity, not quality. Alternatively, the advent of remote sensing technologies has progressed with simultaneous assessment of the vegetation: quantitatively, qualitatively and non-destructively. In addition, these techniques can provide spatial information when integrated with a global positioning system (GPS), which allows interpolation of spatial data and which in turn can lead to exercising precision management practices, in order to maximise the use of resources, whilst minimising the environmental foot-print. For example, a variable rate and precise application of fertiliser can improve nutrient use efficiency and reduce environmental contamination.

Remote sensing is defined as the collection of information on an object or area, without establishing any physical contact with that particular object or area (Lillesand *et al.*, 2004). The information about the object, collected as spectral reflectance, is unique for that object: at each wavelength the reflectance varies, thus giving a spectral signature. These signatures are a function of the intrinsic physical and chemical properties of the observed object. In this case, the object is the pasture canopy. Remote sensors are generally operated from a distance and mounted on a platform. Based on the sensing distance, three types of sensors are available: spaceborne, airborne and ground-based. Ground-based remote sensing has become very popular in recent year, due to its real-time information for decision making; it's increased spatial resolution; and lower cost and availability. These sensors are generally mounted on a vehicle or carried by a hand: and they are also referred to as proximal sensors (Gebbers & Adamchuk, 2010; Pullanagari *et al.*, 2011a).

Based on their spectral properties, the sensors are grouped into panchromatic, multispectral and hyperspectral sensors. In this study, multispectral and hyperspectral sensors were used to study the characteristics of pasture swards. Multispectral sensors typically collect reflected energy in discrete bands of the electromagnetic spectrum. In contrast,

hyperspectral sensors examine the many narrow and contiguous bands (visible to shortwave infrared region) of the electromagnetic spectrum, which then permits detailed study of vegetation (Jungho Im, 2008). The extent of information on vegetation, which is available from remote sensor data, depends on the sophistication of the sensors, our understanding and the methodologies which we apply (Curran, 1989). Proximal sensing tools, particularly hyperspectral sensors, have proved to be successful in estimating foliar chemicals, both in the laboratory (Curran *et al.*, 2001; Kokaly & Clark, 1999) and in the field (Biewer *et al.*, 2009b; Sanches, 2009; Schut *et al.*, 2006). In addition, proximal multispectral sensors (CROPSCAN™ and Crop Circle™) are also found to have a reasonable potential for explaining vegetation features, such as canopy nitrogen content and biomass (Jongschaap, 2006; Trotter *et al.*, 2010; Xue *et al.*, 2004).

## **1.2. Research objectives**

This research investigates the potential of proximal sensing tools (ASD FieldSpec® Pro FR, CROPSCAN™ and Crop Circle™) to assess pasture swards in terms of quantity and quality; these are crucial factors when making decisions related to dairy farm management. The pasture quality parameters assessed included crude protein (CP), acid detergent fibre (ADF), neutral detergent fibre (NDF), ash, dietary cation-anion difference (DCAD), lignin, lipid, metabolisable energy (ME) and organic matter digestibility (OMD). The main objectives of this research are:

- To investigate the ability of a hyperspectral sensor (ASD FieldSpec® Pro FR) to predict pasture quality parameters.
- Assess the potential of a multispectral sensor (CROPSCAN™) to assess pasture quality parameters.
- To examine the temporal robustness of predicting pasture quality parameters over seasons using a multispectral sensor (CROPSCAN™).

- To investigate the potential of a commercial active sensor (Crop Circle™ ACS-470) to estimate pasture biomass and quality while at the same time studying the spatial properties of pasture.

### *1.3. The study areas*

For spectral measurements, the field campaigns were conducted over a two-year period on commercial dairy farms located in various regions across New Zealand. These study sites provided a wide range of pasture samples resulting from varying climatic conditions and botanical compositions. The geographical position of the 14 study sites are depicted in Figure 1.1.



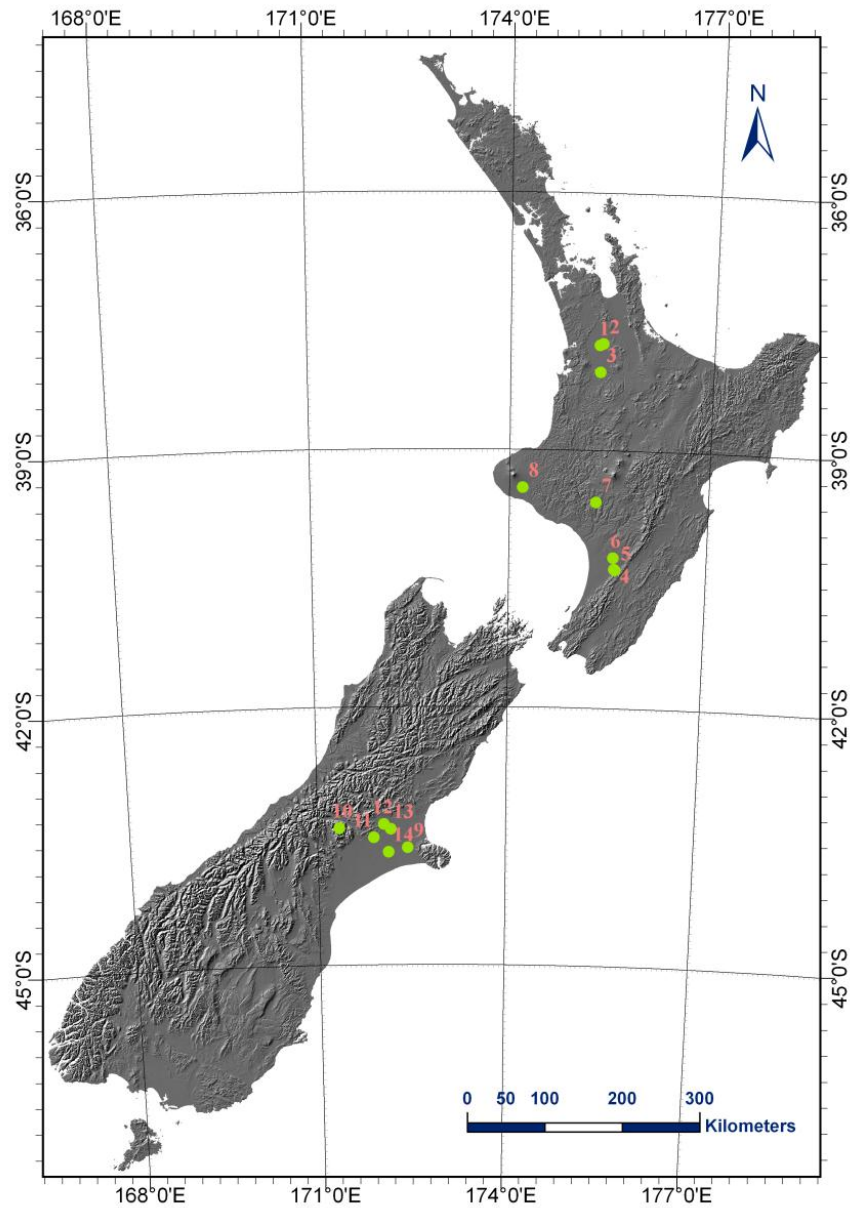


**Figure 1.1 Study farms located across New Zealand; 1) Ruakura dairy farm, AgResearch 2) Tokanui dairy farm, AgResearch 3) Scot dairy farm, AgResearch 4) Dairy No. 1, Massey University dairy farm 5) Dairy No. 4, Massey University dairy farm 6) Aorangi dairy farm, AgResearch 7) WESTPAC dairy farm, DairyNZ 8) Brian dairy farm 9) Lincoln University dairy farm 10) Synlait dairy farm 11) Mackie dairy farm 12) Greendale dairy farm 13) Pang Born dairy farm 14) Ward dairy farm**

### 1.4. Thesis Outline

This thesis comprises 7 chapters. The first two chapters contain the introduction and literature review followed by four stand-alone chapters while the last chapter contains the research discussion and summary. The stand-alone chapters have been developed as individual papers which have been submitted to scientific journals and cited at each chapter and in the author's publications list, each carry an individual introduction, material and methods, results and discussion. The stand-alone chapters had their own style according to the corresponding journal. Consequently, there may be some overlapping and repetition in some of the sections. Although the submitted manuscripts include other authors, my contribution was greatest and appropriate to being the first author in all cases.

- |           |  |
|-----------|--|
| Chapter 1 | Provides the synoptic view of the research background and outlines the objectives and thesis structure.  |
| Chapter 2 | Addresses the review of literature of fundamentals of remote sensing, available remote sensing tools and explains the analysis methods for spectral data.  |
| Chapter 3 | Investigates the ability of proximal hyperspectral sensors to assess pasture quality parameters. For this, the CAPP (Canopy Pasture Probe) enabled ASD FieldSpec <sup>®</sup> Pro FR was used to acquire <i>in situ</i> spectra of the pasture samples. Partial least squares regression (PLSR) was used to analyse the spectral data. This chapter also explores the important wavelengths for explaining pasture quality.  |
| Chapter 4 | Discusses the feasibility of using proximal multispectral radiometer data to estimate pasture quality parameters. A 16-channel CROPSCAN <sup>™</sup> portable radiometer was used to collect <i>in situ</i> diffuse reflectance spectra from pasture canopies. This chapter also explores three statistical methods for the study: Single band model, two-band index models (identifying new combination indices) and a stepwise multiple linear regression model. |

- Chapter 5 Describes the ability of the same multispectral radiometer to predict pasture quality parameters in different seasons of the year. In this chapter, partial least squares regression (PLSR) was adopted for statistical analysis. The *in situ* spectral data of pasture samples were obtained during three different seasons (autumn, spring and summer).
- Chapter 6 Explains the potential capability of the commercially available active proximal sensor (Crop Circle™ Model: ACS-470) for biomass and standing crude protein estimation in mixed pastures. It also evaluates the spatial distribution of pasture biomass in randomly selected paddocks.
- Chapter 7 Summarises the findings of this research and provides discussion and overall conclusions to the work.

## **CHAPTER 2**

### **Literature Review**



### 2.1. General background of remote sensing

Remote sensing is defined as “the science and art of obtaining information about an object, area, or phenomenon through the analysis of data acquired by a device or sensor that is not in contact with the object, area, or phenomenon under investigation (Lillesand *et al.*, 2004). The term “remote sensing” was used for the first time by the geographer Evelyn Pruitt in the mid-1950's for meteorological data analysis (NASA, 1998). Generally, remote sensing devices (spectrophotometers, spectroradiometers and radiometers) detect emitted and reflected electromagnetic (EM) energy and convert it into a signal that can be represented as numerical data or as an image. Electromagnetic energy or radiation can be classified as gamma rays, X-rays, ultraviolet (UV), visible, infrared, microwaves, radio waves and long waves. Each group of radiation is typically presented by wavelength ( $\lambda$ ) and frequency ( $f$ ) units (CCRS, 2011a). The continuum of wavelengths or frequencies of electromagnetic radiation referred to as EM spectrum is illustrated in Figure 2.1 and shows the longest wavelength (radio waves) to the shortest wavelength (gamma waves).

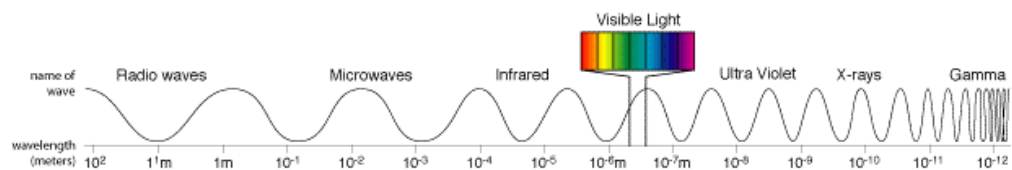


**Figure 2.1 Electromagnetic spectrum (NASA, 1998)**

The wavelength and frequency units are nanometer (nm) or meter (m) and hertz (Hz) respectively. The wavelength region and the terminology of each energy group vary between publications and applications. According to the ASD FieldSpec Pro 3 User Manual (ASD, 2010), the spectral regions are configured as follows: UV (1-400 nm); visible (400-750 nm); near infrared (NIR, 750-1000 nm); shortwave infrared-1 (SWIR-1, 1000-1800 nm); shortwave infrared (SWIR-2, 1800-2500 nm). Lillesand *et al.* (2004) categorise the visible region between 400 nm and 700 nm, the infrared region between 700 and 14000 nm and the microwave between  $10^6$  nm (1 mm) and  $10^9$  nm (1 m). They further divided the

infrared region into the near IR (700-1300 nm) and mid IR (1300-3000 nm). The mid IR is also ascribed to as shortwave infrared region (SWIR) and the thermal IR (3000-14000 nm).

Depending on the study goal, the remote sensing system uses different regions of the spectrum. For example, the visible region from (400 nm) to SWIR (2500 nm) has been used in vegetation studies (Flynn *et al.*, 2008; Pullanagari *et al.*, 2011b) and the thermal infrared and radio are waves used in heat emission studies (Lillesand *et al.*, 2004). A variety of sensors have been used to study the interactions (absorption, transmittance and reflectance) between energy and object. The primary source of electromagnetic energy is the sun. The sensors that depend on sun light to collect the reflectance from the target are called passive sensors. Most space and airborne sensors rely on sunlight for the light source. In contrast, certain sensors use their own source of energy for illumination directed toward the target to be investigated, and often also denoted as “active sensors”. Hence, they can be used any time of the day, night and season regardless of natural light changes. Examples for active systems are synthetic aperture radar (SAR; airborne sensor) and Crop Circle™ (proximal sensor). A camera has both an active and passive system (Lillesand *et al.*, 2004). The human eye that acts as sensor can detect only the visible region of the electromagnetic spectrum.

When the solar radiation hits a target it can be absorbed, transmitted and reflected. These energy components are a function of wavelength ( $\lambda$ ). The proportion of each component varies with object properties. In remote sensing, spectral reflectance ( $\rho_\lambda$ ) is used as a feature to depict the object properties as a function of wavelength (Lillesand *et al.*, 2004). This spectral reflectance is defined as the ratio of the reflected radiation to the total radiation falling upon the object and can be mathematically expressed by the following equation [2.1] (Lillesand *et al.*, 2004).

$$\rho_\lambda = \frac{E_R(\lambda)}{E_I(\lambda)} = \frac{I_o}{I_t} \quad 2.1$$

Where  $\rho_\lambda$  is the spectral reflectance at  $\lambda$  wavelength;  $I_o$  – the energy of wavelength reflected from the object;  $I_t$  – the energy of wavelength incident upon the object. Usually the spectral reflectance is expressed between 0 to 1 with no units or also presented in percentage terms.

The spectral reflectance of each object measured as a spectral response over the spectrum and referred to as the spectral signature is a function object's characteristic features. These unique spectral signatures allow differentiation of various objects. Spectral signatures of selected targets are illustrated in Figure 2.2.

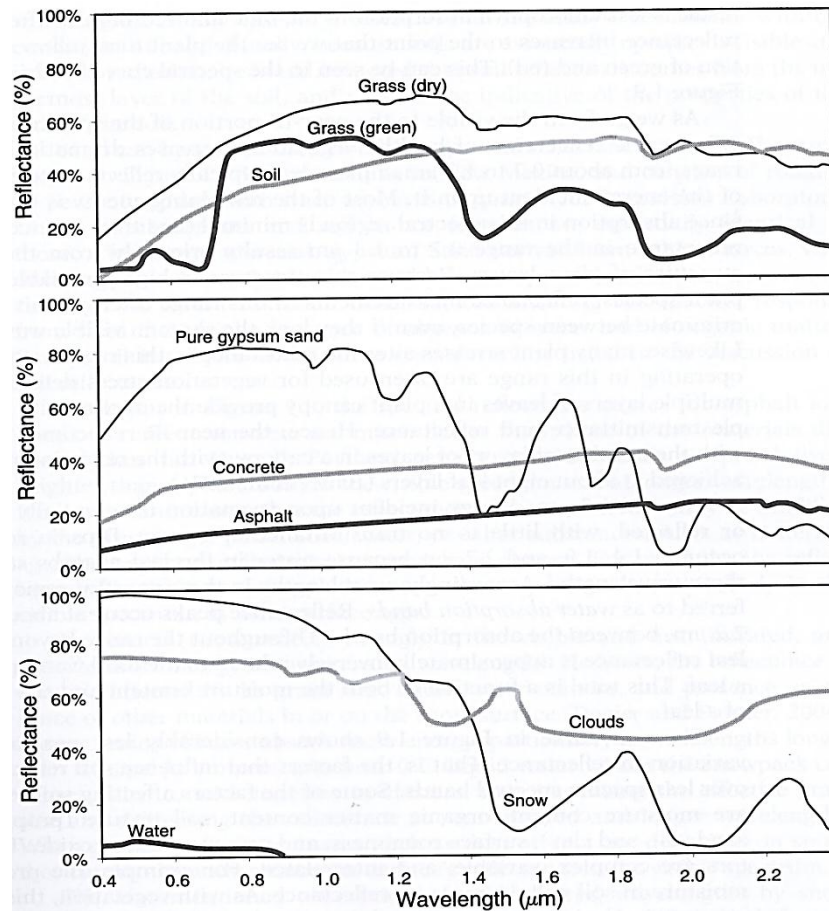


Figure 2.2 Spectral signatures for various feature types (Lillesand *et al.*, 2004)

To collect the spectral reflectance from the target the sensor needs to be placed on a stable platform. For this, satellite based, aircraft based and ground based platforms are available. Spaceborne remote sensing can be used for global scale studies because it covers a large area in a relatively short time. Similarly, airborne sensing investigates the ground objects in a regional scale. While, ground based sensors also called proximal sensors usually operates between 1-2 m distance between the target and sensor hence can able to record detail and real-time information about the target compared space and aircraft based remote sensing



systems. These proximal sensors are generally mounted on a vehicle or carried by hand (Gebbers & Adamchuk, 2010; Pullanagari *et al.*, 2011a).

In remote sensing, the characteristics of the sensor are crucial for evaluation of the study. In this regard, the function and performance of a sensor is characterised by its spectral, spatial, radiometric and temporal resolution (NASA, 1998). Spatial resolution describes the ability of the sensor to recognise the smallest remote object and measures the smallest angular or linear separation between two objects and is usually expressed in radians or meters (CCRS, 2011b). Spatial resolution primarily depends on the sensor field of view (FOV), the solid angle through which a sensor is sensitive to reflectance, and the distance between target and sensor. Generally, space and airborne sensors are far away from the target and have low to medium resolution ( $\approx 5$  m - 5 km) whereas proximal sensors are operated close to the target hence providing a higher spatial resolution ( $\approx 1$  - 2 m). As the sensors have fine resolution, they are more likely to describe detail information about the target. In many instances high spatial resolution may not be necessary and it particularly depends on the scale of study. For example, accounting for global changes of vegetation requires sensing with lower spatial resolution systems.

Spectral resolution refers to the ability of the sensor to resolve or differentiate electromagnetic radiations at different frequencies (CCRS, 2011b) measured by the width of wavelength units. Multispectral sensors generally detect the reflected energy in discrete bands over a range of wavelengths ( $\approx 20$ -400 nm). These broad spectral resolution sensors can't resolve the narrow diagnostic features as the low spectral resolution masks the narrow spectral features (Mutanga, 2004). Currently available multispectral sensors and their characteristics are listed in Table 2.1. Proximal multispectral sensors are widely used in commercial agriculture for determining the nitrogen and biomass variation in standing crops. In contrast, hyperspectral sensors have fine spectral resolution ( $\approx 1$ -20 nm) to detect the reflected energy such as the ASD FieldSpec<sup>®</sup> Pro (proximal sensor) and Hyperion (spaceborne sensor). As the spectral resolution of the sensor increases, better understanding of the object features can be achieved. For example, for quantifying accurate biochemical

concentrations in a heterogeneous environment a high spectral resolution sensor is more appropriate.

**Table 2.1 Selected multispectral sensors and their characteristics**

Sensor	Developer	Spectral Range (nm)	Spectral Resolution (nm)	Spatial Resolution (m)	Platform
Moderate Resolution Imaging Spectroradiometer (MODIS)	NASA, USA	620-2652 (7)	50-1024	250-500	Spaceborne
Advanced Along-Track Scanning Radiometer (ASTER)	NASA, USA	520-11650 (14)	80-700	15-90	Spaceborne
Medium resolution imaging instrument (MERIS)	European Space Agency (ESA)	390-1040 (15)	2.5-30	300	Spaceborne
Landsat-7 +ETM	NASA, USA	450-2350 (6) + 10400-12500 (1)	65-260 + 2100	30	Spaceborne
Multiangle imaging spectroradiometer (MISR)	NASA, USA	446-867 (4)	20-60	275	Spaceborne
Advanced Land Observation Satellite (ALOS)	JAXA, Japan	420-890 (4)	80-130	10	Spaceborne
IKONOS	GeoEye, USA	450-853 (4)	71-96	0.82-3.2	Spaceborne
Quick Bird	Digital Globe, USA	430-918 (4)	115-203	2.44	Spaceborne
Rapid Eye	Germany	440-850 (5)	40-90	5	Spaceborne
Système Probatoire d'Observation de la Terre (SPOT-5)	France	500-1750 (5)	70-170	10	Spaceborne
Korea Multi-Purpose Satellite-2 (KOMPSAT-2)	South Korea ESA	450-900 (4)	60-140	4	Spaceborne
CBERS-2	Brazil and China	450-890	60-120	20-260	Spaceborne
FOMOSAT-2	China	450-900 (4)	60-140	8	Spaceborne
World View-2	Digital Globe, USA	400-1040 (8)	40-180	1.85	Spaceborne
Crop Circle (ACS-470) *	Holland Scientific Inc., USA	440-760 (3)	20-40	< 1	Proximal
Cropscan (MSR-16)	Cropscan Inc., USA	460-1680 (16)	7-16	< 1	Proximal
CropSpec*	Topcon, USA	730-810 (2)	10	< 1	Proximal
GreenSeeker (RT-500) *	N Tech Indus., USA	656 and 774 (2)	25	< 1	Proximal
Yara N-Sensor *	Yara International, Norway	450-890 (45)	10	< 1	Proximal
Skye SKR 1800 *	Skye Instruments Ltd., UK	650-800 (2)	10	< 1	Proximal

The available total number of wavebands (parenthesis)

\* The sensors act as active sensors because it has own light source

At present, the demand for hyperspectral sensors has been growing because of their potential for analysing earth surface features encompassing agriculture, forestry and soil environments. As a result of this, many nations and institutes focused on developing hyperspectral sensors. Existing and future hyperspectral sensors are listed in Table 2.2. The term hyperspectral remote sensing is interchangeable with spectroscopy, NIRS and imaging spectroscopy (Kumar *et al.*, 2002).

Radiometric resolution refers to the sensitivity of the sensing system to the intercepted radiation. The energy (analog data) measured in a range of digital data expressed in bits. High radiometric resolution sensors have the ability to distinguish with a wide range of energy intensities or shades which are very useful in classification studies. For example, Landsat MSS had a resolution of 6 bits image had lower intensity. Conversely, Worldview-2 sensors had 11 bits resolution which distinguishes the object more clearly (Satellite-Imaging-Corporation, 2011). Human eye has 6 bits of radiometric resolution.

Temporal resolution refers to the frequency of temporal coverage of a sensor. Normally, airborne and space borne sensors have a lower temporal resolution as the sensor flyover the same target less frequently. Space borne sensors also have the problem of the target being concealed by cloud cover limit their usefulness for researchers. Proximal sensors offer greater flexibility for a study over time, as the user can be pick the timing of measurement, their main disadvantage is the labour involved in collecting the data. However, when considering situations of high temporal resolution they are generally considered the most suitable for agricultural applications (Gebbers & Adamchuk, 2010). High temporal resolution is an important characteristic for investigating the changes in the target over time. For example, nitrogen status varies at each growth stage of a plant.

Table 2.2 Current and future hyperspectral sensors and their characteristics

Sensor	Developer	Spectral Range	Spectral Resolution (nm)	Spatial Resolution (m)	Status	Platform Type
Hyperion	NASA	400-2500 (220)	10	30	Running	Spaceborne
Environmental Mapping and Analysis Program (EnMap)	DLR, Germany	400 -2500 (249)	5-10	600	2015	Spaceborne
PRecursores IperSpettrale della Missione Applicativa (PRISMA)	Italian Space agency	400-2500 (250)	10	20-30	2018	Spaceborne
Hyperspectral Infrared Imager (HyspIRI)	NASA, USA	400-2500 (210)	8-12	45	2015	Spaceborne
Multi-Sensor Microsatellite (MSMI)	Sun Space, South Africa	400-2350 (> 200)	10	14.5	2016	Spaceborne
Compact high resolution imaging spectrometer (CHRIS)	European Space Agency	415-1050 (63)	1.3	18-36	2001	Spaceborne
Australian Resource Information and Environment Satellite (ARIES-1)	Auspace Ltd., ACRES Geoimage Pty. Ltd, CSIRO, Earth Resource Mapping Pty. Ltd	400-2500 (105)	15-30	30	-	Spaceborne
HySI	Indian Space Research Organisation (ISRO)	400-950	15	80	2015	Spaceborne
Compact Airborne Spectrographic Imager (CASI-1500)	ITRES Corp. Canada	380-1050 nm	< 3.5	0.25-1.5	Running	Airborne
Airborne Visible InfraRed Imaging Spectrometer (AVIRIS)	NASA, USA	400-2500 (224)	10	20	Running	Airborne
HYperspectral Digital Imagery Collection Experiment (HYDICE)	Naval Research laboratory, USA	400-2500 (171)	-	-	Running	Airborne
Hyperspec VNIR	Headwall Photonics Inc.	400-1000 (837)	2-3	-	Running	Airborne
HyMap	HyVista Corp., Australia	400-2500 (128)	13-17	3.5-10	Running	Airborne
AisaDUAL (AisaHAWK and AisaEagle)	Specim spectral Imaging Ltd., Finland	400-2500 (298)	6.3	320	Running	Airborne
PROBE-1	Earth Search Sciences Inc.	440-2543 (128)	11-18	5-10	Running	Airborne
VNIR-1600 (HySpex)	Norsk Elektro Optikk, Norway	400-1000 (160)	3.7	-	Running	Airborne
Digital Airborne Imaging Spectrometer (DAIS 7915)	DLS, Germany	400-12600 (79)	15	-	Running	Airborne
EPS (Environment Protection System)-H		430-2500 (140)	-	-	Running	Airborne
ASD FieldSpec®	Analytical Spectral Devices Inc., USA	350-2500	3-8.5	< 1	Running	Proximal
GER-3700	Geophysical Environment Research Corporation, USA	350-2500	1.5-9.5	< 1	Running	Proximal
HR-1024	Spectra Vista Corp.	350-2500	3.5-9.5	< 1	Running	Proximal
SE-590	Spectron, Ocean Optics.	356-1124	5	< 1	Running	Proximal
PIMA®	Integrated Spectronics, Australia	350-1100	3	< 1	Running	Proximal
UniSpec-DC	PP SYSTEMS, USA	310-1100	10	< 1	Running	Proximal

The available total number of wavebands (parenthesis)

## 2.2. Remote sensing of vegetation

The importance and application of remote sensing is growing in agricultural, forest, rangeland and ecological vegetation studies, because vegetation is very important for living beings. Moreover, these technologies are potential alternatives to traditional analysis techniques that usually involve tedious procedures such as manual sampling and expensive laboratory analysis.

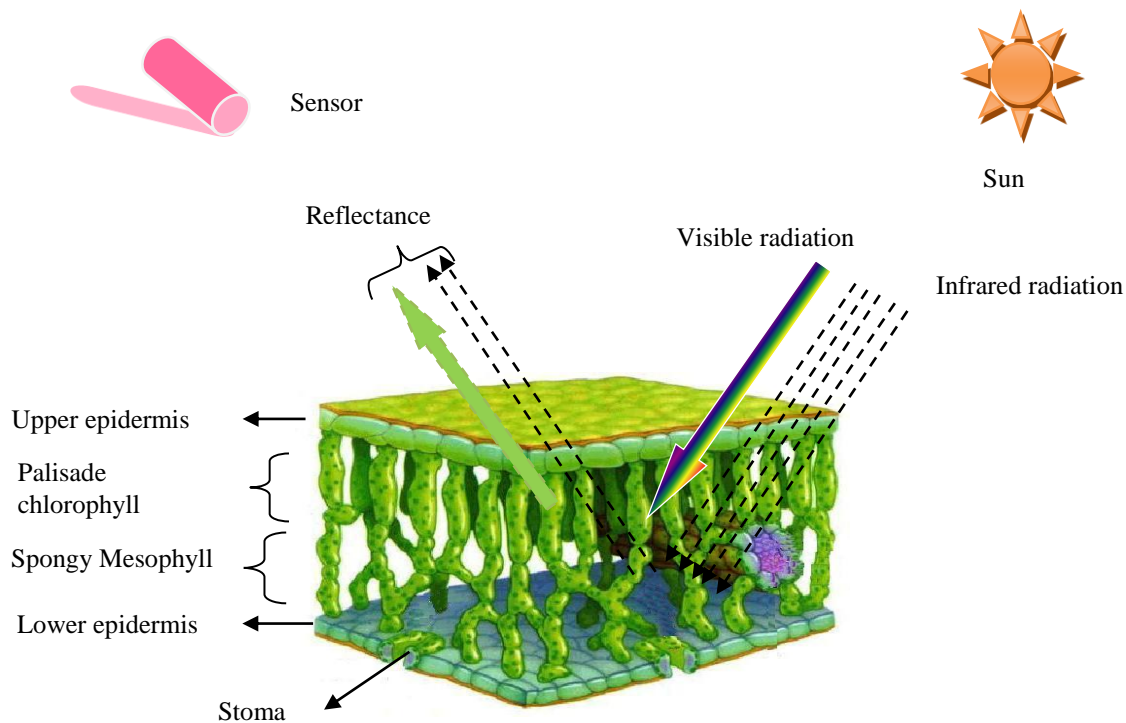


**Figure 2.3 Interaction between energy source, leaf structure and spectral sensor (Lillesand *et al.*, 2004); the diagram of the leaf structure adapted from <https://dbscience3.wikispaces.com/Drew>**

The wavelength regions, which are of greatest interest for vegetation studies are the visible (400-750 nm), the near infrared (750-1000 nm) and the shortwave infrared (1000-2500 nm) regions. The interaction between energy, leaf and spectral sensor is illustrated in Figure 2.3. In Figure 2.3, most of the visible (400-750 nm) radiant energy of the electromagnetic spectrum is absorbed by palisade cells that contain the chlorophyll pigments. The green

radiation reflects back, which is why vegetation appears green in colour. Conversely, the IR is transmitted by epidermis and palisade layer. The reflected radiation is captured by the sensor.

This captured reflectance is presented as a typical spectral reflectance: or spectral signature of green vegetation, in Figure 2.4. The vegetation spectral signature is a function of water, pigments, biophysical (biomass, leaf area index, leaf angles and structure, proportion of green and dead vegetation and proportion of land cover) and biochemical (organic compounds) parameters. These parameters are complex, variable and interrelated (Kumar *et al.*, 2002).

As noted in Figure 2.4, the reflectance of green vegetation contains peaks and valleys across the spectrum. The energy absorption valleys in the visible portion (450-750nm) of the spectrum are caused by pigments (chlorophyll, carotenoids and anthocyanins) which are present in leaves (Gamon & Surfus, 1999). These broad absorptions are caused by electronic transitions and reflected in the green region (495-570nm) (Curran, 1989). These particular absorption areas of the visible spectrum are also called the “chlorophyll absorption bands” (Lillesand *et al.*, 2004). The chlorophyll content in leaf is directly linked to vegetation health: as is photosynthetic capacity, the developmental stage and physiological stresses. Changes in the chlorophyll content of vegetation are reflected in variations in the absorption features of the visible spectrum (Gitelson *et al.*, 2005). Conversely, the reflectance, which is usually high in the near infrared region of the spectrum, primarily results from the scattering at the mesophyll cell wall interfaces of plant leaves (Gausman, 1974). Beyond NIR, three more broad absorption features (valleys around 1400nm, 1900nm, 2500nm) appear in SWIR (Figure 2.4) primarily caused by the bending and stretching of O-H bonds. These bands are also referred to water absorption bands (Lillesand *et al.*, 2004). In addition to as these major absorption features, there are many minor absorption features in NIR and SWIR regions of the spectrum, which are the result of harmonic overtones and combination bands of stretching and bending vibrations of molecular bonds, such as C-O, O-H, C-H and N-H bonds (Curran, 1989). These bonds are very common in many organic compounds, such as nitrogen, lignin, lipid and fibre.

The chemical concentrations of various dried and ground vegetation samples were successfully estimated by using lab-NIRS (1100-2500 nm) and these results were comparable with standard wet chemistry procedures (Williams & Norris, 1987). As a result of these estimates, a lab-NIRS method was manifested by the Association of Agricultural Chemists (AOAC) as the official method for analysing the chemistry of a wide variety of agriculture products.

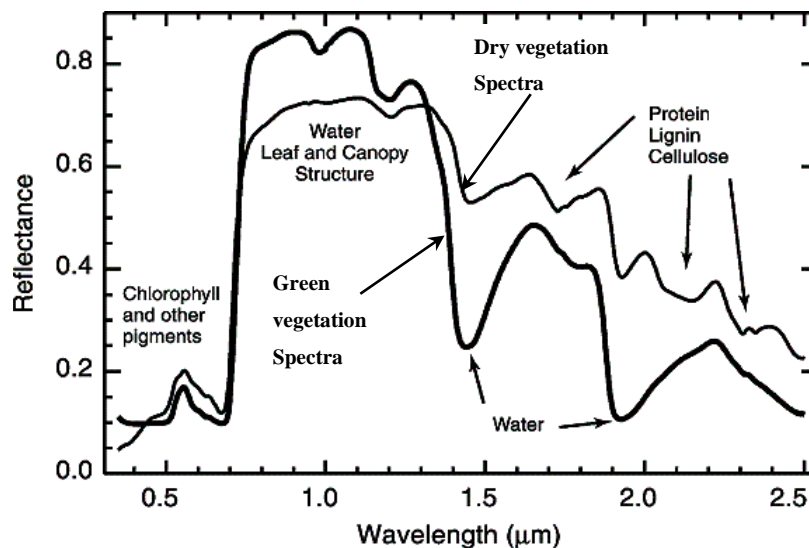


Figure 2.4 Spectral signatures of green and dry vegetation (NASA, 1994)

In contrast, success in estimating biochemistry from green vegetation was limited and the results were associated with uncertainty and low accuracy: and they varied between study sites and vegetation types. There are many factors that influence such results. From these influencing factors, the presence of water in green vegetation is a major problem because it obscures the chemical absorption features particularly in infrared region 900-2500nm (Thulin, 2008). The spectral differences between the corresponding vegetation types (dry and green) are pictured in Figure 2.4. It can be clearly noted that the absorption of protein, lignin and cellulose in the green vegetation spectra are dominated by water peaks (Figure 2.4). Despite these limitations in the field, estimations of pasture characteristics are very important for long-term sustainable dairy farming. In order to establish the strong physical

relationship between the desired pasture parameters and spectra obtained from different sensors, various computational approaches have been developed.

### 2.3. Computation of spectral data

Several computational approaches have been developed, in order to establish relationships between spectral data and vegetation characteristics. These approaches include empirical, physically based, and the integration of empirical and physically based. Each method has its advantages and disadvantages.

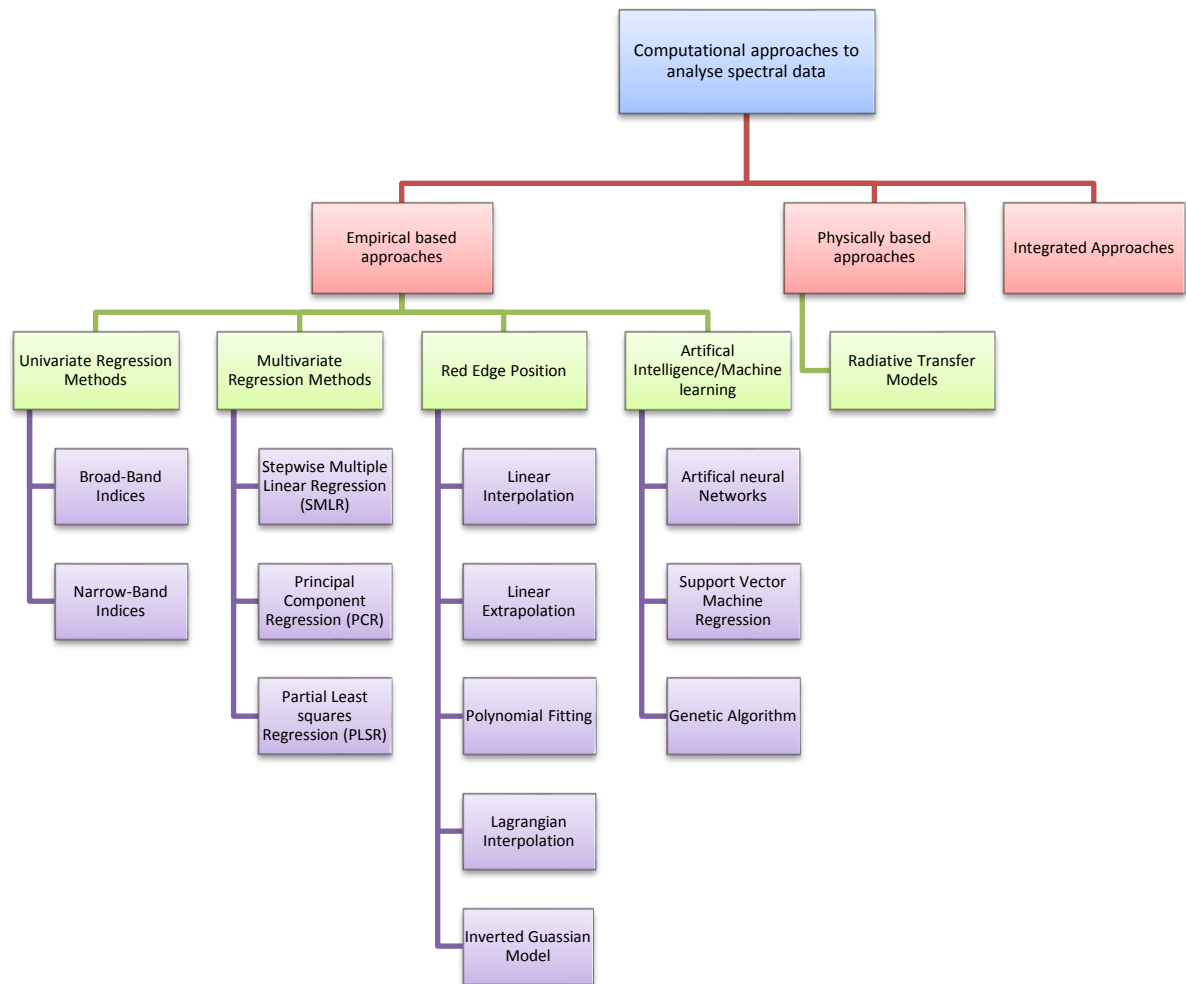


Figure 2.5 The various computational approaches for analysing spectral data



Empirical-based approaches have been widely used for developing correlations between spectral data and various measured pasture characteristics, such as leaf area index (LAI), biomass, vegetation fraction, chlorophyll and nitrogen content etc.

### **2.3.1. Empirical based approaches**

#### **2.3.1.1. Univariate Statistical Methods**

Univariate statistical methods were used to relate the vegetation characteristics to the individual or ratio combination of discrete visible and infrared wavebands (vegetation indices). Generally, the vegetation indices are represented as a single value and regressed against desired vegetation properties. The usage of vegetation indices is dominated in remote sensing studies, due to their simplicity in interpretation.

The retrieval of canopy spectral information, within a limited number of wavebands, is known to be affected by many confounding external factors, such as soil background; soil moisture; structures of leaf and canopy (number of leaves per unit area, leaf angle, orientation and foliage clumping); vegetation optical properties; and the differences between species. In addition, a distinct effect of the sensor view angle and illumination geometry has been seen on vegetation indices (Qi *et al.*, 1994). In order to overcome some of these problems, many scientists have consequently worked towards developing many indices to determine parameters, such as the biophysical (LAI, vegetation cover and botanical and vegetation composition) and biochemical (concentrations and contents of chlorophyll, nitrogen, protein, fibre and pigments) characteristics of plant and canopy, while minimising the effect of external perturbing changes on vegetation indices. The function of each index is majorly influenced by the spectral resolution and property of interest. Multispectral sensors are dominant in remote sensing, since they provide spectral information in broad discrete wavebands, in order to study vegetation properties. A variety of vegetation indices (Table 2.3) have been developed for studying the various properties and to minimise any perturbing problems. Based on the spectral resolution of the sensor, the indices can be divided into multispectral and hyperspectral indices.

Table 2.3 Various vegetation indices listed in literature

Vegetation index	Abbreviation	Formula	Reference
<b>Atmospheric Indices</b>			
Atmospheric Resistant Vegetation Index	ARVI	$\frac{(R_{NIR} - (R_{RED} - R_{BLUE}))}{(R_{NIR} + (R_{RED} - R_{BLUE}))}$	(Kaufman & Tanre, 1992)
Soil and Atmospherically Resistant Vegetative Index	SARVI	$(1 + L)(R_{800} - R_{670}) / (R_{800} + R_{670} + L)$	(Kaufman & Tanre, 1992)
<b>General and Structural Indices</b>			
Normalized Difference Vegetation Index	NDVI	$\frac{R_{NIR} - R_{RED}}{R_{NIR} + R_{RED}}$	(Rouse <i>et al.</i> , 1973)
Simple Ratio Index	SR	$R_{NIR} / R_{RED}$	(Jordan, 1969)
Renormalized Difference Vegetation Index	RDVI	$\frac{(R_{800} - R_{670})}{\sqrt{R_{800} + R_{670}}}$	(Roujean & Breon, 1995)
Perpendicular Vegetation Index a= slope of the soil line, b= soil line intercept	PVI	$\frac{1}{\sqrt{a^2 + 1}} (R_{NIR} - a \times R_{red} - b)$	(Richardson & Wiegand, 1977)
Difference Vegetative Index	DVI	$R_{NIR} - R_{RED}$	(Jordan, 1969)
Enhanced Vegetation Index	EVI	$2.5 \frac{R_{nir} - R_{red}}{R_{nir} + 6R_{red} - 7.5R_{blue} + 1}$	(Liu & Huete, 1995)
Modified Simple Ratio	MSR	$\left( \frac{R_{800}}{R_{670}} - 1 \right) / \sqrt{\left( \frac{R_{800}}{R_{670}} + 1 \right)}$	(Chen, 1996)
Wide Dynamic Range Vegetation Index	WDRI	$\frac{[(\alpha + 1)NDVI + (\alpha - 1)]}{[(\alpha - 1)NDVI + (\alpha + 1)]}$	(Richardson & Wiegand, 1977)
Zarco-Tejada & Miller	ZTM	$R_{750} / R_{710}$	(Zarco-Tejada <i>et al.</i> , 2001)
<b>Soil-Line Indices</b>			
The following indices developed to account the changes in soil optical properties such as soil background and to minimize the background influence.			
Soil-Adjusted Vegetative Index	SAVI	$(1+L) (R_{800}-R_{670}) / (R_{800}+R_{670}+L)$	(Huete, 1988)
Transformed Soil Adjusted Vegetative Index	TSAVI	$\frac{a(NIR - a \times Red - b)}{a \times NIR + Red - a \times b}$	(Baret <i>et al.</i> , 1989)
Modified Soil Adjusted Vegetative Index	MSAVI	$\frac{1}{2} \left[ 2R_{NIR} + 1 - \sqrt{(2R_{NIR} + 1)^2 - 8(R_{NIR} - R_{RED})} \right]$	(Qi <i>et al.</i> , 1994)
Modified Second Soil-Adjusted Vegetation Index	MSAVI2	$\frac{1}{2} \left[ 2R_{NIR} + 1 - \sqrt{(2R_{NIR} + 1)^2 - 8(R_{NIR} - R_{RED})} \right]$	(Qi <i>et al.</i> , 1994)
Optimized Soil-Adjusted Vegetation Index	OSAVI	$(1 + 0.16) \left( \frac{R_{800} - R_{670}}{R_{800} + R_{670} + 0.16} \right)$	(Rondeaux <i>et al.</i> , 1996)
Triangular Vegetation Index	TVI	$0.5 [120(R_{750} - R_{550}) - 200(R_{670} - R_{550})]$	(Broge & Leblanc, 2000)
Modified Triangular Vegetation Index	MTVI-1	$1.2 [1.2(R_{800} - R_{500}) - 2.5(R_{670} - R_{550})]$	(Haboudane <i>et al.</i> , 2004)
Modified Second Triangular Vegetation Index	MTVI-2	$\frac{1.5 [1.2(R_{800} - R_{550}) - 2.5(R_{670} - R_{550})]}{\sqrt{(2R_{800} + 1)^2 - (6R_{800} - 5\sqrt{R_{670}} - 0.5)}}$	(Haboudane <i>et al.</i> , 2004)

<b>Pigment and LAI Indices</b>			
The following indices developed to reduce the combined and independent effects of soil background and non-photosynthetic material.			
Normalized Pigment Chlorophyll Index	NPCI	$(R_{680} - R_{430}) / (R_{680} + R_{430})$	(Peñuelas <i>et al.</i> , 1994)
Modified Chlorophyll Absorption in Reflectance Index	MCARI	$[(R_{700} - R_{670}) - 0.2 \times (R_{700} - R_{550})] \times R_{700} / R_{670}$	(Daughtry <i>et al.</i> , 2000)
Transformed CARI	TCARI	$3[(R_{700} - R_{670}) - 0.2(R_{700} - R_{550})(R_{700} / R_{670})]$	(Haboudane <i>et al.</i> , 2002)
MCARI was a modification to minimize the combined effects of the soil reflectance and the non-photosynthetic materials.			
Modified Chlorophyll Absorption in Reflectance Index	MCARI-1	$1.2[2.5(R_{800} - R_{670}) - 1.3(R_{800} - R_{550})]$	(Haboudane <i>et al.</i> , 2004)
Modified Chlorophyll Absorption in Reflectance Index	MCARI-2	$\frac{1.5[2.5(R_{800} - R_{670}) - 1.3(R_{800} - R_{550})]}{\sqrt{(2R_{800} + 1)^2 - (6R_{800} - 5\sqrt{R_{680}}) - 0.5}}$	(Haboudane <i>et al.</i> , 2004)
Anthocyanin Reflectance Index	ARI	$(1/R_{550}) - (1/R_{700})$	(Gitelson <i>et al.</i> , 2001)
Carotenoid Reflectance Index	CRI	$(1/R_{510}) - (1/R_{550})$	(Gitelson <i>et al.</i> , 2002)
Carotenoid Reflectance Index-2	CRI-2	$(1/R_{510}) - (1/R_{550})$	(Gitelson <i>et al.</i> , 2002)
<b>Water Indices</b>			
Normalized Difference Water Index	NDWI	$(R_{860} - R_{1240}) / (R_{860} + R_{1240})$	(Gao, 1996)
Simple Ratio water Index	SRWI	$R_{858} / R_{1240}$	(Zarco-Tejada <i>et al.</i> , 2003)
Plant Water Index	PWI	$R_{970} / R_{900}$	(Peñuelas <i>et al.</i> , 1997)

### 2.3.1.1.1. Multispectral Indices

The most widely used and best-known classic index developed by Rouse *et al.* (1973)-normalized difference vegetative index (NDVI)- shows contrast between soil and vegetation. A number of scientists (Brown *et al.*, 2008; Donald *et al.*, 2010; Flynn, 2006; Gamon *et al.*, 1995; Hill *et al.*, 1999; Montandon & Small, 2008) have attempted to correlate NDVI with a range of vegetation properties. Donald, *et al.* (2010) developed an NDVI based model (using MODIS imagery) to predict plant growth rate in mixed pastures in Western Australia. This model accounted 70% of variability in plant growth rate over the three years of study. With a similar type of imagery, Kawamura *et al.* (2005) conducted a

study on grasslands in Mongolia, in order to monitor the forage biomass and standing crude protein and they found that the MODIS derived EVI had the potential to estimate live biomass, total biomass and standing crude protein with  $r^2$  values of 0.79, 0.76 and 0.73 respectively. He *et al.* (2009) used satellite imagery, from SPOT-4, to derive the leaf area index in native grasslands in Canada. This study has shown that the ATSAVI has a significant correlation ( $r^2=0.66$ ) with leaf area index.

Proximal sensors have proved that they have the potential to predict grain yield in wheat (Raun *et al.*, 2001) and nitrogen variation in maize (Roberts, 2009; Solari *et al.*, 2008). However, there was limited research on the use of proximal sensing in grassland science, due to the presence of complex heterogeneity. For instance, Flynn, *et al.* (2008) found that there was a significant correlation ( $r^2=0.64$ ) between the pasture biomass of tall fescue (*Schedonorus arundinaceus*) and NDVI obtained from the proximal active sensor, Greenseeker. Based on an above calibration, they further developed spatial maps for pasture biomass. Similarly, NDVI derived from Greenseeker, is well correlated ( $r^2=0.69$ ) with nitrogen uptake in Bermuda-grass (*Cynodan dactylon* L.) (Mosali, 2007). Trotter *et al.* (2010) used an vegetation index, soil adjusted vegetation index (SAVI), derived from proximal active sensor (Crop Circle; Model-ACS210), in order to predict the herbage mass in tall fescue (*Festuca arundinacea* var. Fletcher) and found a  $r^2$  value of 0.71.

#### **2.3.1.1.2. Hyperspectral Indices**

The advent of hyperspectral sensors has led to the development of narrow band indices to resolve narrow vegetation features, which are completely masked in the broad band indices. The narrow band indices have proven that they have the potential to explain the biochemical features with improved accuracy compared to broad band indices (Stagakis *et al.*, 2010). The majority of hyperspectral indices use similar mathematical equations to broad band indices (Table 2.3), with an ideal combination of wavelengths and spectral resolution. Stagakis *et al.* (2010) conducted a study that focused on hyperspectral imagery, acquired from the CHRIS sensor, to monitor vegetation biophysical and biochemical characteristics through narrow band indices in Mediterranean ecosystem fully covered by semi-deciduous shrub *Phlomis fruticosa*. This study has proved that narrow band indices

are very useful and highly accurate in prediction of the leaf area index, leaf biochemical content (chlorophyll a, chlorophyll b, carotenoids) and leaf water potential. In an airborne study, Liu *et al.* (2004) used MTVI2, calculated from CASI, to estimate absorbed photosynthetically active radiation (APAR) in corn, soybean and wheat fields. Haboudane *et al.* (2002) proposed a new combined index, TCARI/OSAVI, which is very sensitive to chlorophyll content variations and more resistant to variations of LAI, soil background and solar zenith angle. This study was conducted on corn crops, using CASI imagery.

The assessment of closed canopies with high density biomass using broad band indices is a well-known problem, due to the broad band index such as NDVI being saturated after certain level of biomass content or LAI and, hence, this limits the prediction accuracy (Gao, 2006; Tucker, 1977). In order to overcome such a problem, Mutanga *et al.* (2004b) proposed narrow band indices and they successfully estimated ( $r^2=0.80$ ) the high density biomass of *Cenchrus ciliaris* grass, by using a new combination of narrow bands- SR (simple ratio) index. Similarly Thenkabail *et al.* (2000) developed narrow band NDVI models, in order to explain the biophysical variables (LAI, canopy cover, wet biomass, plant height and yield) in cotton, potato, soybean, corn and sunflower. Yoder *et al.* (1994) used narrow band NDVI (developed from proximal hyperspectral sensor) to explain leaf area index, light absorption capacity and photosynthetic potential in tall Douglas-fir (*Pseudotsuga menziesii*) seedlings. In a heterogeneous Mediterranean grassland, Darvishzadeh *et al.* (2008) conducted a laboratory experiment for estimating leaf area index in natural vegetation, by using a proximal hyperspectral sensor and this confirmed that SAVI-2 ( $\lambda_1=727\text{nm}$ ;  $\lambda_2=1967\text{ nm}$ ) estimated the leaf area index with high accuracy ( $r^2=0.78$ ). Zhao *et al.* (2007a) developed new narrow band indices, which proved to be more accurate than broad band indices, when estimating the LAI and canopy chlorophyll density in cotton (*Gossypium hirsutum* L. cv. Sumian 3).

### 2.3.1.2. Multivariate Regression methods

As the number of wavebands of the sensors increased, the available information from different wavelengths of the spectrum has been increased and results in complex and redundant data. In order to extract the adequate information from many numbers of

wavebands, multivariate statistics are necessary. As the reference of recent reports (Biewer *et al.*, 2009b; Sanches, 2009), the multivariate analysis methods are found to be better estimates of vegetation characteristics than univariate analysis. This is probably because of hundreds of wavebands were used to extract object details, whereas univariate analysis uses a limited number of wavebands.

#### **2.3.1.2.1. Step wise multiple linear regression (SMLR)**

This is a traditional multivariate regression method used widely in laboratory based NIRS mainly due to simplicity compared to other multivariate methods (Marten *et al.*, 1985). Basically, this method involves selecting a few optimal wavebands in order to explain a large proportion of variation in the property of interest. The selection of wavebands is predetermined and varies with property of interest and the environmental conditions. SMLR effectively works when there are a greater number of observations than independent variables (wavebands) and also when the independent variables have less inter-correlation also referred to as multicollinearity. Mutunga *et al.* (2005) employed SMLR to the estimate pasture quality components (nitrogen, phosphorus, potassium, calcium, magnesium and neutral detergent fibre) from canopy spectral reflectance, using proximal hyperspectral sensor. However, the SMLR has been criticized by the researchers due to the problems of over fitting, the existence of multicollinearity affects the prediction power and lack of consistency in wavelength selection (Grossman *et al.*, 1996). Moreover, it can't deal with high dimensional data, when the number of independent variables greater than the number of observations.

To overcome some of the problems of SMLR, principal component regression (PCR) was proposed as a two-step multivariate calibration method: principal component analysis (PCA) and multiple linear regression (MLR). PCA converts the numerous independent variables (wavebands) to a limited number of latent variables or principal components through an orthogonal transformation (Esbensen *et al.*, 2009). The new variables are uncorrelated and explain most of the variance of the original dataset (spectra). Of the total variation, the first principal component (PC1) accounts maximum variation and the subsequent component, PC2, accounts second most variation and so on. The component

values of each observation are represented by scores. These score values of different components are graphically presented by score plot which is useful for studying the similarities between observations and to detect the outliers in the dataset (Miller & Miller, 2005). After developing components, MLR was applied to develop a model between independent variables (principle components) and dependent variables (measured values).

#### 2.3.1.2.2. Partial Least Squares Regression (PLSR)

PLSR is developed by Herman Wold in the 1960's to address problems in economic path modelling. PLSR is a prominent method in chemometrics because it effectively deals with numerous, multicollinear variables and also when the number of independent variables (also known as explanatory variables) are greater than the number of observations (Wold *et al.*, 2001). PLSR method is slightly different from PCR method where PLSR extracts the new components as a function of both dependent and independent variables, hence the PLS components show high correlation with dependent variables (Kusumo, 2009). The number of components optimized by the cross-validation procedure (Wold *et al.*, 2001). Based on the number of dependent variables, two types of PLSR: PLSR1 and PLSR2 are available. PLSR1 method deals with only one dependent variable whereas PLSR2 consists more than one dependent variable (Miller & Miller, 2005).

Ollinger *et al.*, (2002) examined regional level variation of canopy biogeochemistry in White Mountains National Forest, New Hampshire, USA, using AVIRIS sensor and mapped the variation of canopy lignin:N ratio by applying PLSR method. Sanches *et al.* (2009) utilized the PLSR through proximal hyperspectral sensing to assess the macronutrients concentration and dry matter of pastures in dairy and sheep farms with four explanatory variables (reflectance, first-derivative, BDR, and NBDI). In a field based imaging spectroscopy study, Schut *et al.*, (2005) estimated DM mass of standing grass herbage accurately and the macronutrient (N, P, K, S, Ca, Mg, Mn, Zn and Fe) content and feeding value (fibre, ash and sugars) with satisfactory results using PLSR method. Biewer *et al.*, (2009b) determined the concentrations of CP, ADF, ash, ME of legume-grass mixtures (*Lolium perenne* L., *Trifolium repens* L., *Trifolium pratense* L.) with canopy

reflectance, made from proximal hyperspectral sensor, using MPLSR (Modified Partial Least Squares Regression). All above experiments were yielded high prediction accuracy.

### 2.3.1.3. Red Edge Position (REP)

Red edge position (REP) or red edge index (REI) is defined as the spectral position of the inflexion point in the red edge region (670-780 nm) (Clevers *et al.*, 2002; Horler *et al.*, 1983), a new and unique method for estimating the vegetation parameters from the spectral reflectance. REP mainly caused by the combined effects of strong chlorophyll, hence high nitrogen concentration, absorption and leaf internal scattering (Dawson & Curran, 1998) causes a shift from shorter wavelengths to longer wavelengths and vice versa with lower concentration (Horler *et al.*, 1983). For accurate measurement of REP, the spectra should be continuous from 670 nm to 780 nm hence the hyperspectral sensor data is more suitable. Several researchers found that the REP is strongly correlated with LAI, chlorophyll content (Clevers *et al.*, 2002), nitrogen content (Mutanga & Skidmore, 2007) and vegetation stress compared to vegetation indices because it is less influenced by the diverse soil and atmosphere conditions and, sensor view angles (Cho, 2007).

There are several methods available for calculating the variation of the red-edge position: linear interpolation method (LIP), linear extrapolation method (LEP), inverted guassin method (IGM) and lagrangian interpolation method. Although many techniques are available to account for the variation in REP, each method has its own advantages and limitations for estimating various characteristics of vegetation.

#### 2.3.1.3.1. Linear Interpolation

The linear four-point interpolation method relies on the reflectance particularly at four wavelengths of 670, 700, 740 and 780 nm of the REP (670-780 nm) (Guyot & Baret, 1988). Therefore, this method can also be applied to multispectral data which have similar wavebands. The computation of this method includes two steps (Cho & Skidmore, 2006): Calculation of the reflectance at the inflection point ( $R_{re}$ ) using the following equation [2.2]

$$R_{red} = \frac{(R_{670} + R_{780})}{2} \quad 2.2$$



Calculation of the red edge position is computed by the following equation [2.3]

$$REP = 700 + 40 \left( \frac{R_{red} - R_{700}}{R_{740} - R_{700}} \right) \quad 2.3$$

Ruiliang *et al.* (2003) found that the linear four-point interpolation method is more practical for estimating forest LAI using Hyperion data. Similarly, Jago *et al.* (1999) used field (SE-590) and airborne (CASI) sensors for estimating chlorophyll concentration in grassland and winter wheat. Strong correlations ( $r^2=0.84$  and  $0.83$ ;  $0.73$  and  $0.86$ ) were observed between REP, using a linear interpolation technique, for field and airborne data at the sites of grassland and winter wheat, respectively.

### 2.3.1.3.2. Linear Extrapolation

This method is based on the occurrence of double-peak feature in the REP of the first derivative reflectance spectrum. “It involves linear extrapolation of two straight lines on the far-red (680 to 700 nm) and NIR (725 to 760 nm) flanks of the first derivative reflectance spectrum” and the values of these straight lines represented by the following equations [2.4 and 2.5] (Cho & Skidmore, 2006):

$$\text{Far-red line} = m_1\lambda + c_1 \quad 2.4$$

$$\text{NIR line} = m_2\lambda + c_2 \quad 2.5$$

Where  $m$  and  $c$  are the values of slope and intercept values of the lines, and  $\lambda$  is the wavelength.

The REP is defined as equation [2.6]:

$$REP = \frac{-(c_1 - c_2)}{(m_1 - m_2)} \quad 2.6$$

Cho and Skidmore (2006) successfully used the linear extrapolation technique for estimating the nitrogen concentration in rye canopy, maize leaf and mixed grass/herb leaf

stack using the proximal hyperspectral sensor (GER-3700) and stated that the results were comparable with other REP techniques.

### 2.3.1.3.3. Polynomial fitting technique

This method is very simple fitting the REP curve, from minimum reflectance at red region (670 nm) to the maximum reflectance at NIR shoulder (780 nm), with a fifth-order polynomial function. The polynomial fitting model computed using equation [2.7] (Ruiliang *et al.*, 2003).

$$REP = a_0 + \sum_{i=1}^5 a_i \lambda^i \quad 2.7$$

Generally, the curve includes the available number of wavebands from 670 to 780 nm. This technique proved as a robust method for estimating vegetation parameters under variation of canopy structure and soil background conditions (Ruiliang *et al.*, 2003). However, it requires first derivative spectra for calculating the REP.

### 2.3.1.3.4. Lagrangian Technique

Dawson and Curran (1998) introduced a new technique to interpolate the REP which uses three point Lagrangian model on the first derivative spectral reflectance. In this technique, the model applies second-order polynomial curve to the three band first derivative spectrum (Ruiliang *et al.*, 2003). After that, to determine the maximum slope position, a second derivative is performed on Lagrangian equation [2.8] (Dawson & Curran, 1998):

$$REP = \frac{A(\lambda_i + \lambda_{i+1}) + B(\lambda_{i-1} + \lambda_{i+1}) + C(\lambda_{i-1} + \lambda_i)}{2(A + B + C)} \quad 2.8$$

Where

$$A = \frac{D\lambda_{(i-1)}}{(\lambda_{i-1} - \lambda_i)(\lambda_{i-1} - \lambda_{i+1})}$$

$$B = \frac{D\lambda_{(i)}}{(\lambda_i - \lambda_{i-1})(\lambda_i - \lambda_{i+1})}$$

$$C = \frac{D\lambda_{(i+1)}}{(\lambda_{i+1} - \lambda_{i-1})(\lambda_{i+1} - \lambda_i)}$$

In the above equation,  $\lambda_{(i)}$  represents the wavelength position at maximum first derivative and  $\lambda_{(i-1)}$  and  $\lambda_{(i+1)}$  are the positions either side of the  $\lambda_{(i)}$  position;  $D\lambda_{(i-1)}$ ,  $D\lambda_{(i)}$  and  $D\lambda_{(i+1)}$  are the first derivative values with their corresponding wavelength positions.

### 2.3.1.3.5. Inverted Gaussian (IG) fitting technique

This technique uses inverted-Gaussian (IG) function to fit with the reflectance curve at the REP (670-780 nm). According to Miller *et al.* (1990), the IG model is represented by the following equation [2.9].

$$R(\lambda) = R_s - (R_s - R_0) \exp\left(\frac{-(\lambda_0 - \lambda)^2}{2\sigma^2}\right) \quad 2.9$$

Where  $R_s$  and  $R_0$  is the maximum and minimum spectral reflectance, respectively;  $\lambda_0$  is the position of the minimum spectral reflectance;  $\lambda$  is wavelength;  $\sigma$  is the Gaussian function variance, then the REP is calculated using the following equation [2.10] (Cho & Skidmore, 2006).

$$REP = \lambda_0 + \sigma \quad 2.10$$

To determine the parameters of the IG model, two approaches are available: iterative optimization fitting procedure and linearized fitting approach (Bonham-Carter, 1988). For determining the land cover classification based on canopy pigment at the BOREal Ecosystem-Atmosphere Study (BOREAS), Zarco-Tejada *et al.* (1999) applied IG model approach to the CASI and showed the classification accuracy exceeded 68% for all classes.

#### 2.3.1.4. Artificial intelligence (AI)

With the advancement of computational power and resources new approaches such as artificial intelligence have been developed for making intelligent decisions in data analysis. Although there is a potential scope for studying the complicated environment using AI, computationally expensive and difficult in understanding (Lary, 2010). Depend on the study environment, AI rooted into various subfields. Machine learning, broad subfield of artificial intelligence, is concerned with the design and development of algorithms and techniques that allow computers to learn automatically extracting the information from data (Lary, 2010). In remote sensing, machine learning is promising technique in regression and classification studies. Generally, two type's machine learning algorithms are used in remote sensing: artificial neural networks (ANN) and support vector machines (SVM).

##### 2.3.1.4.1. Artificial Neural Networks

ANN is a computational model or architecture which consists of numerous interconnected network of simple processing elements, artificial neurons, to process the remote sensing data (Kimes *et al.*, 1998). The basic element of ANN is the neuron or node.

The advantages of ANN in remote sensing studies are illustrated (Jungho Im, 2008; Kimes *et al.*, 1998):

- Generally, the results of ANN are more accurate than the statistical methods.
- The technique is highly effective in a complex environment. For example, estimating canopy biophysical and biochemical characteristics in a forest.
- It can effectively handle the problems of non-linearity.
- We can incorporate a priori knowledge and physical constraints in the analysis.
- It can handle large amount of remote sensing data. For example: long term temporal remote sensing studies.
- This technique uses the data rather than the model in classification studies.
- It can process the data from multiple sensors which have different designs and configurations in order to produce comparable input (Brown *et al.*, 2008).

There are many types of neural networks available, feed-forward back-propagation multi-layer perceptron (MLP) type commonly used in remote sensing applications (Jungho Im, 2008). So far, this technique has been used in land cover and forest classification studies, the research in estimating pasture quality is limited. Mutanga and Skidmore (2004a) used feed-forward back-propagation multi-layer perceptron (MLP) algorithm to map nitrogen concentration in an African savanna rangeland using airborne hyperspectral sensor (HyMap). In this experiment, continuum-removed absorption features ( $R_{550-757}$ ) and ( $R_{2015-2199}$ ) and, the REP of the vegetation reflectance were used as input to the neural network algorithm.

#### **2.3.1.4.2. Support Vector Machine (SVM)**

Vapnik (2000) introduced the concept of support vector machine (SVM), it is a group of supervised learning methods that analyse the data for classification and regression problems. It can handle high dimensional data and uses fewer samples in the model development and, has generalisation capability (Wang *et al.*, 2010). The application of SVMs in remote sensing is more focused on classifications studies while little research has been done in regression studies. In classification studies, this method found improved accuracy over other classic statistical methods because it depends on margin-based “geometrical” criterion rather than a purely “statistical” criterion (Melgani & Bruzzone, 2004). Durbha *et al.* (2007) used SVR based algorithms to retrieve the LAI from green vegetation using multiangle imaging spectroradiometer (MISR) data. In this, they found good correlation between the SVR model and LAI. A study by Wang *et al.* (2010) used 15 hyperspectral bands of ASD field Spec Pro to determine LAI in paddy using three approaches (MLR, PLSR, SVM) concluded that the SVM algorithm is a better estimator than MLR and PLSR.

#### **2.3.2. Physically based approach**

Despite the success of these empirical approaches, these models suffer from a lack robustness, generalization and transferability and tend to be rather dependent on the vegetation species, study location, time, sensor and environmental conditions (Cho, 2007; Colombo *et al.*, 2003). In addition, these empirical relationships highly influenced by canopy architecture and optical properties of within and between the species. Alternatively,

physically based approaches have been developed to extract information from spectral data and it can handle some of the limitations of empirical approaches such that these models can be applied to different sites and sampling conditions. Of these physically based approaches, radiative transfer models are promising in remote sensing studies which involve the transfer and interaction between radiation and vegetation using physical principles (Jacquemoud & Baret, 1990). Inversion of these models simulates the vegetation optical properties (reflectance, scattering and absorption) as a function of their physical, water and biochemical properties. Jacquemoud and Baret (1990) developed a model, PROSPECT, based on the leaf optical properties of broad leaf species to analyse the pigment concentration, water content and leaf structure. Recently, updated version of PROSPECT, PROSPECT-4 and 5, resulted in accurate predictions of concentrations of chlorophyll and carotenoids (Feret *et al.*, 2008) and can estimate cellulose, lignin and protein. A canopy based model, SAIL (Scattering by Arbitrarily Inclined Leaves) model designed by Verhoef (1984) for describing LAI and leaf inclination distribution. LIBERTY (Leaf Incorporating Biochemistry Exhibiting Reflectance and Transmittance Yields) model was developed to quantify the biochemicals in dry and fresh pine needles (Dawson *et al.*, 1998). Jacquemoud *et al.* (1995) estimated chlorophyll  $a+b$  concentration with reasonable accuracy by combining the SAIL and LIBERTY models. However, the interpretation radiative transfer models are more complicated and difficult to understand. Furthermore, this method of analysis still in developing stage.

### 2.3.3. Integrated Approaches

It is an approach that integrates all the benefits of empirical and physically based approaches and minimises the problems to describe vegetation phenomena. Conceptually, an empirical approach develops strong relationships between the reflectance and desired vegetation variable whereas physical models minimises the problems of variations occurred in canopy architecture and optical properties of vegetation and soil background. These models effectively can determine the properties of vegetation across a wide range of species thereby very useful for the analysis of complex environments such as forest and grassland. For example, Huemmrich and Goward (1997) used a combination of NDVI and

SAIL model to examine fraction of absorbed photosynthetically active radiation in ten different forest species. Schlerf and Atzberger (2006) made an attempt to map LAI in Norway spruce stands using “Invertible Forest Reflectance Model” INFORM and three layer feedforward backpropagation neural network.

#### 2.4. Summary

This review has summarised the evidence that remote sensing tools have the potential to estimate various vegetation features. However, the research was very limited in determining the properties of pasture, although some publications (Kawamura *et al.*, 2009; Sanches, 2009) have described the possibilities of sensing tools being used to determine some of the properties of pastures. Recently, a programme called “Pastures from Space” was initiated in Western Australia in order to estimate pasture biomass or Feed On Offer (FOO) or pasture growth rate (using a model based on a combination of MODIS NDVI, soil, climate and light-use-efficiency data) both accurately and quantitatively (<http://www.pasturesfromspace.csiro.au/index.asp>) (Edirisinghe *et al.*, 2002). This information on pasture estimates (at paddock scale) was made directly available to the Western Australian sheep and cattle farmers through a web or email-based service: Fairport Technologies (<http://www.fairport.com.au/PastureWatch/>), using the name Pasture Watch™. This near real-time, temporal and spatial pasture information enables the producers to make effective farm-management decisions, such as those involving a pasture budgeting module and the adjustment of stocking rates. However, it has a few limitations, such as the developed models having limited prediction accuracy: and, only 70% variation of the estimates was explained. This has been mainly attributed to the unavailability of localised climate data and the presence of woody vegetation. Moreover, the prediction accuracy varied with the season, years and farms. As yet, similar technologies to estimate pasture quality do not exist and they are still under study.

The author is aware that the majority of these experiments were conducted under controlled environment conditions (Mutanga, 2004; Starks *et al.*, 2008) and confined to a particular location (Kawamura *et al.*, 2009; Trotter *et al.*, 2010) and therefore, it is important to

investigate the application of these technologies under uncontrolled environmental conditions. Biewer *et al.* (2009b) have suggested that the application of these techniques in different environment conditions are to be required. In addition, in the ‘real-world’ there is a large variation present in pastures due to various factors such as nutrient and water variability in the soil, animal interference resulting in dung and urine patches and topography etc., which may limit the application of these technologies. In order to address some of these shortcomings, this experiment was undertaken on commercial dairy farms to explore the practical reliability of these technologies.

In order to develop strong and explicit relations between the spectral and measured data, computation is an essential step of within this process. Section 2.3 explains the various approaches used by the researchers. Empirical approaches (section 2.3.1) have been widely used in experiments due to their flexibility and ease of adoption and ease. For example, vegetation indices (section 2.3.1.1) require a simple computation process for the interpretation of results. Flynn *et al.* (2008) used NDVI to estimate pasture biomass. Similarly, NDVI has been reported as a tool for estimating pasture growth rate in Western Australia (Donald *et al.*, 2010). Extending from vegetation indices to multivariate regression approaches (section 2.3.1.2) involve more sophisticated and complex data analysis, in addition to needs numerous wavebands information. In multivariate analysis, PLSR is an efficient tool to obtain accurate results and it is used in various experiments (Biewer *et al.*, 2009b; Kawamura *et al.*, 2009; Schut *et al.*, 2005) and, this study evaluates these empirical approaches.

Although a variety of space and air borne tools have been used in research (see list in Table 2.1 and 2.2), ground-based remote sensing tools (proximal sensors) have a wider scope in agriculture due to their real-time information, which allows the producer to make immediate decisions. Therefore, in this study, a series of proximal sensors have been involved, in order to evaluate their potential to assess the various properties of pastures. Each sensor has differential characteristics, such as spectral and spatial resolution and the availability of wave bands.



New Zealand pastures are highly variable, resulting in complex measurements of pasture characteristics. In order to address these concerns, a hyperspectral sensor will be used to determine pasture quality characteristics in mixed pastures. Hyperspectral sensors are more promising, since they have the ability to determine the number of pasture characteristics accurately, due to high spectral and spatial resolution and the availability of numerous wavebands. For example, many researchers have used hyperspectral sensors and found them to be a prominent tool, which can accurately estimate pasture quality parameters (Cho & Skidmore, 2006; Mutanga *et al.*, 2005; Sanches, 2009).

CROPSCAN is a passive sensor, which has been used in field crop studies to identify nitrogen status, since it allows for accurate provision of fertilisers, according to plant demand. However, no research has been reported on determining pasture quality characteristics and therefore, this research will be focused on the potential ability to assess the quality characteristics of pasture.

Crop Circle is an active sensor, which has been widely used in field crops. For example, Solari *et al.* (2008) used this sensor to identify nitrogen status and yield potential in maize. With the option of 'on-the-go', it enables the provision of spatial maps across the field, which provide the basic information needed to adopt precise management techniques such as the variable rate application of fertilisers. This sensor needs to be evaluated in pastures for its capability to estimate pasture characteristics.

## CHAPTER 3

# **In-field hyperspectral proximal sensing for estimating quality parameters of mixed pasture**

*This chapter based on:*

Pullanagari, R.R., Yule, I.J., Tuohy, M. P., Hedley, M. J., Dynes, R. A. and King, W. M. 2011. In-field hyperspectral proximal sensing for estimating quality parameters of mixed pasture. *Precision Agriculture* 13(3), 351-369. doi: 10.1007/s11119-011-9251-4.



### ***Abstract***

A study was conducted to explore the potential use of a hand-held (proximal) hyperspectral sensor equipped with a canopy pasture probe (CAPP) to assess a number of pasture quality parameters: crude protein, (CP), acid detergent fibre (ADF), neutral detergent fibre (NDF), ash, dietary cation-anion difference (DCAD), lignin, lipid, metabolisable energy (ME) and organic matter digestibility (OMD) during the autumn season 2009. Partial least squares regression (PLSR) was used to develop a relationship between each of these pasture quality parameters and spectral reflectance acquired in the 500 to 2400 nm range. Overall, satisfactory results were produced with high coefficients of determination ( $R^2$ ), Nash-Sutcliffe efficiency (NSE) and ratio prediction to deviation (RPD). High accuracy (low root mean square error-RMSE values) for pasture quality parameters such as CP, ADF, NDF, ash, DCAD, lignin, ME and OMD was achieved; although lipid was poorly predicted. These results suggest that *in situ* canopy reflectance can be used to predict the pasture quality in a timely fashion so as to assist farmers in their decision making.

### ***3.1. Introduction***

Grazed pasture systems support New Zealand's major export earnings from milk, meat and wool production. The meat and milk industries require high quality pastures to maintain productivity and profitability. In addition, pasture quality is a critical factor in determining animal performance, stocking rates and methane emissions (FAO, 2010). The key components of pasture quality are crude protein, fibre, minerals, ash, organic matter digestibility, sugars and metabolisable energy. Pasture quality is highly variable, and its feeding value depends to a large extent upon the species composition of the pasture, its maturity, stage of growth as well as topography and climatic factors (Holmes *et al.*, 2007).

Intensification of NZ farming systems and consumer demand for changing product specifications are contribute to an increasing need for objective measurement and control of pasture quality. The key components of feed quality estimates have typically been measured using conventional methods of wet chemistry according to the Association of

Official Analytical Chemists (AOAC, 2005). These procedures are time consuming and expensive. The need for faster and cost effective analysis options has led to the wide-spread use of laboratory-based near infrared spectroscopy (NIRS) for estimating foliar chemistry without any chemical treatments and analysis. Lab-NIRS has been widely accepted as a common method to estimate chemical components in materials such as forage (Marten *et al.*, 1983), maize (Volkers *et al.*, 2003), cereals (Stubbs *et al.*, 2009), tuber crop flowers (Lebot *et al.*, 2009), meat (Prieto *et al.*, 2006) and soil (Kusumo *et al.*, 2008). Analysing forage quality using NIRS was initiated by the United States Department of Agriculture (USDA) because it allowed more rapid processing of laboratory samples, multiple analyse with one operation and non-consumption of the sample (Marten *et al.*, 1985). However emerging demand is for ‘real-time’ analysis which overcomes the issues of spatial and temporal variability in pasture quality.

Remote sensing technologies, particularly hyperspectral remote sensing, have enabled field study of vegetation biochemical features at a canopy level and can also record spatial differences (Zarco-Tejada, 2000). This reduces the tedious process of intensive sampling and lab analysis. In the early 1990’s NASA initiated a programme called Accelerated Canopy Chemistry Programme (ACCP) (NASA, 1994). ACCP examined the relationships between spectral data acquired from High Resolution Imaging Spectrometer (HIRIS) and measured foliar chemistry. The nitrogen and lignin concentrations in forest canopy were predicted successfully using this method with  $R^2$  values of 0.87 and 0.77 respectively (Martin & Aber, 1997). Despite the successful application of remote sensing in field crops, grassland provides a more diverse set of challenges when adopting these technologies. In general, pastures have greater diversity as spatial and temporal heterogeneity result from a number of confounding factors, including: diverse species, morphology and interactions of grazing animals, the natural environmental conditions and management practices. To accomplish this task, in such a complex environment, Schellberg *et al.* (2008) has recommended use of a high resolution spectral sensor, where high spectral and spatial resolution proximal sensors could provide reasonable information with high precision. Recently portable or field spectroradiometers (hyperspectral sensors) have been developed with similar features for research studies in various industries. Research by Sanches (2009),

Mutanga *et al.* (2005) and Pullanagari *et al.* (2011b) found significant relationships between nitrogen concentration and *in situ* green vegetation. Although there were problems of water interference with biochemical concentrations (Mutanga, 2004), soil background and canopy structure, satisfactory results with high accuracy were obtained.

This paper investigates the ability of a proximal hyperspectral sensor to estimate pasture quality parameters (CP, ADF, NDF, ME, ASH, Lignin, Lipid, OMD and DCAD) on commercial NZ pastures. It can process large numbers of *in situ* samples cost effectively compared with wet chemistry, creating an opportunity to improve pasture management. Proximal hyperspectral sensors encompass spatial and temporal variations and near real time data is produced to aid effective farm decision processes to be implemented. The objective of this study was to evaluate the spectral differences related to *in situ* pasture quality, as well as developing and validating relationships between acquired reflectance data and pasture quality parameters.

### **3.2. Materials and Methods**

#### **3.2.1. Study area**

The study was conducted on four commercial farms across New Zealand, a total of 320 locations or subplots (Table 3.1) were sampled. The farms and paddocks within farms varied in: ratio of green: dead and vegetative: non-vegetative plant material, geographical location, botanical combinations of pasture, soil type, climate and livestock enterprise (dairy or sheep and beef). All pastures were based on perennial ryegrass (*Lolium perenne* L.) and white clover (*Trifolium repens* L.). A range of less dominate grasses and a small portion of weeds such as: buttercup (*Ranunculus* spp), catsear (*Hypochaeris radicata*), chickweed (*Stellaria media*), docks (*Rumex* spp), Californian thistle (*Cirsium arvense*) and yarrow (*Achillea millefolium*), were also evident.

#### **3.2.2. Spectral measurements**

Canopy spectral measurements were taken during the autumn season of 2009, on 23rd-26th March at Massey University Dairy Farm, Aorangi (sheep and beef), Palmerston North;

from 22nd-23rd April at Lincoln University Dairy Farm and from 27th to 28th May at Ruakura Dairy Farm, Hamilton (Table 3.1). The spectral measurements were acquired *in situ* using an ASD FieldSpec<sup>®</sup> Pro FR spectroradiometer (Analytical Spectral Devices Inc., Boulder, CO, USA).

**Table 3.1 The experimental site locations**

Site No.	Farm Name	Location	Latitude	Longitude	Number of samples	Number of samples considered in analysis
1	Massey University Dairy Farms	Palmerston North	-40.3785	175.6029	80	30
2	Aorangi Research Station, AgResearch	Palmerston North	-40.2523	175.5901	40	18
3	Lincoln University Dairy farm	Lincoln	-43.6399	172.4413	100	92
4	Ruakura Dairy farm, AgResearch	Hamilton	-37.7777	175.3125	100	74

The ground field of view was approximately 25° and covered a sample area of 0.25 m<sup>2</sup>. The spectral range was 350 nm to 2500 nm, with 1.4 nm resolutions in the 350-1000 nm and 2 nm in the 1000-2500 nm. This was re-sampled as 1 nm resolution spectral data (from 350-2500 nm) by using ASD, RS3<sup>™</sup> software. To ensure consistent illumination, the canopy pasture probe (CAPP)-top grip, developed by (Sanches, 2009), was used. This consisted of an inverted black bin coupled with a 50 Watt tungsten-quartz-halogen bulb as the light source. The CAPP-top grip allowed acquisition of consistent reflectance spectra using an artificial light source under variable natural lighting (e.g. cloudy) and weather (e.g. windy) conditions. At each sub-plot, ten spectral measurements were acquired and subsequently averaged, using ViewSpec Pro<sup>®</sup> software, to a single reflectance spectrum.

A total of 214 spectral measurements (Table 3.1) were included in the data analysis. Samples were excluded due to soil contamination the sample submitted for NIR analysis and missing samples. The radiance was converted into reflectance so as to optimise the reflectance by using scans from a reference panel. In this case, a matt white ceramic tile

was used as a reference which has been proven as a reasonable and reliable reflectance standard (Sanches *et al.*, 2009). Figure 3.1 illustrates the population mean reflectance (Fig. 3.1a), and first derivative mean reflectance of 214 pasture measurements at wavebands ranging from 500-2400 nm, (Fig. 3.1b). The first derivative reflectance illustrates most of the variation is in the visible to near infrared with wavelengths of 550-1000 nm followed by 1460-1800 nm and 2000-2300 nm. This indicates the importance of the visible-near infrared region for the study of green vegetation, and is consistent with previous research (Biewer *et al.*, 2009a).

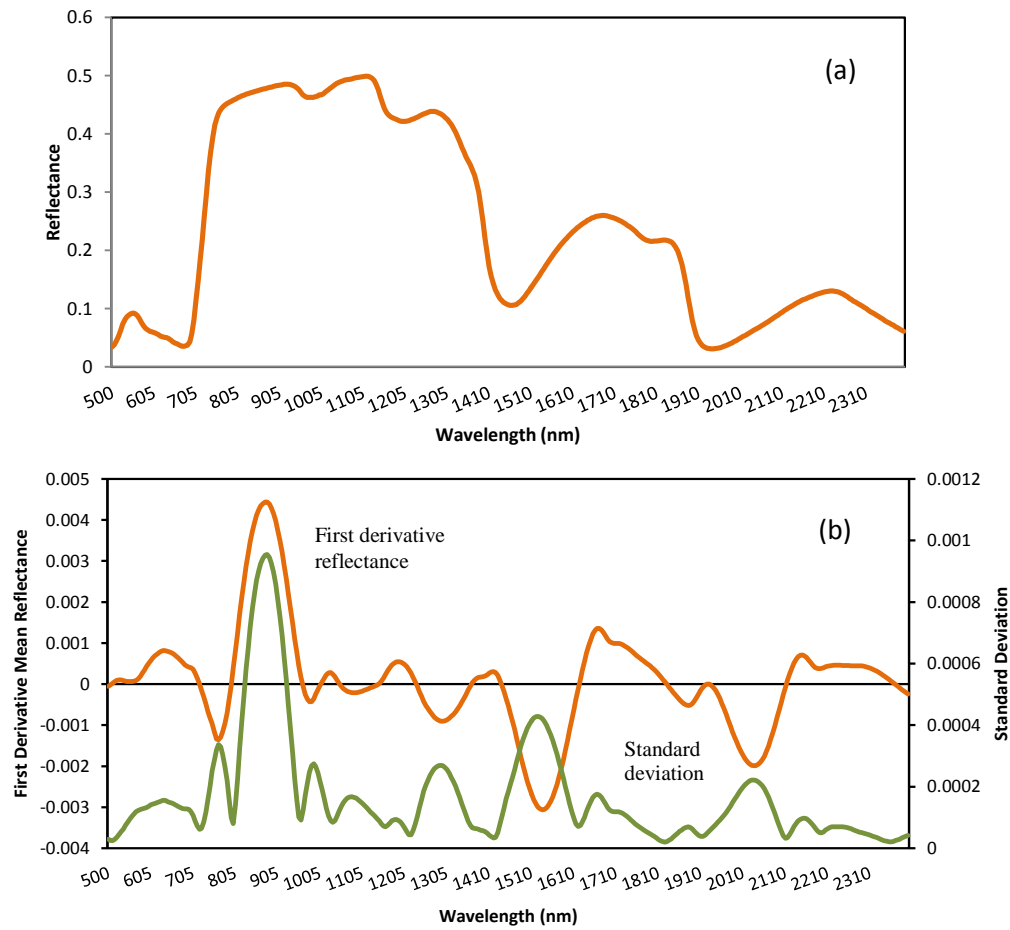


**Figure 3.1 (a) Mean reflectance (b) Mean and standard deviation of first derivative reflectance of acquired pasture samples ( $n=214$ )**

### 3.2.3. Sampling

Subplots in each paddock were selected randomly. At each subplot, a wooden framed quadrant with inside edge dimensions of  $0.5 \times 0.5$  m, was positioned on the pasture so as to



obtain spectral signatures. At each site, after spectral measurements, the herbage samples were cut to ground level with an electric shearing hand piece. The dominant species and ancillary data (e.g. weeds and treading damage) were visually assessed and recorded separately.

#### **3.2.4. Chemical Analysis**

The clipped pasture samples were collected in polythene plastic bags and transported to a laboratory immediately for processing. The samples were oven-dried at 60°C for 24 hours and ground to pass a 1 mm sieve. The crude protein (CP) acid detergent fibre (ADF), neutral detergent fibre (NDF), ash, dietary cation-anion difference (DCAD), lignin, lipid, metabolisable energy (ME) and organic matter digestibility (OMD) contents were estimated using near-infrared reflectance spectroscopy - NIRS at FeedTECH (Corson *et al.*, 1999) laboratory based at AgResearch in Palmerston North, New Zealand.

#### **3.2.5. Data processing and statistical analysis**

##### **3.2.5.1. Data manipulations**

The objective of the research was to build relationships between acquired spectral signatures and pasture quality parameters which are important for livestock management.

The spectral data were manipulated to remove spectral abnormalities which occur randomly across the spectrum and to improve absorption features. These abnormalities might be due to internal (detectors and electronic circuits and baseline fluctuations) (Ozaki *et al.*, 2005) and external factors (light leak and humidity). ViewSpec Pro<sup>®</sup> (ASD Inc.) programme was used to process the raw spectra and eliminated unusual spectra (other than typical green vegetation spectrum) which might reduce the calibration accuracy. In acquired reflectance, spectral data were removed at the two edges of spectra, 350-500 nm and 2400-2500 nm, due to natural light leak into the CAPP. The collected contiguous hyperspectral data (1900/1 nm wavebands) were reduced to 380/5 nm wavebands using Microsoft Visual Basic<sup>®</sup> software. Data transformation, pre-processing and pre-treatment were followed (Viscarra Rossel, 2008) to enhance spectral properties. Initially, transformation, converting spectral data in R units to log (1/R) units, was used to reduce non-linearity. The Savitzky–Golay filter (Savitzky & Golay, 1964), a pre-processing smoothing procedure, was then

used to improve signal-to-noise ratio. The Savitzky–Golay filter had a window size of 30 and polynomial order of 4. The next step of the pre-processing procedure was to compute the first derivative (Tsai & Philpot, 1998) of reflectance differentiation to enhance the absorption spectral features and to minimise background noise. The first derivative (FD) transformation of the reflectance spectrum calculated the slope values from the reflectance which can be derived from the following equation [3.1] (Mutanga *et al.*, 2005):

$$R'_{\lambda(i)} = \frac{(R_{\lambda(j+1)} - R_{\lambda(j)})}{\Delta_{\lambda}} \quad 3.1$$

Where  $R'_{\lambda(i)}$  is the first derivative reflectance at a wavelength  $i$  midpoint between wavebands  $j$  and  $j+1$ .  $R_{\lambda(j+1)}$  is the reflectance at the  $j+1$  waveband,  $R_{\lambda(j)}$  is the reflectance at the  $j$  waveband and  $\Delta_{\lambda}$  is the difference in wavelengths, between  $j$  and  $j+1$ . As a final step of data manipulation, mean centering of pre-treatment was assigned which may minimise multicollinearity (one variable correlated with other variables) (Aiken & West, 1991). It also increased precision and stability of estimates by reducing the standard error and producing least squares of estimates.

### 3.2.5.2. Data Analysis

After data manipulation, multivariate statistics were used by adopting the PARLES software, developed by Viscarra Rossel, (2008), to develop relationships between processed spectral data and measured variables of interest. Among multivariate statistics, partial least squares regression (PLSR) is a prominent modelling method which effectively deals with numerous, multicollinear variables and also when the numbers of explanatory (number of wavelengths) variables are greater than the number of observations (Wold *et al.*, 2001). Before the application of PLSR, principal component analysis was adopted to identify the spectral outliers but in this case none were found.

The calibration model was developed using the PLS technique, then the regression model was developed to predict the unknown quality estimates known as validation or test set. The regression model [3.2] was represented by (Kawamura *et al.*, 2008):

$$Y = \beta X + \varepsilon \quad 3.2$$

Where  $Y$  was the dependent variable (pasture parameters),  $X$  was the independent variable (spectral reflectance),  $\beta$  was the coefficient, and  $\varepsilon$  was the residual. The calibration model was built with the minimum number of components required to minimise the RMSE full cross-validation (leave-one-out method). This predicts each sample, with a PLSR model constructed using the remaining samples ( $n-1$ ) and is a method of estimating the accuracy of the calibration model internally (Kusumo *et al.*, 2009a). The validation errors were then combined into statistical measurements to test the performance of the calibration model. For external validation, the total dataset (214) was divided into 1:1 ratio as calibration (107) and validation (107) sets. The calibration model was used to predict the unknown samples or validation set, thereby estimating the practical accuracy of the developed model. The whole dataset was divided by ranking the samples from smallest to largest. Even and odd number samples were recognised as calibration and validation sets respectively.

### 3.2.6. *Quantifying Model Accuracy*

The accuracy of the calibration and validation models was evaluated by statistical measurements;  $R^2$  (coefficient of determination), RMSE (root mean square error), RMSE% (root mean square error percentage), bias, RPD (ratio prediction to deviation) and Nash-Sutcliffe efficiency (NSE). In general,  $R^2$  indicates the degree of collinearity between predicted and measured data and describes the percentage of variation of the  $X$  variable in the  $Y$  variable. Although  $R^2$  has been widely used for model evaluation, this statistic is oversensitive to outliers and insensitive to additive and proportional differences between model predictions and measured data (Legates & McCabe, 1999).

The difference of standard deviation between the measured and the predicted values of functional properties of pasture was measured as RMSE (root mean square error). The RMSECV and RMSEP, RMSE measure of cross-validated calibration and validation sets respectively, were calculated according to Eq [3.3]. The RMSE is an absolute measure of fit whereas  $R^2$  is a relative measure of fit. Lower values of RMSE indicated a better fit.

RMSE is a measure of how accurately the model predicts the response, and is the most important criterion for fit if the main purpose of the model is prediction.

$$RMSE = \sqrt{\frac{\sum_{i=1}^n (\hat{y} - y)^2}{n}} \quad 3.3$$

Where  $\hat{y}$  indicates predicted value and  $y$  was the measured laboratory value,  $\bar{y}$  was the mean of measured values and  $n$  was the number of samples. Although, RMSE is more sensitive to outliers and therefore, RMSE% was also calculated using Eq [3.4].

$$RMSE \% = 100 \frac{RMSE}{\bar{y}} \quad 3.4$$

The bias, mean difference between the reference data and NIRS-predicted data indicated the systematic error in the model and was computed according to Eq [3.5].

$$Bias = \frac{1}{n} \sum_{i=1}^n (\hat{y} - y) \quad 3.5$$

The RPD is the ratio of the standard deviation of laboratory values of pasture characteristics to the RMSE. This calculation was made to show how much more accurate (measured by the standard error) a prediction from the model was, than simply quoting the overall mean (Kusumo *et al.*, 2008). The RPD values were calculated from Eq [3.6].

$$RPD = \frac{SD(y)}{\sqrt{\frac{\sum_{i=1}^n (\hat{y} - y)^2}{n}}} \quad 3.6$$

In addition, the Nash-Sutcliffe efficiency (NSE) statistic also called the model efficiency was used to examine the relative magnitude of the residues compared to the variance in measured data and was calculated from Eq [3.7] (Nash & Sutcliffe, 1970). The values of

NSE ranged between  $-\alpha$  to 1.0. The acceptable NSE values were from 0 to 1, whereas the negative values ( $< 0$ ) were deemed unacceptable which indicated poor model performance (Moriasi *et al.*, 2007) and (Miehle *et al.*, 2006). However, it is strongly sensitive to the variation within the data (Schut *et al.*, 2006).

$$NSE = 1 - \left( \frac{\sum_{i=1}^n (\hat{y} - y)^2}{\sum_{i=1}^n (y - \bar{y})^2} \right) \quad 3.7$$

Accurate and precise prediction was shown by high  $R^2$ , NSE and RPD, and low RMSE and RMSE %.

After PLSR modelling, the magnitude of each waveband (x) in modelling of y computed using PLS-regression weighted coefficients and represented by variable importance for the projection (VIP) (Wold *et al.*, 2001) and calculated by Eq [3.8]. A larger score indicates the waveband had greater importance in building a model that predicts y, while the waveband having a lower score ( $< 1$ ) had less importance in developing a model.

$$VIP_k(a) = K \sum_a w_{ak}^2 \left( \frac{SSY_a}{SSY_t} \right) \quad 3.8$$

The Eq [8], where  $VIP_k(a)$  is the importance of the  $k^{th}$  predictor (wavelength) variable based on a model with  $a$  factors (PLS-components),  $w_{ak}$  represents PLS-weights of  $k^{th}$  variable in a  $a^{th}$  PLS-factor,  $SSY_a$  is the explained sum of squares of  $Y$  by a PLSR model with  $a$  factors,  $SSY_t$  is the total sum of squares of  $Y$  explained in all  $a$  factors of a PLS model.

### 3.3. Results

#### 3.3.1. Summary statistics of NIRS data

The dataset ( $n=214$ ) comprised of 107 assays for the calibration set and 107 assays for the validation set. The descriptive statistics of pasture quality estimates were analysed by bench-top laboratory NIRS with respective calibration set and validation sets and are presented in Table 3.2.

**Table 3.2 Descriptive statistics of the pasture quality parameters of calibration ( $n=107$ ) and validation sets ( $n=107$ ) measured by NIRS**

Pasture quality parameters	Calibration set (n = 107)					Validation set (n = 107)				
	Mean	Minimum	Maximum	SD	CV (%)	Mean	Minimum	Maximum	SD	CV (%)
CP	20.49	8.08	28.21	4.88	23.82	20.58	9.38	28.41	4.83	23.49
ADF	26.18	19.40	37.31	4.91	18.78	26.27	19.99	38.19	4.96	18.91
NDF	43.95	28.29	67.32	9.16	20.85	44.14	28.66	67.32	9.19	20.84
Ash	10.59	7.35	13.40	1.32	12.49	10.58	7.30	13.58	1.35	12.75
DCAD	632.7	305.30	872.30	123.22	19.48	635.5	311.40	874.40	121.9	19.18
Lignin	2.65	1.30	5.10	0.81	30.61	2.66	1.31	5.14	0.82	30.78
Lipid	2.73	0.97	4.24	0.76	27.98	2.71	0.44	4.18	0.78	28.78
ME	11.24	8.39	12.78	1.16	10.34	11.26	8.51	13.16	1.15	10.26
OMD	77.82	48.77	89.91	10.07	12.94	78.06	53.64	92.23	9.84	12.61

**Note:** CP crude protein (% DM), ADF acid detergent fibre(% DM), NDF neutral detergent fibre(% DM), DCAD, dietary cation-anion difference ( $\text{mEq kg}^{-1}$  DM), ME metabolisable energy( $\text{MJ kg}^{-1}$  DM), OMD organic matter digestibility(% DM), SD standard deviation, CV coefficient of variation.

In this experiment a wide range of pasture quality estimates were found. The variation was mainly due to biotic (botanical composition and weeds) and abiotic (slope, soil, altitude and climate) factors (Mutanga & Skidmore, 2003) and also samples acquired from different locations and different growth stages. To build a robust calibration model Marten *et al.* (1985) recommended a wide range of datasets.

To summarise the descriptive statistics illustrated in Table 3.2, the lignin had the widest variation expressed as a CV(%) with a range of values from 1.30 to 5.14 % followed by lipid (0.97- 4.24 % DM), crude protein (8.08- 28.41 % DM), neutral detergent fibre (28.29 – 67.32 % DM), DCAD (305.30 – 874.40 mEq kg-1 DM), acid detergent fibre (19.40 – 38.19 % DM), OMD (48.77 – 92.23 % DM) ash (7.30 – 13.58 % DM) and ME (8.39 – 13.16 MJ kg-1 DM) in calibration and validation sets. Overall, lignin had the greatest CV of 30.61 and 30.78 %. While, ME had a low CV (10.34 and 10.26 % in the calibration and validation datasets respectively).

**Table 3.3 Intercorrelation coefficients of measured pasture quality parameters**

Pasture quality Parameters	CP	ADF	NDF	Ash	DCAD	Lignin	Lipid	ME	OMD
CP	1.000								
ADF	-0.838**	1.00							
NDF	-0.804**	0.941**	1.00						
Ash	0.731**	-0.439*	-0.414	1.00					
DCAD	0.809**	-0.767**	-0.776**	0.549**	1.00				
Lignin	-0.749**	0.745**	0.743**	-0.442**	-0.742**	1.00			
Lipid	0.617**	-0.731**	-0.683**	0.396**	0.659**	-0.614**	1.00		
ME	0.877**	-0.912**	-0.855**	0.606**	0.820**	-0.786**	0.667**	1.00	
OMD	0.880**	-0.940**	-0.878**	0.603**	0.830**	-0.778**	0.690**	0.984**	1.00

\*\* Significant:  $p < 0.001$

\* Significant:  $p < 0.05$

### 3.3.2. Correlation among the pasture quality parameters

A strong linear intercorrelation existed, listed in Table 3, between various measured quality parameters. The majority of the parameters have intercorrelation at a significance level of  $p < 0.001$ . The CP had shown a strong positive correlation ( $R^2$ ), significance at level of  $p < 0.001$ , with ash (0.73), DCAD (0.81), lipid (0.62), ME (0.88), OMD (0.88) while having a strong negative correlation ( $p < 0.001$ ) with ADF (-0.84), NDF (-0.80) and lignin (-0.75). ADF had shown significant correlation with all pasture quality parameters with a range of  $R^2$  (-0.94 to 0.94) values. Similarly, NDF had significant correlation with all quality constituents except ash. Ash had stronger correlation with CP ( $R^2$  0.73) while other components correlated with moderate  $R^2$  values. Lignin and lipid had significant correlations with all quality parameters except with ash.

### 3.3.3. Principal component analysis

After mathematical transformations of the reflectance spectra, a principal component analysis (PCA) was conducted to visualise the spectral variance and detect any influence of each object's spectral data within the whole dataset (Esbensen *et al.*, 2009).

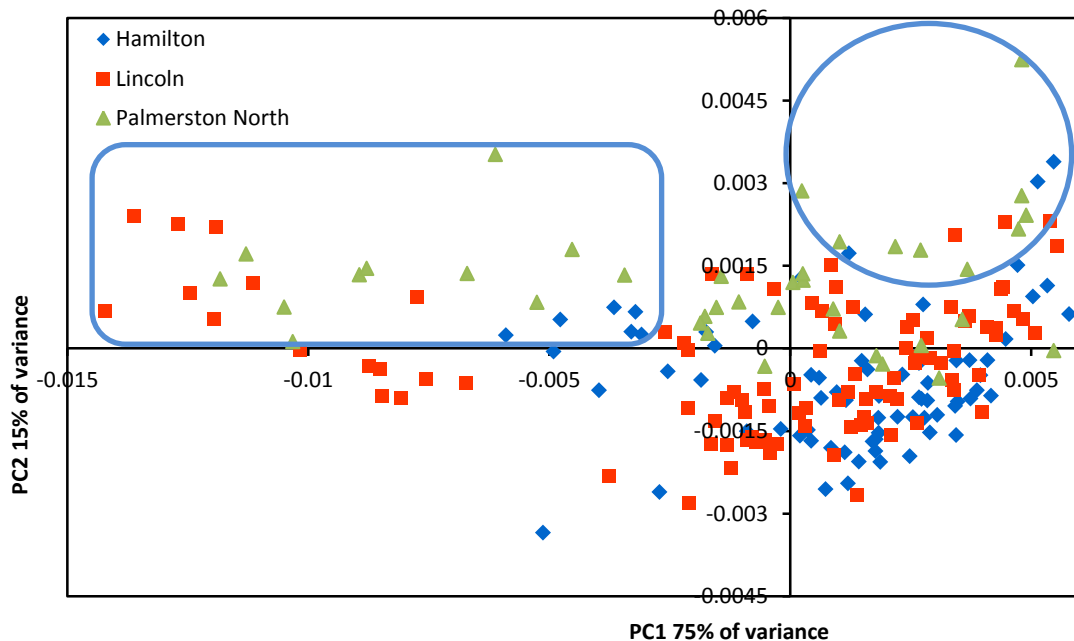


**Figure 3.2** Score plot of first and second principal components from the PCA of reflectance spectra



In the process of PCA decomposition, the available spectral data were transformed into non-linear principal components or latent variables. This described the majority of variation present in the spectra. Furthermore, the score plot spectral distinctions were useful for identifying outliers and to discriminate the spectral differences as clusters which were used for model development. The resulting biplot (Figure 3.2) illustrated 90 % of variance in total spectra: PC1 (principal component 1) accounts for 75% and PC2 (principal component 2) accounts for 15% of the variance. Geographical location had little impact on spectral variation. The location-specific spectral discrimination was not strong, therefore the score values of four quadrants in the score plot (Figure 3.2) were evaluated with recorded ancillary data and visual images.

#### **3.3.4. PLSR models for calibration and validation datasets**

From the calibration and validation datasets the quality estimates of CP, ADF, NDF, ash, DCAD, lignin, ME and OMD were significantly predicted using the spectral data (Table 3.4). The results of the prediction models and regression equations were described in Table 4. High levels of coefficient of determination ( $R^2$ ) values ranging from 0.71-0.83 were accompanied by low RMSE values, indicating high accuracy. From this, it can be deduced that the performance of the PLSR models were consistent among the calibration and validation datasets with a slight variation of  $R^2$  values (0 to 5.2%) and RMSE values (0-13%). Although  $R^2$  is a commonly used calibration statistic, it is not the best measure of the merit of a calibration model because it depends on range of dataset (Davies & Fearn, 2006). To offset this problem, RPD was calculated for the above parameters and found to range in value between 1.88 to 2.46. Under laboratory conditions, the desired level of prediction accuracy is:  $R^2 > 0.8$  and  $RPD > 2$  (Kusumo *et al.*, 2009a). For field measurements, however, lower RPD values are acceptable according to Biewer *et al.* (2009b). The NSE values for the above pasture quality parameters ranged between 0.63 to 0.83, which indicated competent performance of the models. In contrast, the remaining quality parameter, lipid was not predicted well by the spectra with results of low  $R^2$  values: 0.52, and 0.18 respectively. Although lipid had a wider range (CV, 24 - 28%) in the dataset, the precision and accuracy were low.

### 3.3.5. Important wavebands explaining the variance of pasture quality components

The contribution of each waveband can be visualised by computing the variable importance in projection (VIP), which was illustrated in Figure 3.3. As expected, the majority of the important first derivative reflectance wavebands with high VIP scores occurred in the visible region (500-750 nm) (Figure 3.3). This was attributed to absorbance of visible radiance by green vegetation. In addition to this, the near infrared region (800-1000 nm) and shortwave infrared region from 1900-2400 nm had shown importance in corresponding to each pasture quality parameter.

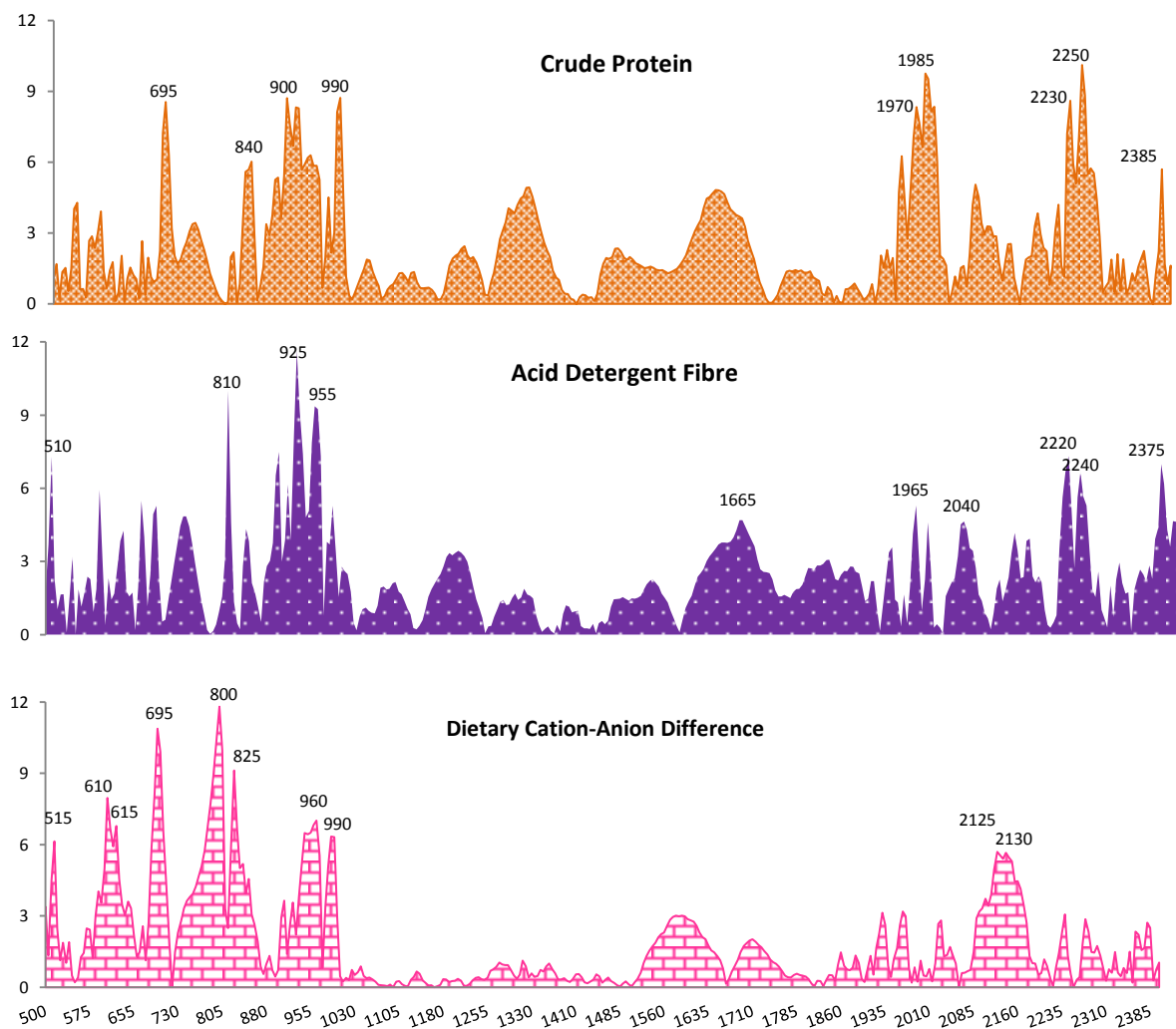


**Figure 3.3** Variable importance in projection (VIP) plot showing the importance of each waveband in developing a model of pasture quality attributes across the electromagnetic spectrum; X-axis represents wavelength (nm) and Y-axis represents VIP-scores.

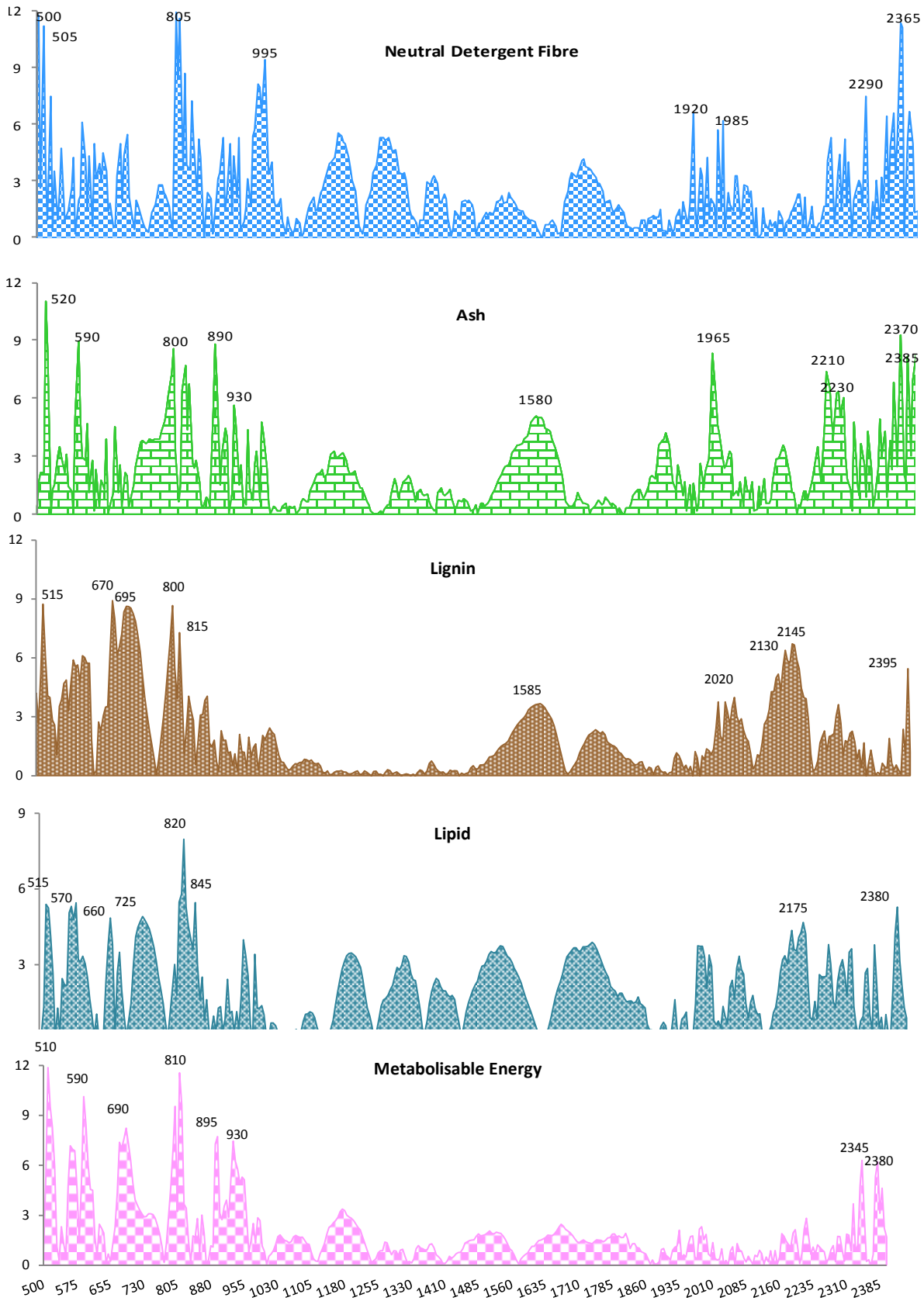


Figure 3.3 Continued

**Table 3.4 PLSR results between first derivative reflectance and pasture quality concentrations for cross-validated calibration and validation datasets**

Pasture quality parameters	Cross-validated calibration set							Validation set					
	R <sup>2</sup>	RMSECV	RMSECV%	Bias	RPD	NSE	Regression equations	R <sup>2</sup>	RMSEP	RMSEP%	Bias	RPD	NSE
CP	0.82	2.08	10.10	0.07	2.34	0.81	$y = 0.849x + 3.18$	0.78	2.33	11.32	-0.12	2.04	0.75
ADF	0.81	2.13	8.163	-0.02	2.28	0.80	$y = 0.841x + 4.12$	0.82	2.23	8.54	0.52	2.11	0.77
NDF	0.77	4.22	9.703	-0.07	2.08	0.76	$y = 0.755x + 10.7$	0.75	4.63	10.56	-0.15	1.95	0.72
Ash	0.65	0.74	6.931	0.00	1.68	0.63	$y = 0.725x + 2.94$	0.65	0.74	6.95	0.01	1.70	0.64
DCAD	0.77	55.92	8.891	0.31	2.10	0.77	$y = 0.814x + 117$	0.73	63.58	9.85	0.38	1.90	0.72
Lignin	0.71	0.41	15.60	0.00	1.87	0.71	$y = 0.739x + 0.695$	0.71	0.42	16.31	0.06	1.84	0.69
Lipid	0.56	0.47	16.82	0.01	1.51	0.55	$y = 0.604x + 1.11$	0.55	0.48	17.08	-0.01	1.44	0.50
ME	0.83	0.46	4.082	0.01	2.46	0.83	$y = 0.859x + 1.59$	0.83	0.46	4.074	-0.05	2.48	0.83
OMD	0.83	4.13	5.30	0.01	2.43	0.83	$y = 0.869x + 10.3$	0.83	4.02	5.14	0.22	2.46	0.83

CP crude protein, ADF acid detergent fibre, NDF neutral detergent fibre, DCAD, dietary cation-anion difference, ME metabolisable energy, OMD organic matter digestibility, R2 coefficient of determination, RMSECV root mean square error of cross validation, RMSECV% root mean square error of cross validation percentage, RMSEP root mean square error of prediction, RMSEP% root mean square error of prediction percentage, RPD ratio prediction to deviation, NSE nash-sutcliffe efficiency,  $y$  = measured parameter,  $x$  = predicted parameter using reflectance.

### 3.4. Discussion

The majority of forage quality prediction experiments using hyperspectral sensors, so far, are confined to reasonably well controlled experimental sites and have produced satisfactory results (Albayrak, 2008; Beeri *et al.*, 2007; Mutanga *et al.*, 2005). In order to evaluate the practical application of these sensors and to develop suitable methodologies for the analysis of data, this study was conducted under commercial field conditions. Using single wavebands or broad band indices to explain the variation in foliar chemistry is limited (Zhao *et al.*, 2005). Single band values are not directly related to any plant chemical constituent due to overlapping of chemical absorption features. Therefore, the use of contiguous spectral wavebands, with a full-spectrum approach, was investigated to determine if the relationships between reflectance measurements and *in situ* pasture quality could be improved. The models were developed using acquired and processed spectral data using 380 wavebands with 5 nm resolution and data produced from lab-NIRS measurement of pasture quality. Although many mathematical transformations are available to develop a best functional relationship between measured pasture quality parameters and *in situ* reflectance measurements, the first derivative (FD) of Log (1/R) was found to be useful in prediction with an improved statistical accuracy compared to reflectance alone. This study has shown that using PLSR analysis resulted in predictive models with high  $R^2$ , RPD and NSE, and lower RMSE and RMSE % values. Biewer *et al.* (2009b) stressed the importance of using full spectral data using a modified partial least squares regression (MPLSR) algorithm for estimating quality parameters of CP, ME, ash and ADF in highly variable mixed swards with high  $R^2$  and RPD values rather than two-wavebands ratios (low  $R^2$  values). A similar pattern was also observed with the results of Mutanga *et al.* (2005). Zhao *et al.* (2007b) also reported the significant performance, with improved  $R^2$  values, of PLSR models used to predict forage quality parameters, compared with simple reflectance ratio and multiple regression (MAXR) with 10-waveband models.

Principal component analysis (PCA) showed the reasons for major spectral discrimination in the score plot may be due to the presence of dead material (highlighted by the rectangle, Figure 3.2), variance in botanical composition and pasture colour (highlighted by the circle,

Figure 3.2). On the top-left corner of the score plot, the samples in the marked region contained some dead material, and the top-right quarter of the score plot samples had light green coloured pasture. These observations were consistent with Sanches (2009). In addition, Biewer *et al.* (2009b) has highlighted the spectral reflectance values obtained from dried grass swards and regarded these as outliers to improve the model accuracy. Principal component regression (PCR) was applied to investigate the predictive ability of pasture quality parameters, but weaker relationships were obtained, with  $R^2$  values of 0.15 - 0.45 (data not shown). However, PCA is useful for recognising major sources of variance (fraction of green and dead vegetation) rather than small variances (chemical concentrations) in the vegetation spectral data. This implied that the majority of spectral variance might be influenced by confounding factors such as canopy structure, chemical interactions with other factors, soil background and botanical composition. To offset this problem, PLSR analysis was performed where the spectral PLS-components were more strongly directed towards parameters of interest by providing these parameters with extra weight (Esbensen *et al.*, 2009).

In this study, the pasture quality estimates of CP, ADF, NDF, ash, DCAD, lignin, ME and OMD were predicted with high accuracy, a wide range of chemical constituents of pastures samples caused by natural heterogeneity in permanent pastures (Schellberg *et al.*, 2008) may support improved accuracy. Added to this, fertiliser application rates, varieties and measurement times also contributed to create a large variance (Nguyen *et al.*, 2006). For developing a best fit model a wide range of data within the dataset is essential (Williams & Norris, 1987). However, lipid was not predicted well, which might be due to the lower fraction present in the sample. Despite satisfactory results in prediction of biochemical concentrations in green vegetation there is no consistency of statistical accuracy in various experimental studies (Kawamura *et al.*, 2008; Mutanga *et al.*, 2005; Schut *et al.*, 2006). It could possibly depend on the range of samples used in datasets and the influence of confounding factors (biotic and abiotic). Moreover, there was high level of intercorrelation (Table 3.3) between quality parameters, which will assist with more precise predictions. However, there are still opportunities to improve the accuracy of models which might be influenced by various interference factors such as: different botanical and floristic

composition, weeds (Schut *et al.*, 2006), growth stages, soil background effects (Kokaly, 2001) and canopy structure.

Developing calibration equations using the data estimated by laboratory-NIRS has some limitations since there were significant errors associated with prediction and in addition to this, standard error (SE) varies with each chemical compound. For example, the SE of CP of hay was higher than ADF, might be due to an absence of precise methods to analyse detergent fibres rather than CP (Marten *et al.*, 1985). In addition, Biewer *et al.* (2009b) has explained the relative importance of using wet chemistry values as a reference for reducing the prediction errors as seen in NIRS analysed samples. Considering this statement, this study has used laboratory-NIRS to predict chemical composition of dried samples of each sward. Therefore the accuracy of the measurements might be slightly lower compared to standard procedure (wet chemistry). This suggests that the wet chemistry might improve the model accuracy.

The predictive contribution of each waveband can be visualised by computing the VIP, an output of PARLES (Viscarra Rossel, 2008) and shown in Figure 3.3. However, as expected, the majority of the important first derivative reflectance wavebands occurred in the visible region (400-750 nm), near infrared region (800-950 nm) and in the shortwave infrared region (1950-2350 nm). This can be attributed to absorbance of visible radiance by chlorophyll, which is abundant in green vegetation. Past studies have shown that there was a strong relationship between chlorophyll concentration and nitrogen content in plants due to the presence of N-H bonds (Curran, 1989). The leaf organic materials such as: lignin, protein, starch, cellulose, hemicellulose and sugar have common fundamental molecular bonds such as O-H and C-H. The vibrational and bond stretching absorbance's associated with these bonds lie across the spectral region of shortwave infrared from 1.720  $\mu\text{m}$  to 2.350 $\mu\text{m}$  (Kokaly & Clark, 1999). The wavelength at 2.078  $\mu\text{m}$  is responsible for O-H stretch/O-H deformation bond, which are the prominent bonds in starch or sugar (Curran, 1989) and water. Absorptions around 1960 nm, 1980 nm, 2100 nm 2240 nm and 2340 nm are responsible for O-H, N-H, O=H and O-H combinations, C-H (aromatic), C-H and O-H

combination bonds respectively (Curran, 1989) which are the common bonds in pasture quality parameters.

Protein is the major nitrogen containing biochemical component in plants. For CP, the peaks with higher VIP values surrounded the wavebands from 695- 990 nm, and from 1950-2400 nm. Absorption in the spectral region from 2100-2200 nm has also been attributed to N-H bonds in proteins (Martin & Aber, 1997). The absorptions at 2.054  $\mu\text{m}$  and 2.172  $\mu\text{m}$  is directly related to the presence of C-N and N-H bonds in proteins (Kokaly, 2001). This implies that the visible and near infrared wavebands are reliable when estimating biochemical concentrations in pasture.

Accurate and real-time estimation of pasture quality enables farmers to adopt precise management practices. Such practices include fertiliser application which can be applied in response to pasture quality status thereby, fertiliser use has been optimised. Moreover, field or spatial variability maps can be obtained when the sensor integrated with global positioning system (GPS) which allow for the identification chronically poor and high productive areas. These variability maps allow farm managers to maintain pasture evenly across the field using site-specific practices. Murray and Yule (2007) clearly indicated the economic benefit and increased fertiliser use efficiency by adopting the variable rate application technology as site-specific practice.

Regular monitoring of forage nutrient status provides an opportunity to schedule rotations in an efficient way in order to meet the requirements of stock while maintaining threshold levels in the field, thereby supplements can be provided when there is an inadequate level of nutrient from pasture. Based on the information of available nutrients at the paddock level, stocking rate would be allocated as to meet animal needs. Finally, the successful adoption of precise management practices on grasslands leads to economic and environmental benefits and better utilization of pastures and ensures animal health and performance.



### 3.5. Conclusion

This paper explains the potential use of in-field hyperspectral proximal sensing to estimate mixed pasture quality using a PLSR algorithm. Satisfactory results were obtained that reflect the strong relationship between spectral measurements and pasture quality parameters. The PLSR models predicted measured attributes with reasonable precision (high  $R^2$ , NSE and RPD values) and accuracy (low RMSE and RMSE % values) compared to other models.

The PLSR algorithm performed better in estimating pasture quality attributes such as CP, ADF, NDF, ash, DCAD, lignin, ME and OMD, while, the estimates of lipid was predicted with lower precision for various reasons. The information produced using in-field hyperspectral proximal sensing of pasture would help pastoral farmers and graziers to improve their productivity, on-farm performance and build business resilience, by enabling them to make more accurate and timely decisions. There are, but not limited to: manipulation of stocking rates, grazing intervals, optimising timing of grazing individual paddocks, benchmarking each paddock within their farm to optimise and tailor capital inputs of fertiliser, plan from which paddocks conserved feed is to be made, and gauge what the quality of the pasture is before harvesting. To extend the results of this study towards a practical outcome for farmers, it is recommended that further research be carried out to investigate the spectral changes in permanent pastures throughout the year and across the seasons with the view of evaluating the need for seasonal calibration of NIRS to pasture quality.

### Acknowledgement

The authors are grateful for the technical support received from: Michael Killick, Massey University, Palmerston North, New Zealand; Grant Rennie, AgResearch, Ruakura, Hamilton, New Zealand; Brian DeVantier, AgResearch Grasslands, Palmerston North, New Zealand; Staff from AgResearch, Lincoln, New Zealand and comments on the manuscript from Carolyn Hedley and Cathe Goulter.

## CHAPTER 4

# Multispectral radiometry to estimate pasture quality components

*This chapter based on:*

Pullanagari, R. R., Yule, I. J., Tuohy, M. J., Hedley, M. P., Dynes, R. A. and King, W. M. 2011. Multispectral Radiometry to Estimate Pasture Quality Components. *Precision Agriculture (Accepted)*



**Abstract**

Multi-spectral remote sensing of green vegetation provides an opportunity for assessing biophysical and biochemical properties. This technique could play a crucial role in pasture management by providing the means to evaluate pasture quality in-situ. In this study, the potential of a 16-channel multi-spectral radiometer for predicting pasture quality, crude protein (CP), acid detergent fibre (ADF), neutral detergent fibre (NDF), ash, dietary cation-anion difference (DCAD), lignin, lipid, metabolisable energy (ME) and organic matter digestibility (OMD) was evaluated. In-situ canopy spectral reflectance was acquired from mixed pastures, under commercial farm conditions in New Zealand. The multi-spectral data were evaluated by single wavelength, linear and non-linear RDVI index (renormalized difference vegetation index), and stepwise multiple linear regression (SMLR) models. The selected non-linear, exponential fit, RDVI index models described ( $0.65 \leq r^2 \leq 0.85$ ) of the variation of pasture quality components (CP, DCAD, ME and OMD), while CP, ash, DCAD, lipid, ME and OMD were estimated with moderate accuracy ( $0.60 \leq r^2 \leq 0.80$ ) by the SMLR model. The remaining pasture quality components ADF, NDF and lignin were poorly explained ( $0.40 \leq r^2 \leq 0.58$ ) by the models. This experiment concluded that the multi-spectral radiometer has potential to rapidly estimate pasture quality in the field using non-destructive sampling.

**4.1. Introduction**

Remote sensing tools have proven to be useful for monitoring changes in characteristics of vegetation and have become widely used in experimental agriculture. The application of remote sensing techniques to grazed production systems is more difficult due to the complexity of these environments. Grassland systems are highly variable in composition, structure and age and are continually changing in response to a range of drivers including grazing, pest and weed ingress, fertility and moisture status. These factors result in significant spatial and temporal variability, as compared to cropping systems. Adoption of remote sensing technologies in grassland systems remains difficult due to the presence of high levels of heterogeneity among and within fields (Schellberg *et al.*, 2008). Proximal

remote sensing tools with higher spatial and spectral resolution could overcome some of the challenges of complex pastoral environments. Pasture quality and the quantity that is eaten drive production of milk and meat in pastoral systems. Accurate, cost-effective and rapid pasture quality information would inform farm management decisions required to maximise productivity while managing environmental impacts of the system.

Simple linear regression, using individual wavelengths or vegetation indices as univariates, is a commonly used procedure to establish a functional relationship between crop reflectance and properties of interest. White *et al.*, (2000) found that pasture canopy nitrogen concentration in a dry/ground sample was predicted from a single wavelength with the highest correlation ( $r^2 = 0.77$ ). Although moderate relationships exist between single wavelengths and the desired variables, the level of these relationships are not consistent and usually not statistically significant (Starks *et al.*, 2006a). In their study, the degree of association between single broad wavelengths and quality components of Bermuda grass (*Cynodon dactylon* L.) was found to be very low. Hence, a combination of two or three wavelengths has been required for robust vegetative indices from reflectance data. Broadband vegetative indices have been used to predict variables: such as leaf area index, plant height, biomass and yield (Thenkabail *et al.*, 2000). Raun *et al.*, (2001) estimated grain yield of wheat (*Triticum aestivum* L.) using crop reflectance as normalised difference vegetative index (NDVI), a mathematical combination of red and near infrared wavelengths. In addition, NDVI has been used as a potential tool to increase wheat yield, while preventing over-application of nitrogen fertiliser (Mullen *et al.*, 2003). Donald *et al.* (2010) have demonstrated the combination of NDVI, derived from a remote sensor, Moderate Resolution Imaging Spectroradiometer (MODIS) imagery, climate and soil data and a light-use-efficiency (LUE) model to predict the plant growth rate of pasture at a paddock scale, with an average error at paddock scale of  $10.4 \text{ kg DM ha}^{-1} \text{ day}^{-1}$ .

To date, vegetative indices to predict vegetation biochemistry have been successfully utilised in mono-species (Xue *et al.*, 2004) but have been confined to specific locations (Starks *et al.*, 2006a). However, the sensitivity of vegetative indices to requirements such as sensing nitrogen for example, is confounded by many factors, such as: viewing and radiation geometry, canopy morphology, denudation of underlying soil and optical

properties of the plant (Xue *et al.*, 2004). Consequently, a variety of indices, as reported and illustrated in Yule and Pullanagari (2009) have been proposed to minimise the impact of confounding factors. For example, Trotter *et al.* (2010) have found that soil adjusted vegetation index (SAVI) has an improved correlation with green dry matter, with a root mean square error (RMSE) of 288 kg/ha, compared to NDVI which has a RMSE of 341 kg/ha in tall fescue (*Festuca arundinacea* var. Fletcher). However, the small number of wavelengths used in the vegetation indices limits the information available to describe the complexity of the sward and perhaps limits progress towards increased precision and accuracy of prediction.

A possible alternative to the univariate regression for quantifying pasture quality components is through multi-variate regression. With this method, specific wavelengths can be selected to develop a model that could improve the capability and accuracy of prediction. Among multi-spectral regression approaches, stepwise multiple linear regression (SMLR) has been widely used in near infrared spectroscopy (NIRS) protocols by selecting a greater number of wavelengths in order to explain a large proportion of the variation (Kokaly & Clark, 1999; Marten *et al.*, 1985). Grossman *et al.*, (1996) used stepwise multiple linear regression (SMLR) to select important wavelengths that correlate to leaf level biochemical properties. Mutanga *et al.* (2005) also demonstrated the use of SMLR to estimate pasture quality (nitrogen, phosphorus, potassium, calcium, magnesium and neutral detergent fibre) from canopy spectral reflectance. This was achieved, using a hyperspectral sensor and resulted in  $r^2$  values ranging from 0.32 to 0.87. Curran *et al.* (2001) successfully employed SMLR for estimating 12 foliar biochemicals from reflectance spectra. However, fewer studies have focused on estimating pasture quality using a multi-spectral radiometer. A study by Trenholm *et al.* (1999) found that turf grass quality rankings were closely associated with spectral broad-bands of 661, 813 and 935 nm, obtained from a Cropscan™ radiometer (Cropscan Inc., Rochester, MN, USA). Jiang *et al.* (2007) used a Cropscan™ multispectral radiometer to assess turf quality and leaf firing characteristics and recommended using three to five broad-band models based on multiple regression compared to indices such as NDVI1 ( $(R_{760} - R_{710}) / (R_{760} + R_{710})$ ), NDVI2 ( $(R_{950} - R_{660}) / (R_{950} + R_{660})$ ), stress index 1 ( $R_{710} / R_{760}$ ), stress index 2 ( $R_{710} - R_{810}$ ).

This paper evaluates the feasibility and reliability of using a 16 channel CropsScan™ multi-spectral radiometer to estimate pasture quality components, including CP (crude protein), ADF (acid detergent fibre), NDF (neutral detergent fibre), ME (metabolisable energy), ash, lignin, lipid, OMD (organic matter digestibility) and DCAD (dietary cation-anion difference). It also investigates different statistical approaches to process pasture canopy reflectance data for pasture quality prediction. If these tools provide accurate and real-time information, then farmers can make informed on-farm decisions relating to feed budgeting, stocking

#### 4.2. *Materials and methods*

From December 2009 to March 2010, spectral data were collected on commercial farms at three different locations in New Zealand: Taranaki, Waikato and Canterbury with geographical positions of -39.608 and 174.306; -37.936 and 175.330; -43.704 and 172.286, respectively. At each location, high performing dairy farms were selected as experimental sites. Individual farms were selected to provide differing environmental conditions, soil type and a wide range of pasture quality components. Each farm practiced rotational grazing and pastures were available at different stages of the grazing cycle giving a range of biomass and quality levels. The mixed pastures were mainly composed of perennial ryegrass (*Lolium perenne* L.) and white clover (*Trifolium repens* L.). A total of 2500 multi-spectral measurements, ten spectra from each plot, were taken from 250 plots. Then the spectral measurements (n=10) of each plot were averaged to one spectral measurement which resulted in 250 spectral measurements to represent 250 plots. Of the total spectra, only 151 spectral samples (plots) were considered in data analysis, with the remaining omitted from the analysis due to poor solar irradiance and soil contamination of samples preventing accurate NIRS analysis. After acquisition of spectra, the corresponding sward samples were harvested to ground level with hand-held clippers and returned to the laboratory for drying (70°C) and milling to < 1 mm particle size for near-infrared spectroscopy (NIRS) analysis. CP, ADF, NDF, ME, ash, lignin, lipid, OMD and DCAD were estimated using NIRS at FeedTECH (Corson *et al.*, 1999) laboratory, AgResearch in Palmerston North, New Zealand.

#### 4.2.1. Reflectance readings

Canopy spectral reflectance was measured using a hand-held Cropscan™ multi-spectral radiometer (MSR) 16R with 16 upward and downward facing interference-type band pass filters. The spectral reflectance from this radiometer included sixteen different wavelengths, each with 7-16 nm spectral width. The following filters were fitted: 460/10, 480/7, 530/8.5, 620/11, 670/10, 700/12, 740/13, 770/10, 800/11, 930/13, 970/10, 1080/15, 1200/12, 1300/12, 1580/15 and 1680/16 nm.

The radiometer was held 1m above and perpendicular to the soil surface. The MSR software enabled a data logger to be configured to capture ten consecutive measurement scans of each plot. The field-of-view of the radiometer is 28°, producing a viewing area of approximately 0.5 m diameter. Reflectance measurements were collected between 10 am and 4 pm to ensure the broadband incident radiation was within a range of 400-1200 watts m<sup>-2</sup> because the radiometer is a passive sensor requiring adequate natural light to measure incident irradiance. The intensity of incident radiation was measured by one of the channels of the radiometer which was calibrated to simulate a pyranometer (Cropscan™, 2001). Reflectance measurements which were outside the recommended range of light intensity together with associated pasture samples were discarded from further analysis.

The design of the radiometer allowed for near simultaneous inputs of voltages representing incident as well as reflected irradiation. This feature permitted accurate measurement of reflectance from crop canopies when sunlight conditions were less than ideal; useful readings may even be obtained during cloudy conditions (Cropscan™, 2001). The cosine properties for upward sensors allow the multi-spectral radiometer to inherently correct for varying angles of irradiance. The acquired reflectance was converted to a millivolt signal for subsequent analog-to-digital (A/D) conversion using analog multiplexers and stored in the instruments data logger.



### 4.2.2. Data analysis

Several statistical approaches have been employed to estimate functional relationships between spectral reflectance and pasture quality components. In this study, simple linear regression with individual wavelengths, vegetation indices and SMLR were executed using MINITAB (MINITAB, 2007) statistical software.

Relationships between pasture quality properties with the 16 individual wavelengths were calculated. Subsequently, various widely used traditional vegetative indices such as NDVI (Rouse *et al.*, 1973), transformed vegetation index (TVI) (Rouse *et al.*, 1973), Difference Vegetative Index (DVI) (Jordan, 1969), simple ratio (Jordan, 1969) optimized soils-adjusted vegetation index (OSAVI) (Rondeaux *et al.*, 1996) and renormalized difference vegetation index (RDVI) (Roujean & Breon, 1995) were evaluated (data not shown). Among those, RDVI was considered as the best index for predicting pasture quality components with high  $r^2$  values, and was further used in this study for predicting pasture quality components. For selecting the best combination of RDVI, a sequential regression with all possible two-band combinations of the spectra ( $16 \times 16 = 256$ ) using the mathematical Eq. (4.1) was performed with each pasture quality component.

$$RDVI = \frac{(R_{\lambda(i)} - R_{\lambda(j)})}{\sqrt{(R_{\lambda(i)} + R_{\lambda(j)})}} \quad 4.1$$

Where  $R_{\lambda(i)}$  is the reflectance at the  $i^{\text{th}}$  wavelength ( $\lambda$ );  $R_{\lambda(j)}$  is the reflectance at the  $j^{\text{th}}$  wavelength ( $\lambda$ ) and  $i$  and  $j$  consists of 1 to 16 wavelengths spanning from 460 to 1680 nm. The RDVI combinations were ranked based on  $r^2$  values for predicting pasture quality components individually and the top five combinations were selected for developing a regression model.

Stepwise multiple linear regression is a multi-spectral approach used to identify the optimal wavelengths sensitive to a required component. Accordingly, of the 16 wavelengths, each wavelength which acted as a regressor was evaluated with a significance test ( $p < 0.05$ ) against the measured values. The significant regressors were retained in the model for predicting the measured component. This process was repeated for each pasture quality

component. The developed regression model as shown in Eq. (4.2) was validated using a separate validation dataset.

$$\text{Pasture quality component concentration} = a_0 + \sum_{i=1}^N a_i \times R_{\lambda(i)} \quad 4.2$$

Where  $R_{\lambda(i)}$  is the reflectance at  $i^{\text{th}}$  wavelength ( $\lambda$ ) and  $N$  is the number of wavelengths selected for each pasture quality component model presented in Table 4;  $a_0$  and  $a_i$  are the coefficients at selected wavelengths. For validating the RDVI two-wavelength combination and SML regression models, the total data set was divided into calibration and validation datasets in a proportion of 50:50. The total dataset generated by ranking the measured pasture quality content from the lowest to the highest content was partitioned using odd and even ranked numbers which were allocated to calibration ( $n = 75$ ) and validation ( $n = 76$ ) datasets, respectively. The goodness-of-fit of the regression and validation model was tested with coefficient of determination ( $r^2$ ) and root mean square error (RMSE) values.

### 4.3. Results

#### 4.3.1. Summary of reflectance spectrum and pasture quality components data

The mean and coefficient of variation of individual spectra at 16 wavelengths are shown in Figure 4.1. The mean canopy reflectance of 151 samples resembles the typical spectral reflectance of green vegetation.

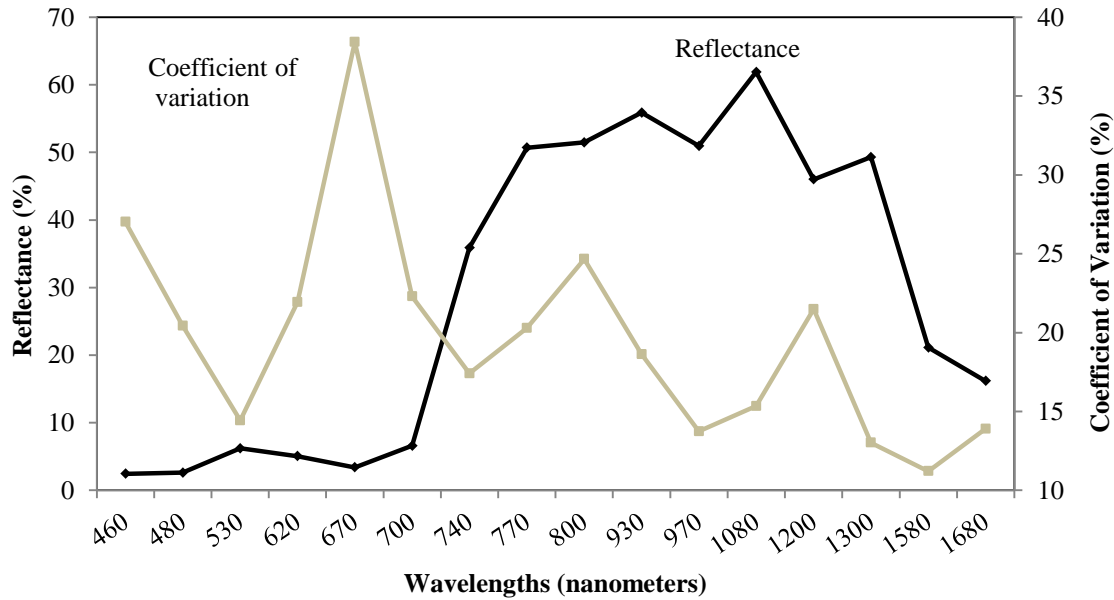


**Fig. 4.1** Canopy spectral mean reflectance (n=151) and coefficient of variation values at 16 wavelengths

Wavelength 670 nm had the greatest variation followed by wavelength of 460 nm. Overall, a larger coefficient of variation in spectral bands of the visible region (460-740 nm) and modest variation in the infrared region (770-1680 nm) (Figure 4.1) was observed.

**Table 4.1** Descriptive statistics of pasture quality components

	Calibration set (n = 75)					Validation set (n = 76)				
	Mean	Minimum	Maximum	SD	CV (%)	Mean	Minimum	Maximum	SD	CV (%)
CP	19.49	9.73	34.47	5.14	26.38	19.56	10.12	32.15	5.00	25.61
ADF	28.72	20.62	38.33	4.00	13.95	28.72	21.00	37.66	4.00	13.93
NDF	53.76	33.09	66.68	6.84	12.73	54.07	37.84	66.38	6.54	12.12
Ash	10.59	7.11	13.51	1.34	12.66	10.62	7.71	13.30	1.30	12.30
DCAD	532	200	775	135	25.31	536	219	756	131	24.51
Lignin	3.34	0.96	4.90	0.70	21.16	3.36	1.44	4.77	0.67	20.00
Lipid	2.81	0.51	5.84	1.19	42.23	2.84	1.06	5.66	1.18	41.76
ME	10.28	8.47	12.70	0.99	9.67	10.30	8.60	12.61	0.99	9.61
OMD	69.28	50.54	86.82	8.94	12.91	69.50	53.52	86.73	8.85	12.74

Table 4.1 summaries pasture quality components measured at different sites. The pasture samples collected had a wide range of values of different quality components, expressed as coefficient of variation ranged between 9.67-42.23 %. Lipid had the highest CV (42.23 %), while ME had the lowest at CV (9.67 %).

#### ***4.3.2. Single band relationships for pasture quality estimation***

A total of 16 available discrete wavelengths were correlated with individual pasture quality components (Table 2). There were significant ( $p < 0.001$ ) correlations between canopy reflectance of discrete wavelengths (620-1300 nm) and pasture quality components (CP, ADF, NDF, ash, DCAD, Lignin, Lipid, ME and OMD), but the coefficients of determination ( $r^2$ ) values were low to moderate with a range of 0.12 to 0.69. The maximum  $r^2$  values for ADF (0.42) and NDF (0.21) were found at the red-edge region (770 nm) followed by wavelengths of 930 nm and 1080 nm. For CP and ash, the highest  $r^2$  values were observed at 930 nm (0.60 and 0.53, respectively) and 770 nm (0.58 and 0.50, respectively). DCAD, lignin, ME and OMD had the highest  $r^2$  values of 0.60, 0.20, 0.56 and 0.69, respectively at 770 nm. For lipid, the maximum  $r^2$  value was found at 1080 nm. Overall, of the 16 discrete wavelengths, the red-edge wavelength (770 nm) and near infrared wavelengths 930 nm and 1080 nm showed the strongest relationships to the pasture quality components.

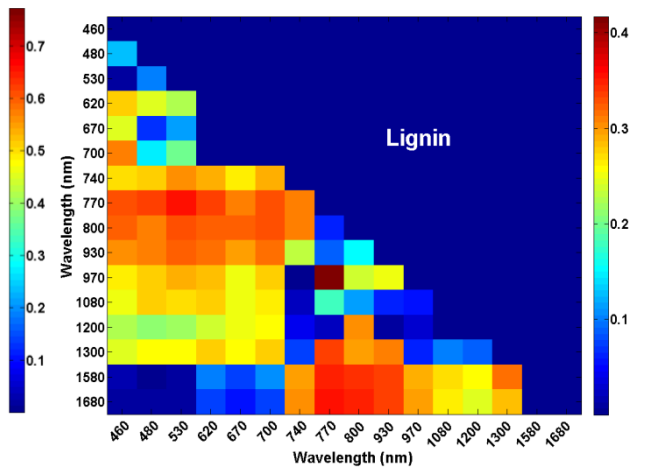
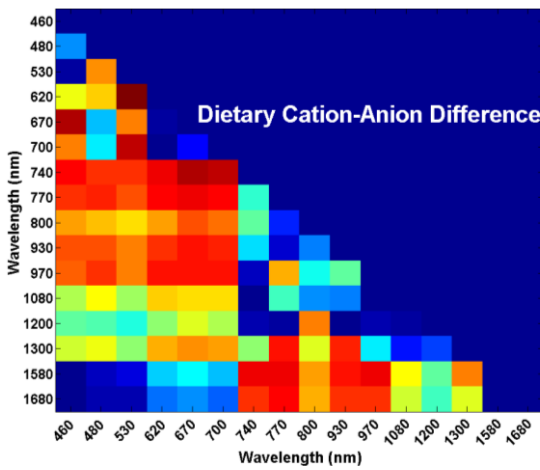
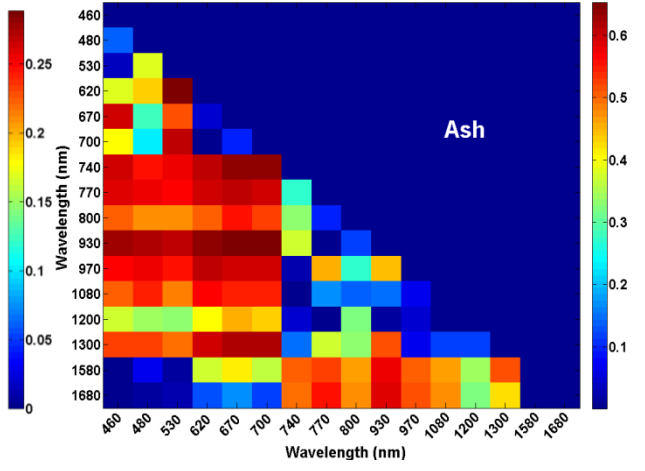
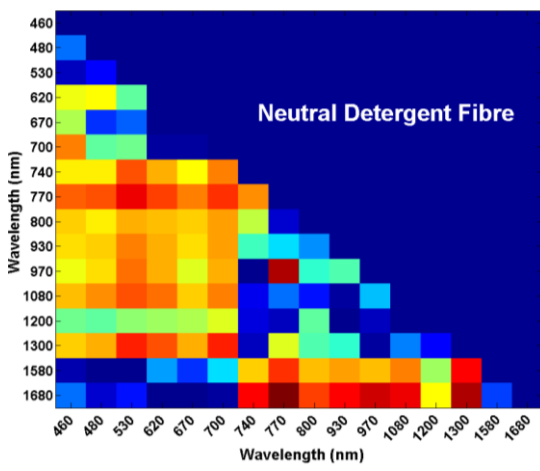
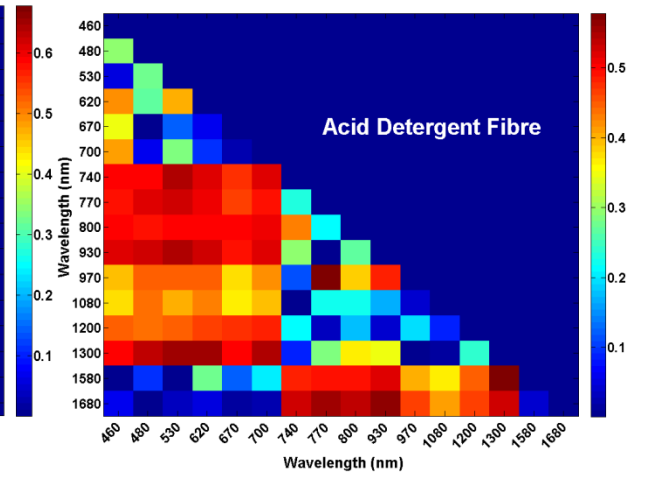
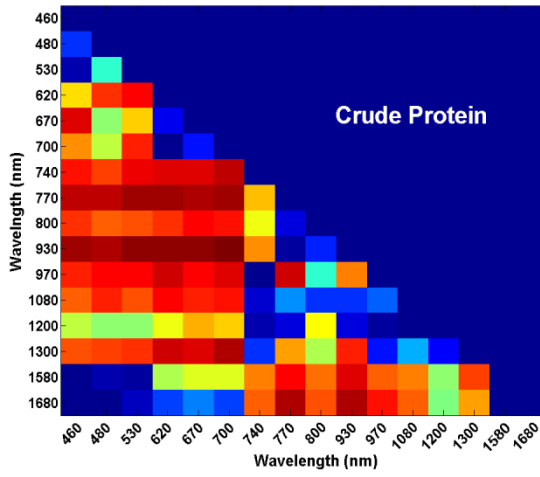
Table 4.2 Coefficient of determination ( $r^2$ ) between canopy reflectance at 16 individual wavelengths and pasture quality components

Quality components	Wavelengths (nm)															
	460	480	530	620	670	700	740	770	800	930	970	1080	1200	1300	1580	1680
<b>CP</b>	NS	0.07**	NS	0.26**	0.20**	0.20**	0.47**	0.58**	0.52**	0.60**	0.52**	0.54**	0.34**	0.46**	NS	NS
<b>ADF</b>	NS	0.05**	NS	0.13**	0.06**	0.09**	0.33**	0.42**	0.37**	0.40**	0.31**	0.40**	0.27**	0.35**	NS	NS
<b>NDF</b>	NS	0.06**	NS	0.12**	0.06**	0.10**	0.15**	0.21**	0.17**	0.17**	0.16**	0.20**	0.11**	0.16**	NS	0.06*
<b>Ash</b>	NS	0.11**	NS	0.30**	0.27**	0.24**	0.44**	0.50**	0.45**	0.53**	0.48**	0.45**	0.28**	0.36**	NS	NS
<b>DCAD</b>	NS	0.13**	NS	0.32**	0.30**	0.26**	0.52**	0.60**	0.51**	0.54**	0.56**	0.48**	0.25**	0.32**	NS	NS
<b>Lignin</b>	NS	0.07*	NS	0.17**	0.11**	0.16**	0.10**	0.20**	0.15**	0.14**	0.15**	0.16**	0.03*	NS	NS	NS
<b>Lipid</b>	NS	0.12**	NS	0.22**	0.16**	0.18**	0.28**	0.40**	0.32**	0.43**	0.29**	0.45**	0.19**	0.30**	NS	NS
<b>ME</b>	NS	0.10**	NS	0.22**	0.17**	0.18**	0.41**	0.56**	0.45**	0.47**	0.44**	0.50**	0.24**	0.34**	NS	NS
<b>OMD</b>	NS	0.09**	NS	0.24**	0.19**	0.18**	0.57**	0.69**	0.60**	0.65**	0.57**	0.63**	0.38**	0.50**	NS	NS

\*\* Significant at the 0.001 P level

\* Significant at the 0.05 P level

NS Not Significant



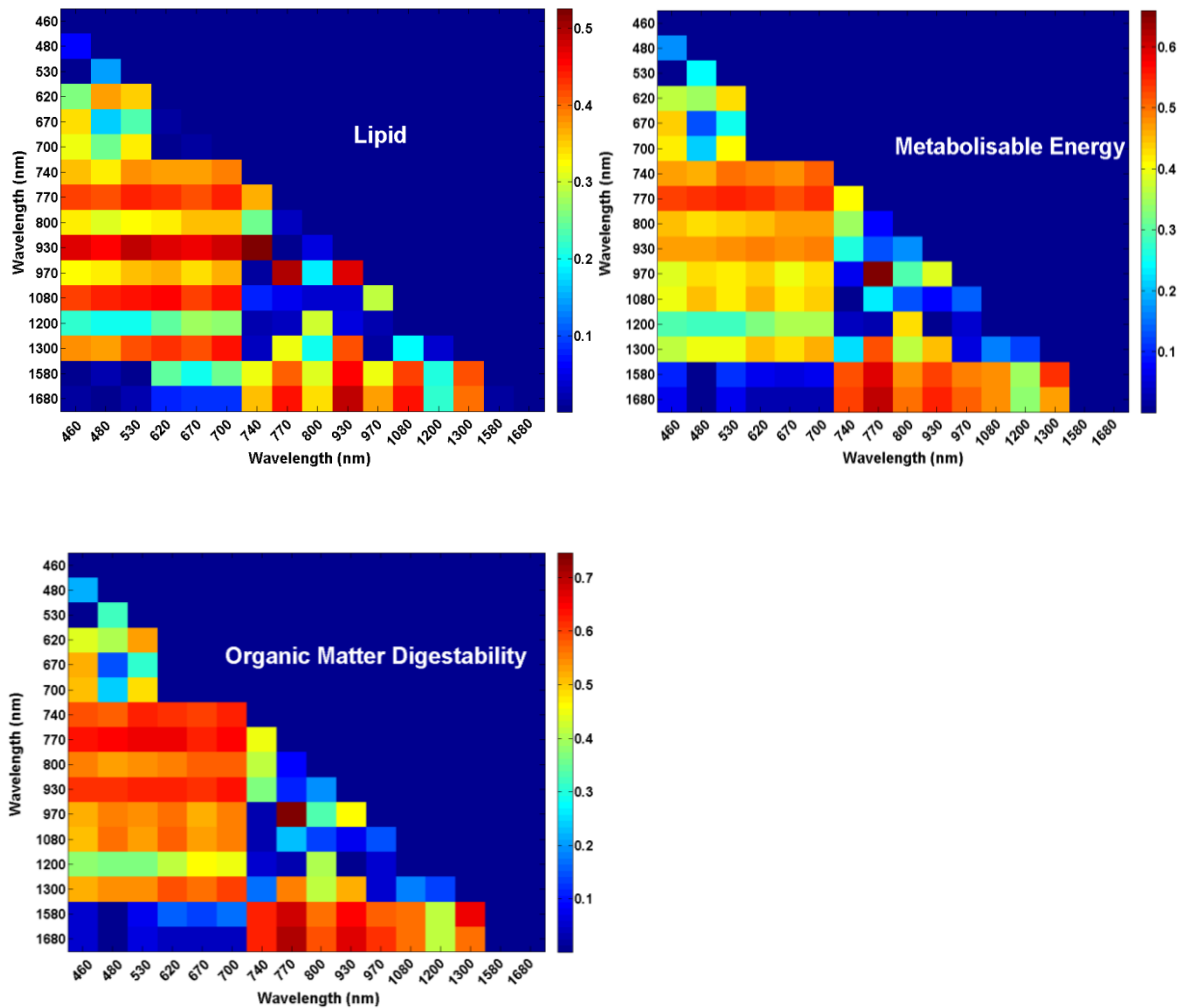


Figure 4.2 The 2-D correlograms showing the amount of variation in pasture quality components explained ( $r^2$  values colour bar) by spectral reflectance acquired in the field and expressed as RDVI indices calculated from 16 discrete wavelengths

#### 4.3.3. *Combinations of broad-band vegetative indices relationships with pasture quality components*

The 16 wavelengths observed by multispectral radiometer offer an opportunity to create a greater number of potential indices for predicting pasture quality. The reflectance ratios, calculated according to Eq. 4.1, of all possible band combinations ( $16 \times 16 = 256$ ) linearly regressed against each pasture quality component are depicted in Figure 4.2.

**Table 4.3 Best performing RDVI indices (top two-band combinations) with high coefficient of determination ( $r^2$ ) values for selected pasture quality components**

Pasture Quality Component	S.No	Selected wavelengths (nm)		Linear		Non-linear (Exponential)	
				Calibration set $r^2$	Validation set $r^2$	Calibration set $r^2$	Validation set $r^2$
		$\lambda_1$	$\lambda_2$				
<b>Crude Protein</b>	1	930	700	0.68	0.65	0.74	0.72
	2	930	620	0.66	0.63	0.70	0.68
	3	930	530	0.66	0.63	0.68	0.68
	4	1300	700	0.64	0.65	0.68	0.70
	5	1300	670	0.62	0.61	0.66	0.67
<b>ADF</b>	1	770	970	0.57	0.51	0.60	0.58
	2	930	1680	0.56	0.52	0.58	0.55
	3	530	1300	0.54	0.52	0.55	0.53
	4	770	1680	0.50	0.48	0.53	0.50
	5	700	1300	0.45	0.41	0.48	0.49
<b>Ash</b>	1	930	700	0.66	0.59	0.71	0.65
	2	930	670	0.65	0.61	0.68	0.60
	3	620	530	0.64	0.59	0.67	0.57
	4	670	460	0.63	0.58	0.67	0.61
	5	930	620	0.60	0.58	0.64	0.59
<b>DCAD</b>	1	740	700	0.73	0.65	0.76	0.72
	2	1580	770	0.72	0.68	0.78	0.71
	3	740	670	0.68	0.67	0.74	0.73
	4	770	700	0.67	0.70	0.73	0.72
	5	770	670	0.67	0.69	0.70	0.68
<b>ME</b>	1	970	770	0.66	0.64	0.69	0.67
	2	1680	770	0.61	0.60	0.64	0.63
	3	1580	770	0.59	0.53	0.63	0.61
	4	770	530	0.55	0.50	0.60	0.58
	5	770	700	0.54	0.53	0.56	0.54
<b>OMD</b>	1	970	770	0.75	0.84	0.75	0.85
	2	1680	770	0.71	0.81	0.73	0.84
	3	1680	930	0.68	0.80	0.71	0.82
	4	770	530	0.67	0.80	0.67	0.81
	5	1580	770	0.66	0.77	0.70	0.82



The best five RDVI two wavelength combinations based on  $r^2$  values were selected and reported in Table 4.3. The calibration and validation models explained 61-68%, 51-60 %, 60-66%, 65-73%, 53-66% and 66-84% of variation in CP, ADF, ash, DCAD, ME and OMD, respectively. It was found that, the  $r^2$  values for nonlinear models (e.g. exponential fit model) of corresponding wavelengths ranged from 0.49-0.82. However, the remaining pasture quality components: NDF, lignin and lipid were predicted with low  $r^2$  values, hence not considered in Table 4.3.

**Table 4.4 Coefficients of determination ( $r^2$ ) between crop reflectance of best regressors and pasture quality components using stepwise linear regression to select important wavelengths**

Pasture Quality component	Selected Regressors (wavelengths) nm	Calibration		Validation	
		$r^2$	RMSE	$r^2$	RMSE
CP	620, 700,930,1080	0.72	2.82	0.70	2.78
ADF	670,700,740,970,1200	0.59	2.69	0.52	2.83
NDF	770, 800, 930, 970	0.45	5.33	0.42	5.38
Ash	670, 930	0.67	0.80	0.60	0.84
DCAD	700,740,1080,1200	0.80	62.25	0.68	76.18
Lignin	700, 740, 770, 930, 1080	0.52	0.51	0.40	0.58
Lipid	480, 670, 930, 970	0.71	0.67	0.65	0.72
ME	770, 930, 970	0.72	0.53	0.65	0.61
OMD	620, 770, 970	0.76	4.57	0.80	3.73

#### 4.3.4. Stepwise multiple linear regression (SMLR) for pasture quality assessment

Multi-wavelength models were developed using stepwise multiple linear regression to select the information-relevant bands from those acquired by the spectroradiometer. The most important and significant ( $p < 0.05$ ) wavelengths for each pasture quality component, with  $r^2$  and RMSE values, are presented in Table 4.4. Compared with the RDVI two band

combinations (Table 4.3), the SMLR multi-wavelength models explained more of the variation in the pasture quality components, particularly CP, ash, DCAD, lipid, ME and OMD with high  $r^2$  values, ranging from 0.65-0.80. Low RMSE values were also observed in calibration and validation sets. In contrast, lignin, ADF and NDF are shown to have low to moderate  $r^2$  values (0.30-0.56).

Figure 4.3 depicts the  $r^2$  values for predicted pasture quality components using various methods. It can be noted that higher  $r^2$  values were derived with a nonlinear (exponential fit) model compared to single wavelength model, linear vegetation index model and SMLR. However, SMLR was better than the non-linear model for explaining NDF, lignin and lipid.

#### 4.4. Discussion

The multi-spectral radiometer was used to acquire pasture canopy reflectance on commercial farms in various locations within New Zealand. The discrete wavelengths from 740 to 1080 nm better explained ( $r^2$  values 0.33 to 0.65, Table 4.1) the variation of pasture quality components such as, CP, ADF, ash, DCAD, ME and OMD than other wavelengths. Overall, individual bands had limited ability to explain the pasture quality information. Daughtry *et al.*, (2000) reported similar results and confirmed that a single wavelength is more susceptible to background variations and less sensitive to the variable of interest.

The most common and widely used spectral models for describing the vegetation characteristics are vegetation indices. In the present work, among the indices investigated, the algorithm of RDVI of all possible combinations of two-wavelength combinations improved prediction of the variation in pasture quality components (data not shown). Roujean and Breon (1995) stressed the advantage of RDVI sensitivity to photosynthetically active radiation over NDVI and DVI. The correlation matrix plot of all possible RDVI combinations (Figure 4.2) showed that the variation in the quality components CP, ash, DCAD, OMD and ME were predicted with reasonable correlation ( $r^2$ - 0.60 to 0.80) in linear and non-linear validation models using the five best RDVI two-band combinations (Table 4.3). The selected RDVI two-wavelength combinations varied in their ability to predict each pasture quality component (Table 4.3). This indicates that the sensitivity of each index differs with the variable of interest. Overall, the results showed that broad-band

indices were better related to pasture quality than individual wavelengths. For example, Xue *et al.* (2004) reported that the ratio vegetation index ( $R_{810}/R_{560}$ ) minimises the contributions from background interference and improves the sensitivity to leaf nitrogen accumulation in rice (*Orza sativa* L.) over single wavelengths. Nevertheless, the relationship was further improved when nonlinear models, particularly exponential curve fitting, was used instead of linear models of new RDVI indices. This is in agreement with Thenkabail *et al.* (2000), who found that non-linear models performed better than linear models between biophysical variables (leaf area index and biomass) and hyperspectral vegetation indices. Similarly, Trotter *et al.* (2010) found that the log transformed soil adjusted vegetative index (SAVI) based model offered best correlation with green dry matter (GDM) of pasture and with low RMSE compared to a linear model. The accuracy of prediction could be further improved when soil and climate data were considered in the model development. For example, Donald *et al.* (2010) stated the capability of the NDVI prediction model, derived from MODIS imagery, for predicting plant growth rate (PGR) had improved accuracy when combined with soil, climate and light-use efficiency information. Furthermore, the overall performance of spectral indices is greatly influenced by growth stage (Li *et al.*, 2010), soil background (Huete *et al.*, 1985) and seasonal variations of floristic composition (Schellberg *et al.*, 2008), therefore it can be understood that the prediction performance of the developed models might be influenced by these factors.

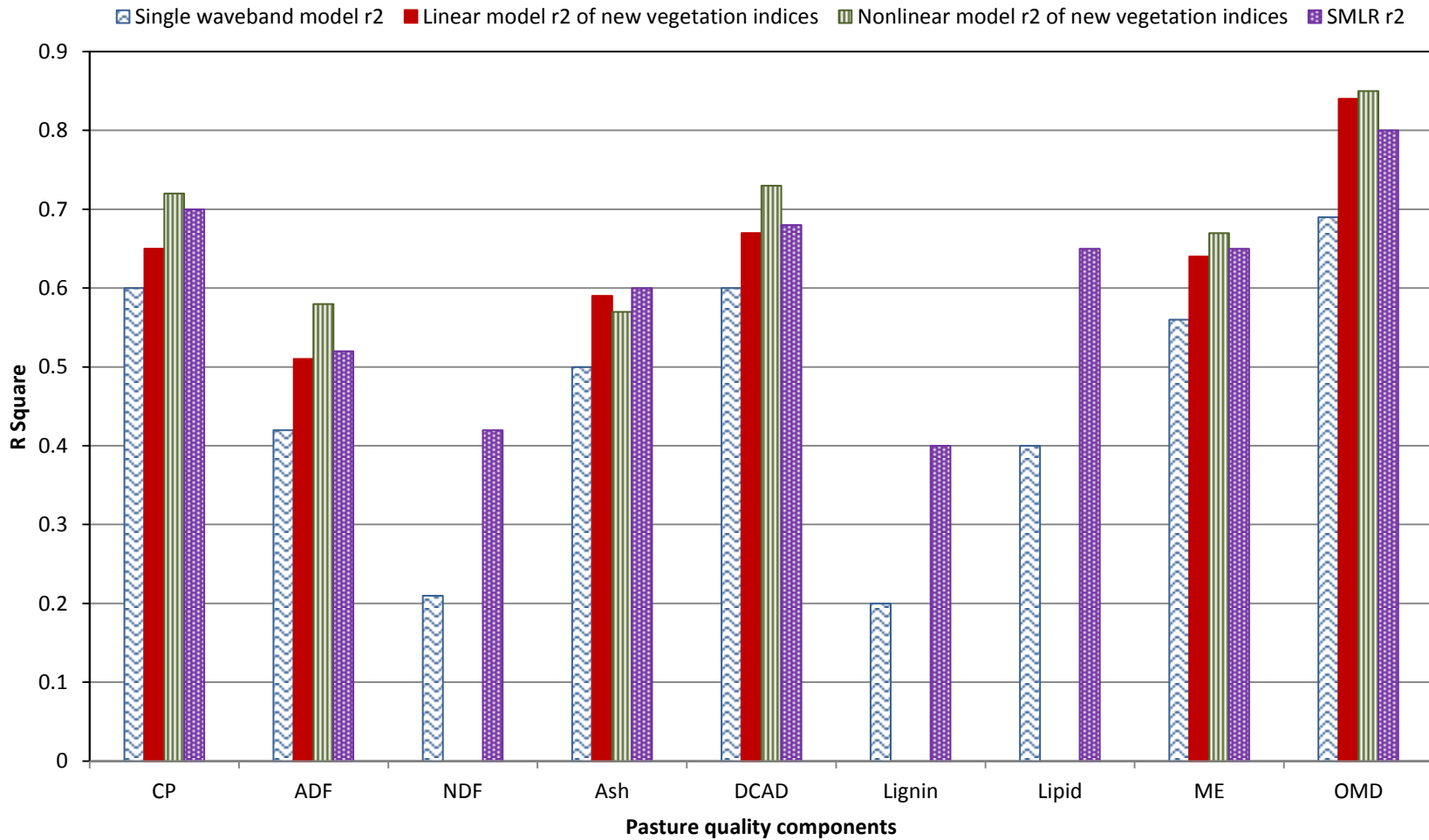


**Figure 4.3** The amount of variation in pasture quality components explained ( $r^2$ ) by spectral reflectance acquired in the field using four different predictive modelling techniques

The remaining quality components (ADF, NDF, ash, lignin and lipid) were poorly explained by the new RDVI two-band combinations. This is probably due to the broad wavelengths masking the essential spectral information and the available wavelengths were not able to explain detailed pasture characteristics (Xue *et al.*, 2004). In support of this statement, Starks *et al.* (2005) found that the canopy reflectance and reflectance ratios acquired as broad wavelengths could explain only a small portion of variance in the forage quality components (ADF and NDF) and in Starks *et al.* (2006b) recommended narrow bands for assessing foliar chemicals concentration with high accuracy in Bermuda grass.

It was noticed that the wavelengths (670-700 nm) around the red-edge region were frequently selected in two-wavelength combinations (Figure 4.2) showing the importance of the red-edge region in predicting the foliar biochemistry, particularly CP, ash and DCAD. Moreover, The 770 nm wavelength features strongly in prediction of ME and OMD, mainly in combination with higher wavelengths. This agrees with the results of Li *et al.* (2010) where he addressed the repeatability of red-edge region wavelength in developed new hyperspectral vegetation indices for identifying the variation of plant nitrogen concentration in wheat (*Triticum aestivum* L.) at Feeks 4-7 growth stage (Large, 1954). Mutanga and Skidmore (2007) also provided the evidence that red-edge position strongly correlated ( $r^2 = 0.89$ ) to nitrogen concentrations at canopy level.

As the statistical approach switched from simple regression to multi-spectral regression, the pasture quality components such as CP, ash, DCAD, lipid, ME and OMD were well predicted, with high  $r^2$  values. Villarreal *et al.* (2006) explained the importance of multiple regression equations which improved the prediction over individual wavelengths and traditional vegetation indices for pasture biomass. This could be due to inclusion of several wavelengths into the model which hold extra information. However, SMLR could not explain the quality components: ADF, NDF and lignin well. This might be due to insufficient spectral data or spectral wavelengths present in the instrument, therefore, a multispectral radiometer with other filters (wavelengths) which are able to explain ADF, NDF and lignin were suggested. To support this statement, Pullanagari *et al.*, (2012b) showed evidence that multi-wavelength data acquired with a

hyperspectral sensor was capable of building multivariate regression models to better predict the ADF, NDF and lignin content of pastures.

#### **4.5. Conclusion**

Pasture reflectance acquired using a hand-held multi-spectral radiometer was capable of accurately predicting some pasture quality components. This real-time pasture quality information can be used to aid pasture management decisions and ultimately improve livestock performance. Overall, this study determined that the use of multi-spectral reflectance of pasture canopy in the range of 460-1680 nm, under a wide range of environmental conditions, predicted pasture quality components such as CP, ash, DCAD, ME, lipid and OMD with reasonable precision. However, some pasture quality components (ADF, NDF and lignin) were not predicted well. The new RDVI two-band combinations were better related with pasture quality components (CP, DCAD, ME and OMD) and these results were further improved when non-linear regression models were developed. However, the accuracy of the non-linear models was slightly better than SMLR. Further research studying the impact of seasonal variations on reflectance and the use of other multi-spectral algorithms may improve the accuracy of the model to predict pasture quality components.

#### **Acknowledgment**

The authors would like to thank the staff of Massey University, New Zealand, Michael Killick; AgResearch, New Zealand, Grant Rennie, Linda Yates, Brian DeVantier, Ray Moss and Westlea Clarke-Hill; and DairyNZ, New Zealand, Laura Rossi for their field work. We extend our gratitude for comments on manuscript from Carolyn Hedley and Cath Goulter.



## CHAPTER 5

# **Proximal sensing of the seasonal variability of pasture nutritive value using multispectral radiometry**

*This chapter based on:*

Pullanagari, R.R., Yule, I. J., Tuohy, M. P., Hedley, M. J., Dynes, R. A. and King, W. M. (2011). Proximal sensing of the seasonal variability of pasture nutritive value using multispectral radiometry. *Grass and Forage Science (Accepted)*.





**Abstract**

The nutritive value of pasture is an important determinant of the performance of grazing livestock. Proximal sensing of *in situ* pasture is a potential technique for rapid prediction of nutritive value. In this study, multispectral radiometry was used to obtain pasture spectral reflectance during different seasons (autumn, spring and summer) in 2009-2010 from commercial farms throughout New Zealand. The analytical dataset (n=420) was analysed to develop season-specific and combined models for predicting pasture nutritive value parameters. The predicted parameters included: crude protein (CP), acid-detergent fibre (ADF), neutral-detergent fibre (NDF), ash, lignin, lipid, metabolisable energy (ME) and organic matter digestibility (OMD) using a partial least squares regression analysis. The calibration models were tested by internal and external validation. The results suggested that the global models can predict most of the pasture nutritive value parameters (CP, ADF, NDF, lignin, ME and OMD) with moderate accuracy ( $0.64 \leq r^2 \leq 0.70$ ) except ash and lipid ( $0.33 \leq r^2 \leq 0.40$ ). However, the season-specific models improved the prediction accuracy, in autumn ( $0.73 \leq r^2 \leq 0.83$ ) for CP, ADF, NDF and lignin; in spring ( $0.61 \leq r^2 \leq 0.78$ ) for CP and ash; in summer ( $0.77 \leq r^2 \leq 0.80$ ) for CP and ash, indicating a seasonal impact on spectral response.

**5.1. Introduction**

New Zealand farming systems are pasture based, with cattle and sheep grazing pastures year-round. New Zealand's temperate climate makes it well suited to low cost high productivity pastures. Effective utilisation of pastures is a key performance indicator of business profitability. Animal production is affected by the feeding value of pasture which is a function of voluntary feed intake (and therefore quantity) and nutritive value (NV). Typically, pasture NV or quality is described in terms of crude protein (CP), acid-detergent fibre (ADF), neutral-detergent fibre (NDF), ash, lignin, lipid, metabolisable energy (ME) and organic matter digestibility (OMD) (Holmes *et al.*, 2007). The NV of pasture will determine the production response per unit of pasture consumed. High NV is essential for high performance dairy farming. In addition, lower protein and high sugar content in pastures can reduce the nitrate toxicity in the rumen and the enteric methane emissions (FAO, 2010).

Current laboratory methods used to quantify the pasture nutritive value are expensive and time-consuming, which sometimes means the results of the analysis arrive at the farm *after* the pasture has been grazed. Furthermore, because of the high cost of analysis, field sampling is usually confined to a few specific points within the farm and limits the opportunity to manage or exploit the inherent variability within and between pastures. Proximal sensing techniques offer a rapid and non-destructive approach for quantifying vegetation characteristics and estimating NV. Here, proximal sensing refers to the technique of acquiring real-time reflectance data from the sward canopy in the field using a spectroradiometer.

Reflectance is defined as the ratio between the amount of radiation reflected by an individual leaf or canopy and the amount of incident radiation (FAO, 2010). The spectral reflectance of green vegetation has unique features that are a function of structure and chemical composition. Vegetation reflectance studies illustrate that there is strong absorption in the visible region spanning from 400 to 750 nm, hence low reflectance is observed, mainly due to the presence of photosynthetic (Schröder *et al.*, 2000) pigments. Conversely, high reflectance in the near infrared (NIR) region is due to microcellular structures, water and biochemicals (Chappelle *et al.*, 1992). Extensive research has described the functional relationships between vegetation reflectance and biophysical and biochemical variables (Curran, 1989). For instance, a number of studies (Rouse *et al.*, 1973; Tucker, 1979) have successfully predicted pasture characteristics from the *infield* spectral reflectance. As a result, numerous vegetation indices have been developed and are listed in a review by Yule and Pullanagari (Sanchez, 2009; Starks *et al.*, 2006b; Trotter *et al.*, 2010; Yule *et al.*, 2010). For example, Xue, *et al.* (2009) found that the ratio of NIR (810 nm) to green (560 nm) showed a strong relationship with leaf nitrogen concentration (LNC) on a dry matter basis with high precision and accuracy in rice (*Oryza sativa* L.) when using a multispectral radiometer (MSR 16, CropScan). In a study by Starks *et al.* (2004), the ratio of canopy reflectance in NIR to red ( $R_{\text{NIR}}/R_{\text{red}}$ ) were moderately correlated ( $r^2 = 0.65$ ) with the concentration of herbage CP in Bermuda grass (*Cynodon dactylon* L.) using hyperspectral data. However, in all cases validation results were poor, indicating these spectral vegetation indices are not generally reliable or stable, and therefore are inaccurate predictors of measured plant properties (Duncan *et al.*, 1993). This was likely due to the influence of many other confounding factors, such as soil background and plant physiological stresses (Hansen & Schjoerring, 2003).

Due to the limitations of two-band vegetation indices measured using multispectral and hyperspectral sensors for describing the vegetation features more accurately, researchers have focused on multivariate statistics to utilise the many wavelengths. In this study, a 16-channel multivariate empirical approach was used to explore the relationships between dependent (NV parameters) and independent variables (wavelengths) by deconvoluting the pasture canopy spectra. Starks *et al.* (2008) demonstrated the  $r^2$  value improved from 0.55 to 0.80 for nitrogen (N) concentration of herbage pasture using a five-band model when compared to a single-band model. Amongst the multivariate statistics, partial least square regression (PLSR) has become prominent when analysing multivariate data, such as multispectral and hyperspectral data (Pullanagari *et al.*, 2012a; Sanches, 2009; Zhao *et al.*, 2007b). The regression analysis also effectively deals with large numbers of independent variables and the problem of multicollinearity. Bronson *et al.* (2005) successfully used the PLSR analysis to build a predictive model for the leaf N concentration in cotton (*Gossypium hirsutum* L.) with reflectance obtained from a 16 channel multispectral radiometer, and a model using two wavelengths was unsuccessful. This research tests the hypothesis that canopy spectral reflectance acquired from a 16-channel multi spectral radiometer can be used to predict pasture NV within and across seasons.

## 5.2. *Materials and methods*

### 5.2.1. *Study Area and sampling*

The study areas comprised four climate regions within New Zealand: Waikato (Lat. -37.76, Long. 175.36) Taranaki (Lat. -39.60, Long. 174.30), Manawatu (Lat. -40.38, Long. 175.61) and Canterbury (Lat. -43.64, Long. 172.44) over three seasons in 2009-2010. These discrete sites and seasons: autumn (March to May, 2009), spring (September to November, 2009) and summer (December, 2009 to February, 2010), were selected to cover a wide range of botanical compositions, growth stages, and variable proportions of leaf, stem and dead material within the pasture sward. Within each region several commercial farms were selected for point sampling. Perennial ryegrass (*Lolium perenne* L.) and white clover (*Trifolium repens* L.) were the dominant species across the sites and seasons.

Spectral reflectance of the pasture canopy was measured using a portable CropScan multispectral radiometer (Model: MSR 16R, CropScan™, Inc., Rochester, MN, USA) at 16 specific wavelengths (460, 480, 530, 620, 670, 700, 740, 770, 800, 930, 970, 1080, 1200, 1300, 1580 and 1680 nm) with a spectral resolution of 7-16 nm, depending on the filter used at each wavelength. The radiometer with a field-of-view (FOV) of about 28° was pointed at the target pasture canopy at nadir position from a height of 1 m, which resulted in an area of just over 0.5 m in diameter. CropScan is a passive sensor, depending on natural light for the source of energy, hence the spectral readings were collected between 12:00 and 14:00 hours New Zealand Standard Time. A pyranometer (CropScan™, Inc., Rochester, MN, USA) was used to measure the intensity of light. The reflectance samples that were recorded under low intensity ( $n = 67$ ) and the reference samples (for near infrared spectroscopy (NIRS) analysis) that were contaminated with soil were discarded from the analysis ( $n = 13$ ). Finally, the total analytical dataset ( $n = 420$ ) comprised of three seasons data; autumn ( $n = 235$ ), spring ( $n = 85$ ) and summer ( $n = 100$ ).

The areas of pasture scanned on-farm were cut to ground level and collected in a perforated plastic bag then transported to the laboratory. The herbage samples were dried at 60°C for 24 hours in a forced-draught oven and ground to a 1mm particle size for estimating the contents of CP, NDF, ADF, ash, ME, lignin, lipid and OMD using laboratory based NIRS (Corson *et al.*, 1999) at the FeedTECH laboratory, Palmerston North, New Zealand. The FeedTECH NIRS (Fourier Transform Near Infrared spectroscopy, Model: MATRIX™ Bruker Optics, Ettlingen, Germany) was calibrated with an extensive dataset of pasture samples that have been analysed with reference chemistry.

### 5.2.2. Data analysis

Initially, the measured reflectance spectra ( $R$ ) were transformed to apparent absorbance spectra ( $A$ ) using logarithmic transformation:  $A = \log(1/R)$  to reduce any non-linearity that may exist in the spectra (Viscarra Rossel, 2008). Data analysis was done in two steps: PCA (principal component analysis) and PLSR. PCA was applied to the transformed spectra to visualise the distribution and pattern of the samples and interrelationships between the samples (Esbensen *et al.*, 2009). The PCA transforms the

original dataset (wavelengths) into uncorrelated orthogonal or principal components. First few components explains majority of the variation present in the dataset. First principal component (PC1) holds as much of the variation in the dataset as possible and second principal component (PC2) accounts as much of the remaining variation in the dataset as possible, and so on.

The PLSR method was used to establish a relationship between each response variable (NV parameters) and predictor variables (wavelengths), using the MINITAB statistical programme. Usually, the PLSR method reduces high dimensional data into a reduced number of uncorrelated components, or latent factors, based on the covariance between the predictor and response variables. Moreover, PLSR can effectively handle the problem of multicollinearity; and situations where the numbers of predictor variables are greater than the number of samples (Wold *et al.*, 2001). The statistical programme, Minitab 15 uses the nonlinear iterative partial least squares (NIPALS) algorithm to perform PLSR (MINITAB, 2007). The accuracy of the models was tested internally and externally. In order to develop a global model across the sites and seasons, the total analytical dataset (n=420) was divided into calibration (n=210) and validation (n=210) datasets using a random selection procedure. The calibration dataset was used for developing the calibration model and then internally validated by “leave-one-out” cross-validation procedure. The number of latent factors in the model was optimised by using the values of predicted residual sum of squares (PRESS). The model with smaller PRESS value has better predictive ability (MINITAB, 2007). The calibration model was again externally tested on unknown samples (validation dataset). To assess the ability of multispectral radiometry to predict pasture NV within each season, the total analytical dataset was divided into three separate datasets corresponding to each season: autumn, spring and summer. Owing to the small number of samples in the seasonal datasets, only internal validation was carried out. In the developed calibration and validation models the samples that had a standardized residual >2.0 were recognised as outliers (n = 9 in calibration and n = 3 in validation data sets), and were therefore removed from the models (Kusumo *et al.*, 2009b). The predictive ability of the models was evaluated by coefficient of determination ( $r^2$ ), root mean square error (RMSE) and ratio prediction to deviation (RPD). The RMSE was calculated according to Eq [5.1]:

$$RMSE = \sqrt{\frac{\sum_{i=1}^n (\hat{y}_i - y_i)^2}{n}} \quad 5.1$$

Where  $\hat{y}_i$  and  $y_i$  were predicted and measured values for the  $i_{th}$  sample, respectively, and  $n$  is number of samples in the dataset. RMSE is a function of direct estimates of modelling error expressed in original measurement units.

Ratio prediction to deviation is the ratio of the standard deviation (SD) of the measured variable (NV) to the RMSE and is calculated according to Eq [5.2]:

$$RPD = \frac{SD(y)}{\sqrt{\frac{\sum_{i=1}^n (\hat{y}_i - y_i)^2}{n}}} \quad 5.2$$

The best model is shown by the highest  $r^2$  and RPD, and the lowest RMSE.

### 5.3. Results

#### 5.2.1. Relationship between pasture nutritive value parameters and spectral reflectance

The total number of spectral readings was  $n = 500$  representing 500 plots but only 420 readings were considered in the experimental analysis. By adopting PCA to the spectra, six principal components (PCs) were found as holding the majority of the variation (98.26 %) in the total dataset, and the percentage values with respective components are illustrated in Figure 5.1a. Among the six PCs, PC3 and PC4 were selected for describing the samples distribution with clear seasonal discrimination and the samples highlighted by the oval had a high proportion of dead pasture (Figure 5.1b). The descriptive statistics of the calibration analytical dataset of pasture NV parameters are summarised in Table 5.1. The parameters CP, lignin and lipid had greater coefficients of variation ( $CV \geq 20\%$ ) than those of ADF, NDF, ash, ME and OMD ( $10\% \leq CV \leq 20\%$ ) in the calibration. The statistical performance of the cross-validated-calibration PLSR models is described in Table 5.1. The cross-validated calibration model estimated the CP, ADF, NDF, lignin, ME and OMD with an  $r^2$  of 0.60, 0.61, 0.59, 0.65, 0.66 and 0.68, respectively. Moreover, the RPD values occurred between 1.53 to 1.77. In contrast,  $r^2$  values for ash and lipid of 0.33 and 0.37 were lower than other NV parameters.

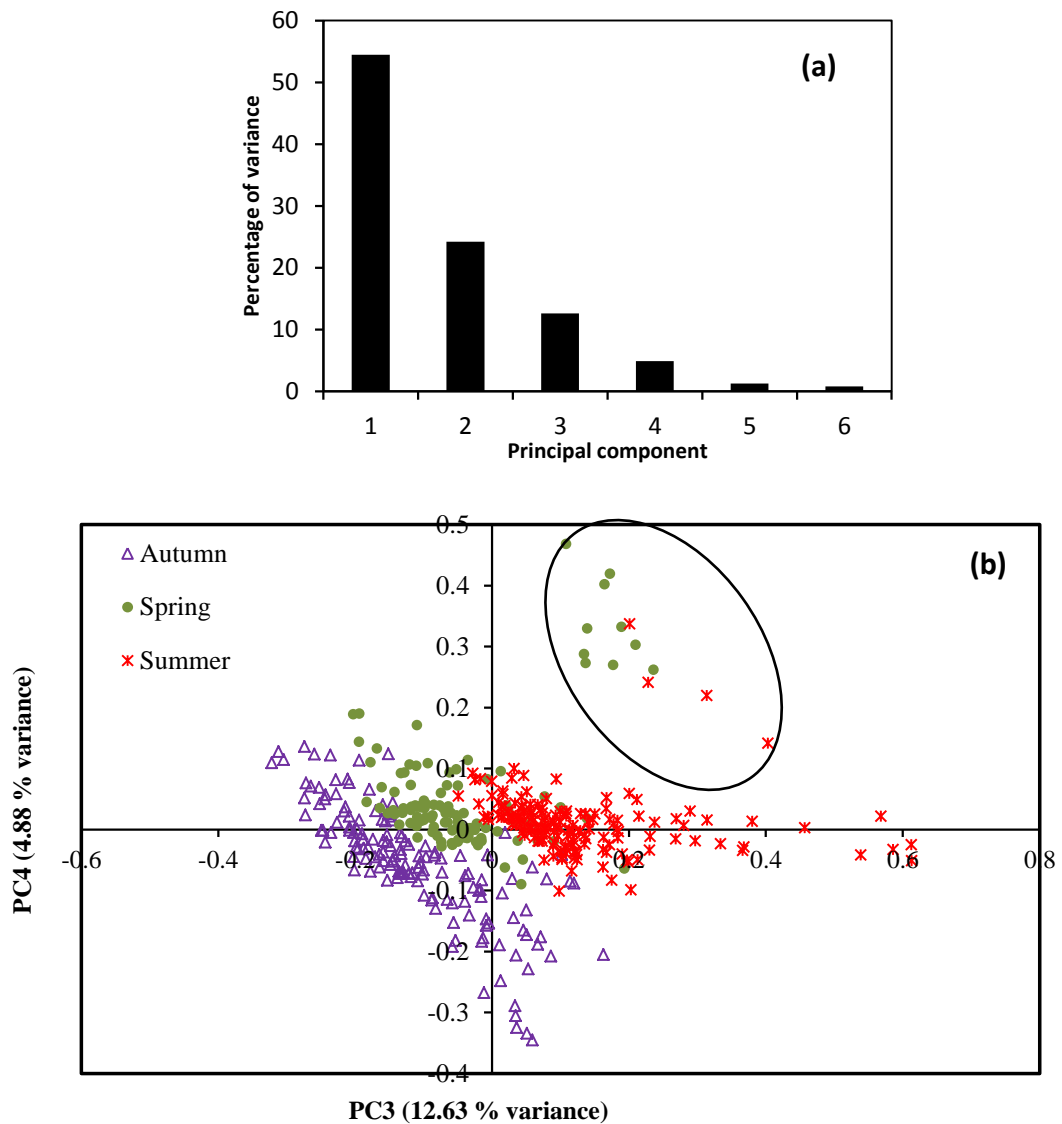


**Figure 5.1** (a) The relative proportion of variation explained by the six principal components in the principal component analysis (PCA) (b) The score plot of third and fourth principal components with respective seasons (autumn, spring and summer) in 2009-2010.

The better predicted parameters (CP, ADF, NDF, lignin, ME, and OMD) were further validated by the external dataset and the respective graphs are presented in Figure 5.2. The descriptive statistics of the validation analytical dataset illustrated in Table 5.2. The results were slightly better than calibration models and predicted with modest accuracy ( $0.64 \leq r^2 \leq 0.70$ ;  $1.65 \leq \text{RPD} \leq 1.83$ ).



**Table 5.1 Descriptive statistics (mean, minimum, maximum, standard deviation; SD, coefficient of variation %; CV) of pasture nutritive value parameters for the calibration dataset (n=210) and calibration model results measured at four sites during three seasons (autumn, spring and summer) in 2009-2010 in Waikato, Tarnaki, Manawatu and Catebury regions, New Zealand.**

Statistics	Pasture nutritive value parameters							
	CP	ADF	NDF	Ash	Lignin	Lipid	ME	OMD
Mean	18.57	27.89	50.05	10.19	3.03	2.53	11.08	75.45
Minimum	10.09	20.50	28.29	7.48	1.44	0.51	8.47	50.54
Maximum	27.72	38.33	67.32	13.12	5.14	4.17	12.92	89.45
SD	4.53	4.18	8.45	1.24	0.81	0.68	1.13	9.35
CV (%)	24.39	14.98	16.88	12.16	26.73	26.87	10.19	12.39
	Calibration model results							
$r^2$	0.60	0.61	0.59	0.33	0.65	0.37	0.66	0.68
RMSE	2.88	2.66	5.53	1.01	0.48	0.54	0.65	5.27
RPD	1.58	1.57	1.53	1.22	1.69	1.26	1.73	1.77

**Table 5.2 Descriptive statistics (mean, minimum, maximum, standard deviation; SD, coefficient of variation %; CV) of pasture nutritive value parameters for the validation dataset (n=210) measured at four sites during three seasons (autumn, spring and summer) in 2009-2010 in Waikato, Taranaki, Manawatu and Canterbury regions, New Zealand**

Statistics	Pasture nutritive value concentrations							
	CP	ADF	NDF	Ash	Lignin	Lipid	ME	OMD
Mean	18.06	28.16	50.75	10.08	2.93	2.53	11.04	75.04
Minimum	7.01	20.45	31.80	6.23	1.37	0.44	8.39	48.77
Maximum	28.41	37.31	67.32	14.32	4.43	4.24	12.98	89.57
SD	4.61	4.19	8.42	1.40	0.78	0.73	1.16	9.58
CV (%)	25.52	14.87	16.59	13.88	26.62	28.85	10.50	12.76

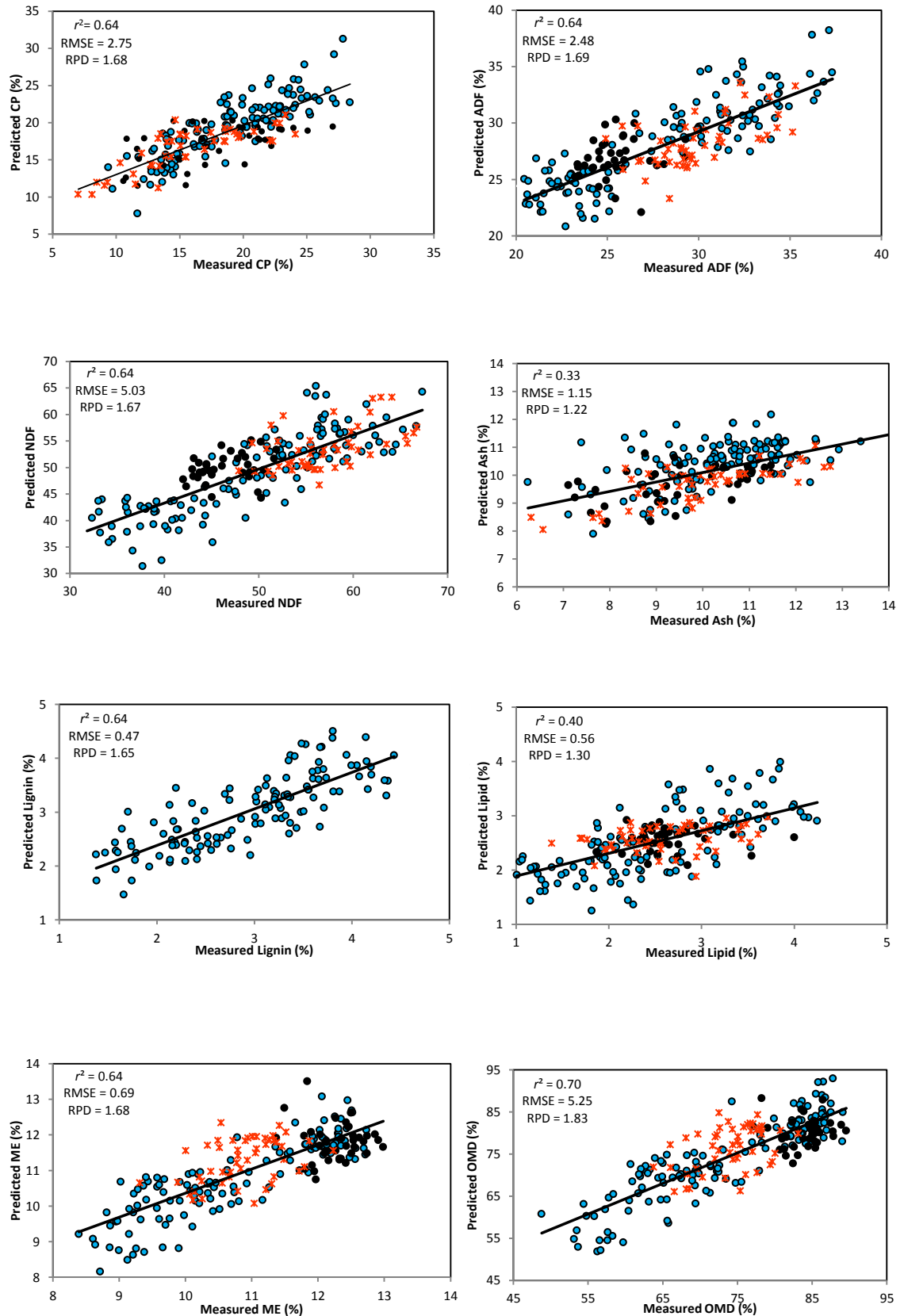


**Figure 5.2** Relationship between near infrared spectroscopy (NIRS) measured pasture nutritive values and values predicted by multispectral radiometer of validation ( $n = 210$ ) dataset of total (autumn  $\bullet$ , spring  $\bullet$  and summer  $\ast$  datasets) dataset using partial least squares regression (PLSR) method

### 5.2.2. Seasonal-specific models between pasture nutritive value parameters and spectral reflectance

The descriptive statistics of the pasture NV parameters for each season are reported in Table 5.3. The data population in spring (n=85) and summer (n=100) seasons was smaller than the autumn (n=248) dataset. Overall, the maximum variation in pasture NV parameters (CV range 11.48-36.34%) was observed in the autumn dataset, whereas the lowest variation occurred in spring (CV range 3.05- 22.18%) (Table 5.3). In the autumn dataset, lipid had the highest CV (32.63%) while in the spring and summer datasets CP had the highest CV's (22.18% and 28.11% respectively). In three seasons, ME had the lowest CV (11.38%, 3.05% and 5.33%).

**Table 5.3** Descriptive statistics (mean, minimum, maximum, standard deviation; SD, coefficient of variation %; CV) of pasture nutritive value parameters measured at four sites for individual seasons (autumn, spring and summer) in 2009-2010 in Waikato, Taranaki, Manawatu and Canterbury regions, New Zealand.

Statistics	Pasture nutritive value concentrations (g kg <sup>-1</sup> DM)							
	CP	ADF	NDF	Ash	Lignin	Lipid	ME	OMD
	<b>Autumn season (n=235)</b>							
<b>Mean</b>	19.20	28.10	49.42	10.44	2.96	2.48	10.73	72.76
<b>Minimum</b>	9.73	20.45	30.74	7.11	1.37	0.92	8.39	48.77
<b>Maximum</b>	28.41	37.66	67.32	13.58	4.43	4.17	8.39	89.45
<b>SD</b>	4.41	4.84	9.07	1.19	0.76	0.80	1.22	10.64
<b>CV (%)</b>	23.00	17.28	18.37	11.48	25.69	32.63	11.38	14.62
	<b>Spring season (n=85)</b>							
<b>Mean</b>	18.20	25.44	46.17	9.50	-	2.64	12.32	84.18
<b>Minimum</b>	10.57	23.12	38.63	7.11	-	1.86	11.37	77.19
<b>Maximum</b>	27.06	29.27	51.86	11.52	-	4.00	12.98	89.57
<b>SD</b>	4.03	1.40	2.94	1.17	-	0.36	0.37	2.77
<b>CV (%)</b>	22.18	5.51	6.39	12.31	-	13.76	3.05	3.30
	<b>Summer season (n= 100)</b>							
<b>Mean</b>	16.44	29.69	56.14	9.98	-	2.62	10.94	74.70
<b>Minimum</b>	7.02	25.42	44.47	6.31	-	1.38	9.31	63.76
<b>Maximum</b>	27.36	35.30	66.72	13.12	-	3.80	12.27	83.13
<b>SD</b>	4.62	2.28	4.86	1.49	-	0.52	0.58	4.12
<b>CV (%)</b>	28.11	7.70	8.66	15.00	-	19.97	5.33	5.52

Figure 5.3 shows the average canopy reflectance and coefficient of variation corresponding to each season; autumn, spring and summer during the years 2009 and 2010. Overall, the pattern of average reflectance of each season is similar, although differences were observed between seasons in the red-edge (740 nm), NIR (770 nm to 1080 nm) regions and at wavelength (1680 nm) of shortwave infrared (SWIR). In the red-edge and NIR's, the average reflectance was greater during spring followed by summer and autumn. However, the average reflectance at the wavelength of 1680 nm was greater in autumn when compared to spring and summer.

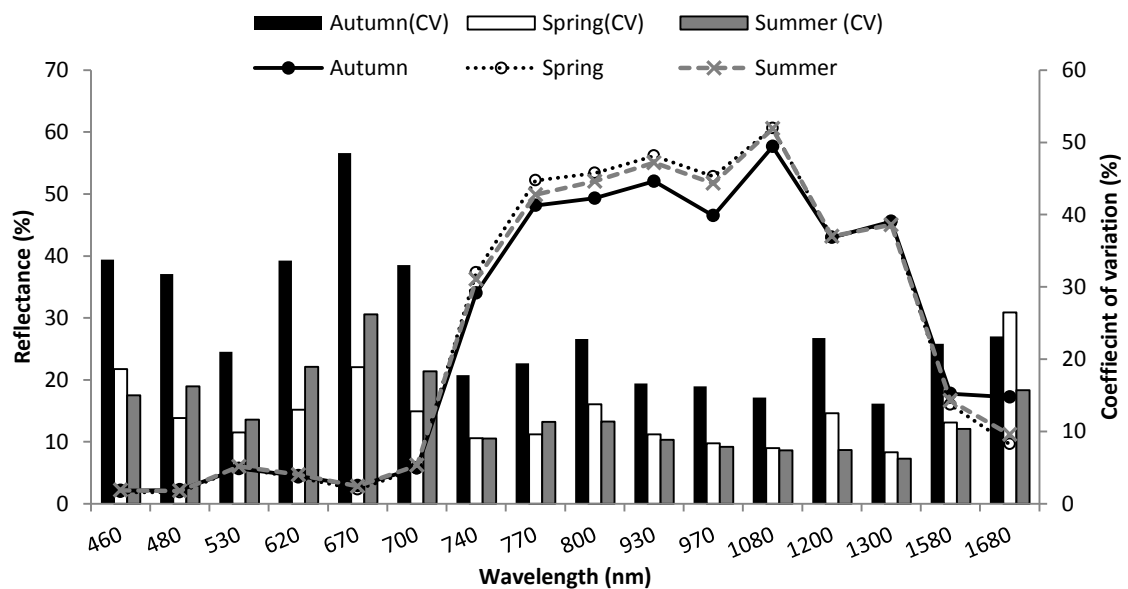


**Figure 5.3** Average pasture canopy reflectance (lines) and coefficient of variation (%) (bars) during autumn, spring and summer seasons in 2009-2010 at the three sites (Waikato, Taranaki, Manawatu and Canterbury) across New Zealand.

The observed spectral variations, expressed by coefficient of variation, across the electromagnetic spectrum vary with each season (Figure 5.3). Overall, the spectral reflectance variations during autumn were greater than the variations during spring and summer, except at the 1680 nm wavelength. The wavelength of 670 nm had greatest variation in autumn and summer, and 1680 nm in spring. In contrast, the reflectance at 1300 nm had the smallest spectral variation in all three seasons.

The cross-validated-PLSR model for predicting the pasture NV parameters with respect to each season are presented in Table 5.4. Season-specific models resulted in improved accuracy for estimating pasture NV parameters compared to the global model. In autumn, CP, ADF, NDF, lignin, ME and OMD had  $r^2$  values ranging between 0.73-0.83 and RPD values between 1.26–2.40 for the cross-validated-calibration dataset. However, ash and lipid were predicted with lower  $r^2$  values and lower accuracy (RMSE).

**Table 5.4 Calibration and cross-validation of spectral and pasture nutritive value data using partial least squares regression (PLSR) at four sites during three seasons (autumn, spring and summer) in 2009-2010 in Waikato, Taranaki, Manawatu and Canterbury regions, New Zealand.**

		Pasture nutritive value							
		CP	ADF	NDF	Ash	Lignin	Lipid	ME	OMD
		<b>Autumn season (n=248)</b>							
Calibration	$r^2$	0.80	0.80	0.80	0.44	0.76	0.63	0.84	0.85
	RMSE	2.05	2.15	4.09	0.9	0.37	0.49	0.49	4.21
Leave-one-out Cross-validation	$r^2$	0.76	0.77	0.76	0.36	0.73	0.57	0.82	0.83
	RMSE	2.2	2.31	4.41	0.94	0.39	0.52	0.52	4.42
	RPD	2.00	2.09	2.05	1.26	1.46	1.53	2.34	2.40
		<b>Spring season (n=85)</b>							
Calibration	$r^2$	0.80	0.55	0.65	0.87	-	0.30	0.5	0.4
	RMSE	1.83	1.08	1.73	0.44	-	0.35	0.27	2.47
Leave-one-out Cross-validation	$r^2$	0.69	0.23	0.5	0.78	-	0.1	0.23	0.2
	RMSE	2.13	1.15	2.07	0.54	-	0.37	0.32	2.57
	RPD	1.89	1.21	1.42	2.16	-	0.97	1.15	1.07
		<b>Summer season (n= 100)</b>							
Calibration	$r^2$	0.86	0.60	0.5	0.84	-	0.52	0.5	0.51
	RMSE	1.84	1.51	3.49	0.61	-	0.37	0.44	3.05
Leave-one-out Cross-validation	$r^2$	0.80	0.45	0.30	0.77	-	0.31	0.28	0.3
	RMSE	2.1	1.7	4	0.72	-	0.41	0.48	3.37
	RPD	2.2	1.34	1.21	2.06	-	1.26	1.20	1.22

During spring, the cross-validated-PLSR model explained the greatest variance ( $r^2$ : 0.69 and 0.78) for CP and ash, respectively, while the remaining NV parameters (ADF, NDF, lipid, ME and OMD) had lower  $r^2$  values. The summer results showed CP and ash were predicted with an  $r^2$  of 0.80 and 0.77, respectively, and the remaining NV parameters were poorly predicted ( $0.28 \leq r^2 \leq 0.47$ ).

#### 5.4. Discussion

A higher level of spectral variation occurred in the visible wavelengths mainly due to high absorption of light for photosynthesis (Viña & Gitelson, 2005) which are crucial for describing green vegetation properties. In this study, most of the pasture NV parameters were predicted with reasonable accuracy from the 16-channel radiometer using PLS-regression. Several researchers (Biewer *et al.*, 2009b; Pullanagari *et al.*, 2011b; Sanches, 2009; Schut *et al.*, 2005; Thulin, 2008) pointed out the value of PLSR for extracting important information from several wavelengths which were well correlated with the measured values. The combined spectra or global model, representing various agro-climatic sites and seasons, explained pasture NV parameters with moderate  $r^2$  values for CP, ADF, NDF, lignin, ME and OMD. However, the remaining parameters (ash and lipid) were poorly predicted. Poor prediction may be related to the lack of corresponding biochemical wavelengths acquired by the radiometer or inadequate dataset for these parameters.

When the total analytical dataset was divided into seasonal datasets the predictive accuracy of the pasture nutritive value parameters was improved (Table 5.4). However the improvement in accuracy varied with season and individual nutritive value parameters. This may be attributed to the influence of seasonal variations and low CV values, which corresponds to the findings of Sanches (2009). To support the statement, Figure 1 clearly shows the discrimination between the seasons. Overall, the autumn season models estimated the CP, ADF, NDF, lignin, ME and OMD with high accuracy, probably due to high CV values. But interestingly, ash had a similar CV in all seasons, even though it was not predicted with high accuracy in autumn, perhaps because of a lack of responsive wavelengths for this season. However, ash was quantified with high prediction accuracy in spring and summer. In these seasons, CP also had greater prediction. The remaining parameters were poorly estimated. It may be attributable to lower CV as seen in Table 5.3. The reasons for the different spectral responses between seasons can be explained as follows:

- Pasture canopy is comprised of green vegetation referred to as photosynthetically active vegetation (PV) and dead vegetation referred as non-photosynthetically active vegetation (NPV). The proportion of PV and NPV affect the spectral responses (He *et al.*, 2009; Irisarri *et al.*, 2009) and changes with seasons ((Holmes *et al.*, 2007). For example, more than 50% of total biomass as NPV masks the response of normalized difference vegetation index (NDVI) which results in reduced accuracy (Beerli *et al.*, 2007). Similarly Kawamura *et al.* (2005) found a poor correlation ( $r^2 = 0.41$ ) between enhanced vegetation index and NPV. The accumulation of dead leaves and understorey litter results in a substantial reduction of herbage NV and spectral response overall, and may therefore reduce the accuracy of NV estimation in pasture. In Figure 5.1b, the pasture samples dominated with dead vegetation were isolated from green vegetation. Similar observations were noticed by Pullanagari *et al.* (2012a).
- To date, the developed empirical models are often sensitive to canopy structure in addition to plant biochemical variations. This makes recognising biochemical changes much more difficult when the canopy structure is variable. Variability is the essence of a heterogenic environment such as pasture (Matson *et al.*, 1994; Schellberg *et al.*, 2008). Pasture comprised of ryegrass and clover has different NV (Hodgson & Brookes, 1999; Holmes *et al.*, 2007), canopy structures and developmental habits respective to each season. These seasonal proportions and variations may reflect spectral responses differently (Jiang and Carrow, 2007).
- Perennial pastures usually have different growth and maturity stages, and the leaf to stem ratio differs in each stage as a result of seasonal growth patterns. These changes have a strong influence on pasture NV (Holmes *et al.*, 2007) which reflects the sensitivity of spectral reflectance differently. Correspondingly, Li *et al.* (2010) concluded that the response of spectral reflectance varies with each growth stage in wheat (*Triticum aestivum* L.).

Reference measurements on the pasture samples were estimated using laboratory NIRS, which would be expected to have an error term associated with the prediction of proximal analysis. In addition grazed pastures are difficult to sample because of the inherent variability within the sward arising from micro-site variation in botanical and chemical composition, sward production and sward structure (Hodgson and Brookes, 1999). These impacts were reduced by collecting a large database of pasture samples with a variety of botanical compositions across seasons and regions. From the results of this study, the seasonal-specific calibration model was the most robust for assessment of pasture NV with high accuracy. Similarly, Irisarri *et al.* (2009) suggested seasonal-specific calibrations for differentiating grass species in mixed canopies.

This research method can also be applied for regional scale mapping by using similar bands to existing airborne or spaceborne multispectral sensors (Aster, Landsat ETM+, SPOT and MODIS) to produce regional maps of pasture NV. But, within New Zealand satellite-based pasture quality mapping is still in its infancy (Ausseil *et al.*, 2011), and has been severely hampered by cloud cover and atmospheric conditions.

### 5.5. Conclusion

This research demonstrated the utility of a PLSR model built from the 16-channel multispectral data has potential to predict pasture NV. Compared to the results of global calibration, seasonal-specific calibrations improved the model's prediction accuracy, suggesting that it may be possible to use seasonal-specific calibrations for estimating pasture NV. However, further tests are required to investigate the influence of seasonal changes on spectral data and whether other wavelengths can be added to improve the accuracy of the PLSR models. For this, a wide range of seasonal datasets would be recommended. Proximal sensing may eventually provide real-time estimates of the NV of pasture so as to improve the efficiency of current feeding strategies. Ultimately, this research can be used for developing spatial maps of pasture NV parameters when the sensor is integrated with a global positioning system (GPS). The generated maps showing some indication of NV will inform farmers and aid management decisions at the paddock-scale to improve pasture NV and grazing management. This research demonstrates that



multispectral instruments used proximally do have the potential to help farmers make more informed decisions about NV. Ultimately better pasture utilisation and improved on-farm productivity could be realised by New Zealand farmers who make use of such technologies.

**Acknowledgement**

The authors wish to thank the people from Massey University (Michael Killick), AgResearch (Grant Rennie, Linda Yates, Brian DeVantier, Ray Moss and Westlea Clarke-Hill) and Dairy NZ (Laura Rossi) for their technical assistance. This research was supported by the P21 Feed Programme (contract No. C10X0604), New Zealand.

## CHAPTER 6

# **Estimation of pasture biomass, standing crude protein and spatial analysis of herbage biomass using an active optical sensor**

*This chapter based on:*

Pullanagari, R.R., Yule, I. J., Tuohy, M. P., Hedley, M. J., Dynes, R. A. and King, W. M. 2011. Estimation of pasture biomass, standing crude protein and spatial analysis of herbage biomass using an active optical sensor. *Agronomy Journal (Under review)*.



### ***Abstract***

Increased concern regarding nitrogen fertiliser use efficiency on grazed dairy pastures has raised interest in real-time measurement of both herbage biomass and quality. Real-time measurements promise adaptable management of dairy cow intakes and fertiliser inputs that will achieve more sustainable dairy farm production. In this study, a three channel optical sensor was used to acquire canopy reflectance from a range of grazed pastures. The objectives of this research were to: (i) develop calibration relationships between canopy reflectance, herbage biomass and standing protein (SCP), (ii) validate the developed calibration models using an external dataset, (iii) use the calibration model, to develop semivariograms for standardising herbage biomass sampling distances. Among the investigated indices, pasture index (PI) showed the greatest correlation with biomass ( $R^2 = 0.69$ ; RMSE = 518 kg ha<sup>-1</sup>) and standing crude protein ( $R^2 = 0.77$ ; RMSE = 110 kg ha<sup>-1</sup>). Semivariograms from ten fields revealed that the spatial variability varied with each field. Across the fields, moderate or strong spatial dependency was observed for biomass.

### **6.1. Introduction**

Accurate and spatial measurement of pasture biomass and quality are important determinants of animal production and their accurate and spatial measurement allow the appropriate allocation of feed to livestock. Real-time in field spatial measurements may optimise management decisions, such as: site-specific application of fertilisers, supplementary feeding, setting break sizes and manipulation of stocking rates.

Direct pasture measurement techniques including hand cutting from quadrats involve destructive sampling and are very time consuming, laborious and expensive on a farm scale, and are not suitable for routine farm monitoring. Alternatively, a number of indirect techniques are suggested for measuring total pasture biomass above ground level. Visual assessment has been a widely used technique and can provide information on pre-grazing herbage mass, post grazing residuals and estimates of pasture quality through assessment of

the content of legume, dead material and reproductive tillers. However, this method is subjective and can show inconsistencies depending on the operator and the season (Holmes *et al.*, 2007) and its prevalence owes more to convenience, than accuracy. Consequently, a range of manual or electronic devices have been used for estimating the herbage biomass such as the rising plate meter (RPM), electric capacitance probe and pasture ruler. These tools still have their constraints, such as appropriate calibration equations, operator bias and are less reliable under extreme herbage biomass conditions and rough surfaces (Hodgson *et al.*, 2000). Several research studies have indicated that these devices rely on universal prediction equations that are more susceptible to variations in management, pastures and climate (Frame, 1993). Sanderson *et al.* (2001) reported that the level of errors from these devices was economically unacceptable. In addition to these errors, these devices require skilled labour as on-farm practice indicates that individual operators can have a significant impact on the results. For example, an operator using a RPM can produce an underestimation of pasture biomass by incorrectly forcing the meter at an angle to the pasture (Thomson *et al.*, 2001). There are also issues around increased error through low numbers of samples being taken and the consistency of sampling sites in sequential measurement events. Moreover, these pedestrian based systems cannot account for spatial information, since they report the mean of spatially discrete estimates and are not linked to a location system. Spatial information of pasture biomass describes the level of heterogeneity occurring at the field scale. It may also describe livestock grazing behaviour (Flynn *et al.*, 2008) and its effect on the grazing system. Recently, the C-DAX Pasturemeter™ was released (Yule *et al.*, 2005), which is towed behind an all-terrain-vehicle (ATV) and enables mapping of the pasture biomass across the farm when integrated with a global positioning system (GPS). However, these instruments provide quantitative biomass information ( $\text{kg DM ha}^{-1}$ ), but not information on pasture quality.

The potential application of remote sensing tools and technologies has increased over recent years, because reflectance data from Vis-NIR (Visible-near infrared) sensors can be used to describe vegetation properties (Kawamura *et al.*, 2009; Mutanga, 2004; Trotter *et al.*, 2010) non-destructively, rapidly and inexpensively. However, the application of remote sensing in grassland systems is still in its infancy due to the variability of pastures and the

environment in which they grow meaning calibration is extremely difficult and expensive. Spatial heterogeneity is greater in grazed systems as it is dependent on a large number of factors, including interactions with the grazing animals, differences in biomass maturity, selective grazing (Correll *et al.*, 2003), urine and dung depositions (Cosgrove *et al.*, 1998), as well as variations in soil fertility and availability of soil water (Hedley & Yule, 2009). Typically, these sensors are usually mounted on a vehicle and operate close (within 1-2 m) to pasture. Consequently, they provide spatially dense, instant, and spatially related information about the desired parameter when the sensor is linked to automatic data logging and global positioning systems (GPS). A range of proximal, multispectral (Berntsen *et al.*, 2006; Eitel *et al.*, 2010; Flynn *et al.*, 2008; Raun *et al.*, 2002) and hyperspectral (Biewer *et al.*, 2009b; Kawamura *et al.*, 2009; Mutanga *et al.*, 2005) sensors have been used in order to determine various vegetation properties. Recently, an active optical sensor, Crop Circle™ was introduced for commercial precision agricultural applications and was successfully used to identify nitrogen variation across a field within a cropping system (Solari *et al.*, 2008).

In order to develop an empirical relationship between the sensor data and the vegetation property the reflectance values are manipulated as vegetation indices. Though many indices are available, the sensitivity of each index varies with the type of vegetation, required characteristic, light intensity and soil background. Pullanagari *et al* (2009) reviewed a number of available vegetation indices that had been used in research and commercial activities. For example, the normalised difference vegetation index (NDVI) correlated well with nitrogen in spring wheat (*Triticum aestivum* L.) (Reyniers & Vrindts, 2006; Tremblay *et al.*, 2009). Similarly chlorophyll index (CI) proved a potential index for predicting nitrogen status and yield potential in corn (*Zea mays* L.) (Solari *et al.*, 2008). The objectives of the present study were to (i) develop an empirical relationship between Crop circle™ derived reflectance data and biomass and standing crude protein (ii) validate the models for prediction accuracy, and (iii) examine the spatial maps for herbage biomass over 10 fields.

## 6.2. Materials and Methods

The experiment was conducted during spring and summer in 2009 at commercial dairy farms located in Manawatu (Lat. -40.39, Long. 175.61), Waikato (Lat. -37.76, Long. 175.31), and Canterbury (Lat. -43.64, Long. 172.44). Different locations were selected to create samples that represented a range of biomass, botanical and chemical compositions, which is important for developing a robust calibration model.

The dominant species included ryegrass (*Lolium perenne* L.), clover (*Trifolium repens* L.), and some weeds: chickweed (*Stellaria media*), Californian thistle (*Cirsium arvense*) and daisy (*Bellis prennis*) distributed across several fields. After spectral measurements, the corresponding pasture quadrat (0.5 × 0.5 metre) samples were harvested to ground level with a shearing hand piece and bagged for laboratory analysis. Before the analysis, the collected samples were washed thoroughly then oven dried at 40°C for 48 hours and weighed. For the analysis of crude protein (CP) concentration, the dried samples were ground through a 1 mm sieve and scanned using near infrared spectroscopy (NIRS)-FeedTECH (Corson *et al.*, 1999) at AgResearch in Palmerston North, New Zealand.

### 6.2.1 Canopy Reflectance

The on-the-go sensor, a three channel Crop Circle™; Model ACS-470 (Holland Scientific Inc.), was used in this study. The sensor has three wavebands which can be selected by using different filters. In this study, we used two visible (670 nm and 730 nm) and one near infrared (760 nm) filters, each with a broad spectral resolution of 20-22 nm. After fixing these filters the sensor was calibrated to optimise the reflectance. The sensor has a field-of view of 32° × 6°. Interestingly, this sensor has its own light source emitting from a modulated polychromatic Light Emitting Diode (LED) array, hence the name active sensor. Therefore, it can be used at any time of the day or night, independent of diurnal variations. The reflected light is detected by an array of silicon photodiodes. To acquire the

reflectance from the target, and to ensure a constant distance, an aluminium platform was constructed at a height of 1m, with the sensor placed on top of the platform attached to a movable frame. Consequently, the sensor frame can move easily from one end to another on the aluminium platform with a constant distance of 1 m from the target. During the scanning process, the sensor was moved forward and back across the platform. The data was then averaged to a single value to represent the plot. To record the sensor output, the sensor was equipped with a GeoSCOUT GLS-400 data-logger, supplied by Holland Scientific Inc.

In another mode, the sensor was mounted on the front of an all-terrain-vehicle (ATV) motor bike in a nadir position 1m above the ground. As the ATV driven around the field, sensors and location data were recorded at 1 second intervals. Accurate locations were measured with an RTK (Real Time Kinematic) GPS (Global Positioning System). The sensor and GPS data were synchronised using a Trimble AgGPS<sup>®</sup> 170 Field Computer to guide the ATV survey in the field. The speed of the bike and swath width ensured at least one reading per 2.5-3.5 m<sup>2</sup>.

## **6.2.2 Data analysis**

The data analysis was done in two stages: First, calibration models were developed for estimating the herbage biomass and standing CP and then validated by an external dataset. Secondly, the spatial variability for herbage biomass was investigated based on the calibration model.

### **6.2.1.1. Development and validation of calibration models**

The acquired reflectance values of discrete bands were transformed into the indices which are listed in Table 6.1. The total dataset comprised  $n=415$  canopy reflectance observations for a corresponding number of plots. The aim of the model development was to explore the explicit relationship between the sensor reflectance values, the herbage biomass and standing crude protein. To develop a calibration model, 50% of the dataset ( $n=208$ ) was



separated from the total dataset using a random selection procedure. Of the 208 samples, 200 samples were used to develop the calibration model and the reflectance observations were linearly regressed against herbage biomass and standing crude protein, the remaining samples ( $n=8$ ) were determined outliers and were therefore discarded from the model dataset. The model was examined for legitimacy by calculating the coefficient of determination ( $R^2$ ) and root mean square error (RMSE) values, and was then further validated by the external dataset ( $n = 207$ ).

**Table 6.1 The selected vegetation indices**

Vegetation Index	Formula	Wavebands
NDVI (Normalized difference vegetation index)-1	$\frac{(\lambda_2 - \lambda_1)}{(\lambda_2 + \lambda_1)}$	$\lambda_1 = 670/22$ nm $\lambda_2 = 760/LWP$
NDVI (Normalized difference vegetation index)-2	$\frac{(\lambda_2 - \lambda_1)}{(\lambda_2 + \lambda_1)}$	$\lambda_1 = 730/20$ nm $\lambda_2 = 760/LWP$
SR (Simple ratio)-1	$\frac{\lambda_2}{\lambda_1}$	$\lambda_1 = 670/22$ $\lambda_2 = 760/LWP$
SR (Simple ratio)-2	$\frac{\lambda_2}{\lambda_1}$	$\lambda_1 = 730/20$ $\lambda_2 = 760/LWP$
PI (Pasture Index)	$\frac{(\lambda_1 - \lambda_2)^2}{\sqrt{(\lambda_2 - \lambda_3)}}$	$\lambda_1 = 760/LWP$ $\lambda_2 = 730$ $\lambda_3 = 670/22$

#### 6.2.1.2. *Spatial analysis of herbage biomass on commercial dairy fields*

Geostatistics, unlike classical statistics, can provide information about the spatial distribution of measurements in the form of a map. For this reason, geostatistics have been used widely for estimating the spatial variability of various soil (Cambardella *et al.*, 1994), vegetation (Flynn *et al.*, 2008; López-Granados *et al.*, 2004) and climatic properties, animal distributions, and ecological studies. In geostatistics, the variance is represented by semivariance ( $\gamma$ ) and is computed by the following equation (Curran & Atkinson, 1998):

$$\gamma(h) = \frac{1}{2m(h)} \sum_{i=1}^{m(h)} [z(x_i) - z(x_i + h)]^2 \quad 6.1$$

Where  $\gamma$  is the semivariance between sample pairs, the spatial distance (lag) between sample pairs measured as  $h$ ,  $m(h)$  is the number of sample pairs at the lag ( $h$ ),  $Z(x_i)$  and  $Z(x_i+h)$  are the sample values at  $x$  and  $x_i+h$  places separated by  $h$ (distance). In this study the lag distance was between 2.5 and 3.5 m. The semivariance was extrapolated graphically by variogram models. In the next step of the process, the observed values were fitted with a mathematical function. The mathematical function may vary with the variable studied and with location. Usually soil variables fit within a spherical model (Cambardella *et al.*, 1994), but in our case exponential, spherical and linear with sill functions were found to have the best fit for explaining the spatial variability of the herbage biomass. Differences between predicted and measured values are presented as root mean square error (RMSE).

The typical shape of a spherical variogram illustrated in Figure 6.1 infers the degree of spatial dependency by the key parameters: nugget, sill, partial sill and range. The nugget ( $C_o$ ) value, when  $h=0$ , represents the random or experimental variance which is unaccountable by the current scale of sampling or the sensor. The partial sill ( $C$ ) is the variability due to the sensor (also referred to as structured variability). The sill ( $C + C_o$ ) is the maximum variance attained in the model (also called total variability). The range ( $a$ ) is the lag distance where the semivariance reaches maximum point (sill). Beyond this, the samples were independent of spatial influence and did not follow the model.

From the results of variogram plots, the spatial dependency ( $Q$ ), function of the ratio between nugget ( $C$ ) and sill ( $C + C_o$ ) was calculated for each field. Values less than 0.25 reflected strongly spatial dependence, the values between 0.25 and 0.75 were considered moderately spatially dependent, and the values more than 0.75 indicated weak spatial dependence (Cambardella *et al.*, 1994). The values of range ( $a$ ) explain the degree of spatial extent for sampling. It gives the average extent of the patches when the spatial dependency ( $Q$ ) is moderate or strong (López-Granados *et al.*, 2004). Semivariograms were calculated using VESPER software (Minasny *et al.*, 2005).

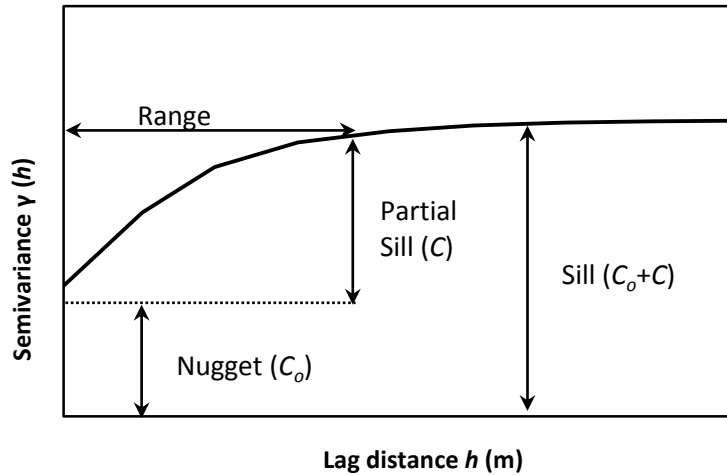


Figure 6.1 Typical shape of a spherical variogram model

### 6.3. Results

Pasture biomass (field cuts) and standing crude protein (NIRS) represented a wide range of values with high coefficients of variation (38 and 45 %), respectively (Table 6.2).

Table 6.2 Descriptive statistics of pasture biomass and standing crude protein for the calibration dataset (n=200)

Statistics	Pasture biomass (Kg ha <sup>-1</sup> )	Standing Crude Protein (Kg ha <sup>-1</sup> )
Mean	2391	506
Minimum	704	139
Maximum	4724	1270
Standard Deviation	924	232
Coefficient of Variation (CV %)	38.68	45.88

Vegetation indices were significantly correlated ( $P = 0.001$ ) to measured herbage DM biomass and standing crude protein (Table 6.3). The NDVI-1 and 2 show coefficients of determination ( $R^2$ ) values of 0.48 and 0.59, respectively for predicting the biomass. However, SR-1 and 2 gave a slightly better correlation than NDVI-1 and 2. Overall, PI gave highest the  $R^2$  value of 0.69. The  $R^2$  between measured standing crude protein and the vegetation indices varied between 0.50 and 0.77. The PI had the highest  $R^2$  value (0.77) and also the lowest RMSE (110 kg ha<sup>-1</sup>). The regression equations for validating the external dataset are stated in Table 6.3.

**Table 6.3 Regression equations for predicting biomass and standing crude protein from various indices**

Vegetation Index	Biomass (Kg ha <sup>-1</sup> )			Standing crude protein (Kg ha <sup>-1</sup> )		
	R <sup>2</sup>	RMSE	Equation	R <sup>2</sup>	RMSE	Equation
NDVI-1	0.48**	667	-2001+5555*NDVI-1	0.50***	163	-1627+2566 × NDVI-1
NDVI-2	0.59**	594	-83+7393*NDVI-2	0.63***	141	-336+2343 × NDVI-2
SR-1	0.61**	577	855+139*SR-1	0.68***	130	-22.2+42.5 × SR-1
SR-2	0.60**	581	-946+1613*SR-2	0.67***	133	-531+478 × SR-2
PI	0.69**	518	1137+2944*PI	0.77***	110	89.9+842 × PI

\*\*\*significance at  $P = 0.001$

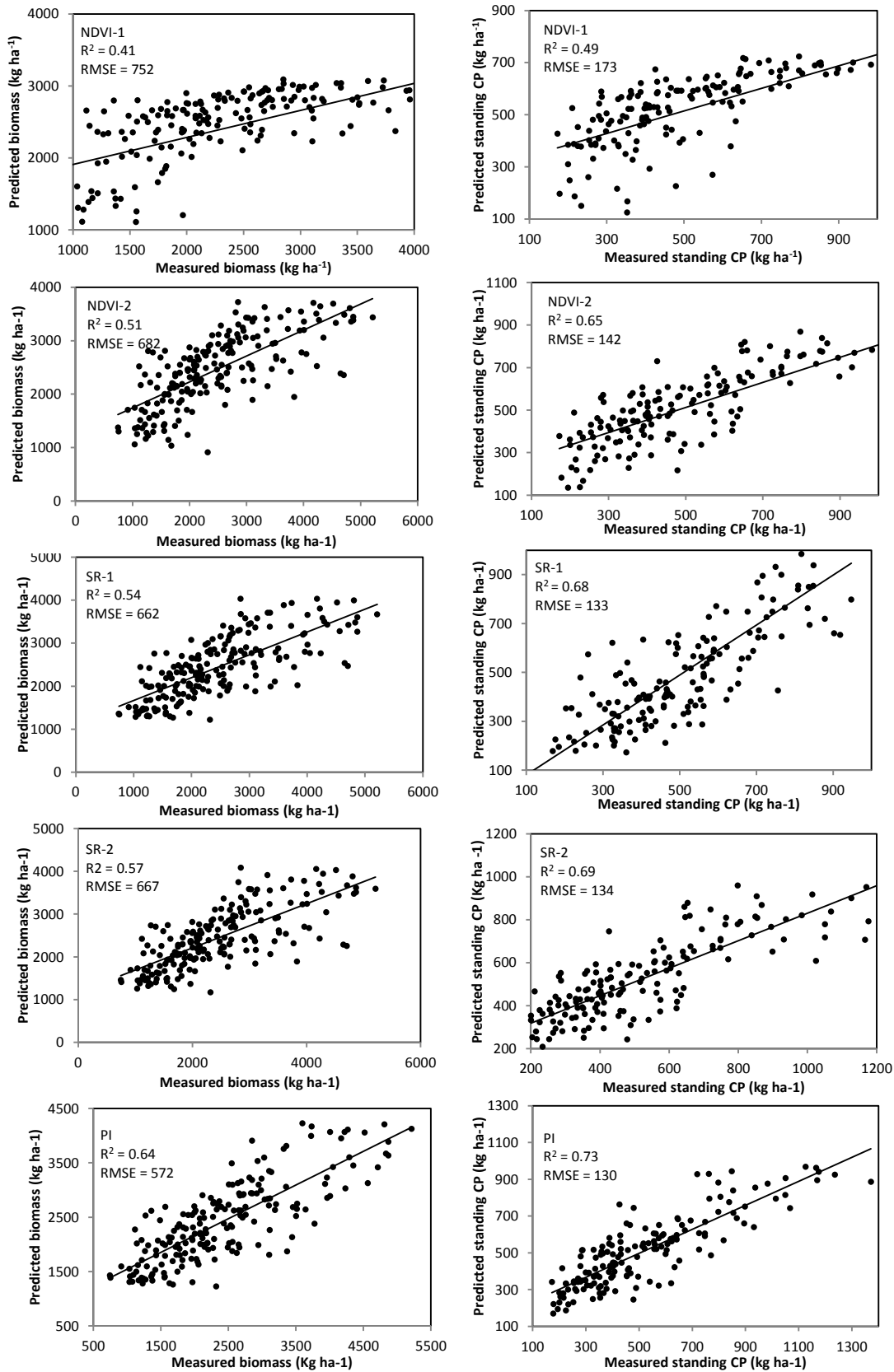


Figure 6.2 Relationship between measured and predicted herbage biomass in the validation dataset (n=207) using vegetation indices

The  $R^2$  between measured standing crude protein and the vegetation indices varied between 0.50 and 0.77. The PI had the highest  $R^2$  value (0.77) and also the lowest RMSE (110 kg ha<sup>-1</sup>). The regression equations for validating the external dataset are stated in Table 6.3. The scatter plots of measured and predicted values for validation dataset are depicted in Figure 6.2. The result show similar  $R^2$  and RMSE values. Overall, the PI predicted biomass and standing crude protein with high precision ( $R^2=0.64, 0.73$ , respectively) compared to other vegetation indices.

Utilising the calibration model and spatially rich data from the sensor, the spatial analysis was developed to examine the distribution pattern of biomass at the field scale. The semivariograms of the 10 fields for herbage biomass fitted well with spherical, exponential and linear with sill models. Most of the models (7) were fitted with an exponential function, two models with a spherical model, and the remaining with a linear with sill model. The geostatistical parameters of the fitted semivariogram models (Figure 6.3) are depicted in Table 4. The nugget and partial sill values were different for each field. The  $Q$  value for mapping herbage biomass ranged from 0.15 to 0.71. The highest  $Q$  value (0.71) was obtained on Field-4 whereas the lowest (0.15) on Field-8. The range ( $a$ ) values varied between fields from 4.1-32 m.

**Table 6.4 Summary of variogram parameters (nugget, partial sill and range), model type and root mean square error (RMSE) of pasture biomass at 10 fields**

Field Name	Size of the field (ha)	Nugget ( $C_0$ )	Partial sill (C)	Q ( $C_0/(C+C_0)$ )	Range	Model	RMSE
Field-1	0.42	20265	10811	0.65	30	Linear with sill	529
Field-2	0.71	16066	28092	0.36	23	Exponential	350
Field-3	1.37	18703	10005	0.65	4.3	Exponential	303
Field-4	9.87	23899	9320	0.71	32	Exponential	645
Field-5	3.82	2934	12851	0.18	29	Spherical	550
Field-6	5.77	2466	2553	0.49	9	Spherical	54
Field-7	5.95	5020	21472	0.18	28	Exponential	620
Field-8	1	761	4212	0.15	7.3	Exponential	25
Field-9	0.37	14290	10000	0.58	16	Exponential	540
Field-10	0.84	1105	511	0.68	4.1	Exponential	38

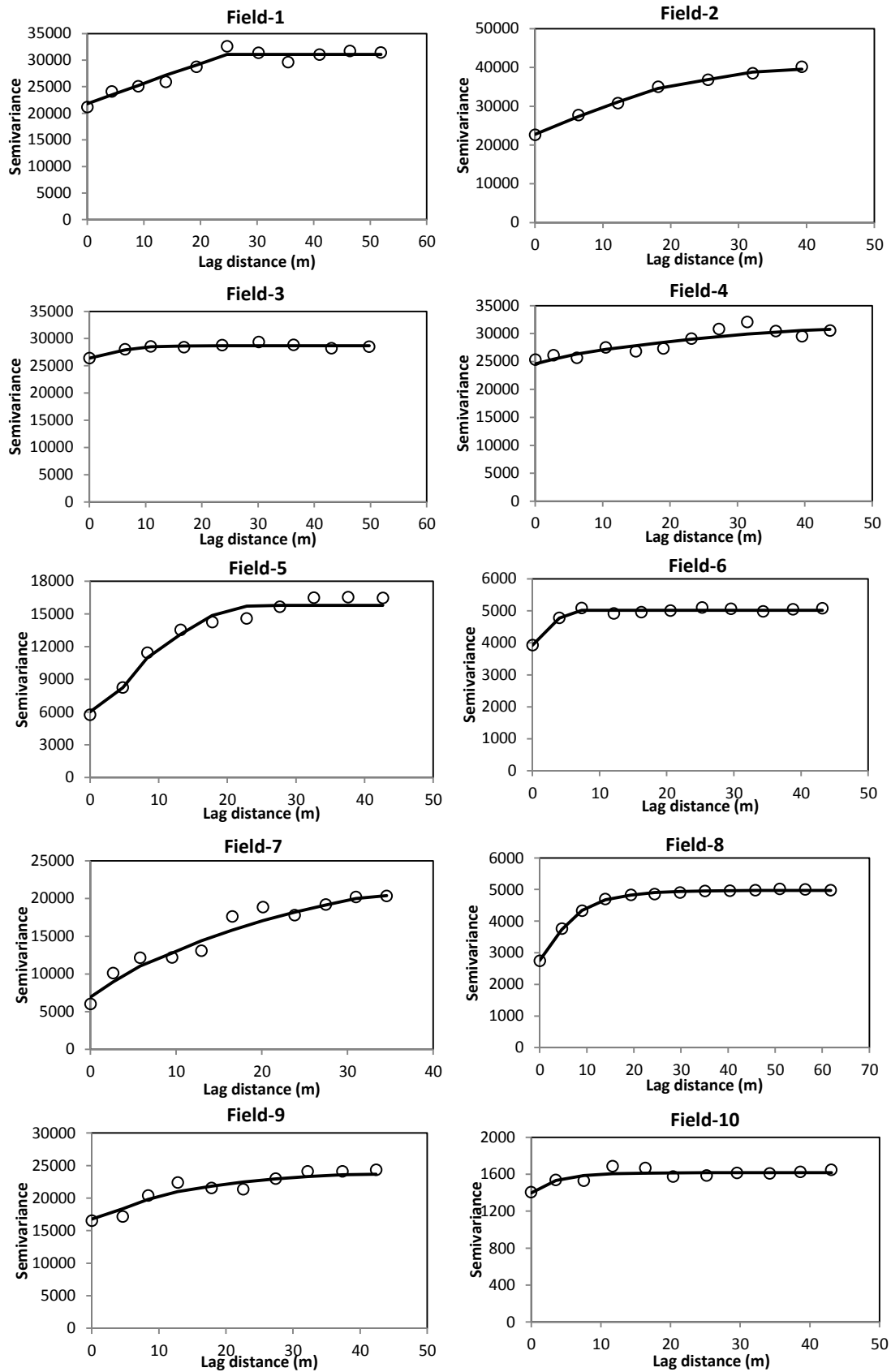


Figure 6.3 Semivariograms of herbage biomass of 10 fields

#### 6.4. Discussion

This study has confirmed that the active optical sensor can provide information on the variation of pasture biomass and SCP across farms and regions and within fields. This finding is consistent with the results of other researchers that examined field estimation of herbage biomass using ground-based active optical sensors. For example, Flynn *et al.* (2008) successfully estimated herbage biomass using NDVI, derived from the GreenSeeker™ sensor. Trotter *et al.* (2010) found a good correlation between green dry matter and soil adjusted vegetation index, computed from a Crop Circle sensor; Model:ACS-210. The wavebands selected in this study, were expected to be strongly correlated with vegetation biomass and protein (Donald *et al.*, 2010; Solari *et al.*, 2008; Stamatiadis *et al.*, 2009), and strong correlations were observed. From the various vegetation indices proposed, PI was substantially better correlated with measured values than other vegetation indices. The accuracy for pasture biomass (572 kg ha<sup>-1</sup>) was better and standing crude protein (130 kg ha<sup>-1</sup>) was slightly lower than the results of Starks *et al.* (2006a) where they reported 1160-1210 kg ha<sup>-1</sup> and 87.5-97.8 kg ha<sup>-1</sup> for biomass and SCP of Bermuda grass (*Cynodon dactylon* L.), respectively. Kawamura *et al.* (2005) reported that an enhanced vegetation index (EVI) (derived from a MODIS imagery) based model accounted for 80% of the variation in live biomass and 74% in SCP in the Xilingol steppe in central Inner Mongolia, China. The reasons for varying accuracy levels appearing in various publications are due mainly to the use of different sensors, waveband combinations and functional relationships. Moreover, most predictions were made on a single species, and in a specific location. Conversely, this study has covered samples from various locations, and multi species creating greater heterogeneity. Compared to two band indices (NDVI and SR), the three band index (PI) performed better when describing the variation of estimates, thus indicating accuracy increases with the number of wavebands.

In this study the semivariogram models and variogram parameter (nugget, partial sill and range) values of various fields were shown differently. This was not surprising since the spatial distribution of pasture biomass is heavily influenced by patch or selective grazing, stocking rate (Flynn *et al.*, 2008), elevation, nutrient status in soil and other environmental



factors. Most of the semivariograms were defined best by the exponential model. Similar model functions were found in pasture biomass studies (Flynn *et al.*, 2008). Conversely, Kawamura *et al.* (2008) found the spherical model to be the best fit for herbage biomass. The spatial dependency ( $Q$ ) for all fields was moderate or strong indicating the sampling interval was optimum. Comparable results (0.34-0.45) were found with Flynn *et al.* (2008). The large nugget variance for each field may indicate the possibility of a measurement error with the sensor. In order to reduce the nugget variance and to make a more-strongly spatial dependent model, the prediction accuracy of the sensor needs to be improved and a smaller lag distance is recommended. It should be noted that sensors with high spatial resolution are tend to be more advantageous for precision grassland management.

The observed range values across the fields suggest that the future sampling interval should be within 4 m for the three channel sensor. However, there are some cautionary remarks for using these results because they rely on the accuracy of the calibration model and sampling strategy done by the three channels Crop circle™ sensor.

Such fine scale spatial information of herbage biomass from sensors allows for more accurate, site-specific management, such as: variable rate fertiliser can be applied to avoid under and over-application of nutrients. A significant reduction in fertiliser use and higher economic returns can be achieved in pastures with the implementation of a variable rate fertiliser practice compared to blanket application (Murray & Yule, 2007). Similar advantages were also observed by López-Granados *et al.* (2004).

## 6.5. Conclusion

In this study, the results have shown that the active optical sensor (Crop circle™) has the potential to predict herbage biomass and SCP in heterogenic grassland systems. Compared to other vegetation indices, the three channels based PI performed best for predicting both properties. This sensor was also used to investigate the spatial variability of herbage biomass at the field scale. Semivariograms of the selected fields revealed that the spatial distribution for herbage biomass varies with field. Consequently, the generated spatial maps

enable farmers to adapt management practices such as variable rate fertiliser application, efficient feeding and manipulation of stocking rates which may lead to more profitable and sustainable dairy farming.

However, the regression model needs to be validated in different fields. For spatial analysis, the impact of sampling orientation and direction need to be further studied. The results from this preliminary study look promising but to provide pastoral farmers with usefully accurate pasture biomass data improvements in the technique are required or the optical sensor readings need to be paired with a co-variate pasture meter reading.

### **Acknowledgement**

We are very grateful to acknowledge the following people for their assistance during field sampling.

Michael Killick (Massey University, New Zealand) Grant Rennie, Linda Yates, Brian DeVantier, Ray Moss and Westlea Clarke-Hill (AgResearch, New Zealand) Laura Rossi (DairyNZ, New Zealand).



## **CHAPTER 7**

### **Overall Summary, Discussion and Recommendations for Future work**



This chapter reviews the findings of the present research, which examine the potential of proximal sensors for estimating the pasture quality and quantity parameters under field conditions, and it also presents recommendations for future research.

### **7.1. Overall Summary**

In dairy farming, real-time and non-destructive assessment of pasture quality allows the farmer to improve animal performance and milk production, through effective grazing management decisions. Remote sensing technology has been proved to have the potential to describe various vegetation features, due to that fact that the corresponding reflectance data is a function of biophysical and biochemical properties. Vegetation reflectance is a result of interaction between light and molecular bonds (C-O, O-H and N-H) of vegetation, which is why the reflectance is sensitive to several to several vegetation biochemical properties (Chapter 2, Section 2.2). Since the availability of remote sensing technologies, considerable progress has been made by researchers to determine vegetation characteristics (Chapter 2). Among these remote sensing tools, proximal sensors have shown more promise in commercial agriculture, due to the importance of real-time information for the producer, which does not require any atmospheric corrections. This study has evaluated potential proximal sensors, which estimate pasture quality parameters. In this study, hyperspectral (ASD FieldSpec® Pro field radiometer) and multispectral (CROPSCAN™ and Crop Circle™) sensors were investigated further, in order to estimate pasture quality parameters in uncontrolled and diverse environmental conditions. A large body of research (Chapter 2) has been completed, which has established strong relationships between canopy reflectance and vegetation characteristics, by using various approaches. However, to date, the proximal sensing of pasture quality has been limited.

#### **7.1.1. Hyperspectral sensor study**

The research in relation to describing pasture quality, through the use of hyperspectral sensors, has been very limited and there has only been success with a few parameters, such as crude protein and fibre. Furthermore, the conducted research has been constrained to specific location and hence, their practical ability in field conditions was not known. In

order to test the performance of a hyperspectral sensor to predict pasture quality parameters, within a range of uncontrolled environmental conditions, an experiment was conducted (Chapter 3). Canopy reflectance was acquired through a portable spectroradiometer (ASD FieldSpec® Pro), which has a spectral range from 350nm to 2500nm; a resolution of 1.4nm in the 350-1000nm; and 2nm in the 1000-2500nm region of the spectrum. This resolution was interpolated and reported in 1nm intervals. The sensor was equipped with a canopy pasture probe (CAPP), which was integrated with an artificial light source (50 Watt tungsten-quartz-halogen bulb), in order to ensure consistent illumination conditions and to avoid a windy environment. After recording the canopy reflectance, the spectral data was processed through pre-processing tools, in order to improve the spectral properties within the spectra.

The relationship between spectral data (reflectance values) and pasture quality parameter values (measured values) were established, by using a partial least squares regression (PLSR). PLSR is an effective method when dealing with larger number of variables (wavebands) than the number of samples: and those variables (wavebands) have a high intercorrelation. The number of PLS components was optimised by a leave-one-out cross-validation procedure. The accuracy of the models was evaluated by a coefficient of determination ( $R^2$ ); root mean square error (RMSE); root mean square error percentage (RMSE%) bias; ratio prediction to deviation (RPD); and Nash-Sutcliffe efficiency (NSE). The calibration models were developed in order to predict each pasture's quality parameter. The developed models were tested on an external dataset (validation dataset), in order to examine the prediction capability of those models. In validation, satisfactory predictions were obtained for CP, ADF, NDF, ash, DCAD, lignin, ME and OMD ( $0.65 \leq R^2 \leq 0.83$ ;  $1.70 \leq RPD \leq 2.46$ ): but lipid was poorly predicted ( $R^2$  0.55, RPD 1.44). These results have advanced our understanding that the majority of pasture quality parameters could be predicted with a hyperspectral sensor within uncontrolled and diverse environmental conditions. The reasons for the low accuracy of predicting lipid appears to be due to the low fraction present in the sample: and other various reasons. The wavelengths which had high importance in the PLSR model prediction were highlighted, by using the variable importance for the projection (VIP) method: and they are different for each pasture quality

parameter. These wavelengths could be useful when selecting the corresponding wavebands required from the multispectral sensors used for predicting pasture quality parameters.

### **7.1.2. Multispectral sensors study**

Although the results of Chapter 3 were satisfactory, these hyperspectral sensors are expensive and they involve significant data computation. Hence, researchers have been devoting their efforts to developing low cost instruments (such as multispectral sensors), in order to define pasture characteristics. However, studies related to pasture quality have been rare. In order to fill this gap, a multispectral sensor (CROPSCAN™) was tested, by collecting canopy reflectance from pasture samples (Chapter 4). This sensor possesses a limited number of wavebands (16). A series of three different empirical approaches (single band, vegetation indices and SMLR) were applied to the reflectance data, in order to estimate pasture quality parameters (Chapter 4). A single band approach resulted in lower prediction accuracy for each pasture quality parameter. New combinations of RDVI's were developed by utilising available wavebands (16) for assessing the pasture quality parameters. Overall, the nonlinear, exponential fit and RDVI indices models described ( $0.65 \leq R^2 \leq 0.85$ ) the variation of pasture quality parameters (CP, DCAD, ME and OMD) with reasonable accuracy, while CP, ash, DCAD, lipid, ME and OMD were estimated with moderate accuracy ( $0.60 \leq R^2 \leq 0.80$ ) by a SMLR model. However, ADF, NDF and lignin were poorly explained ( $0.40 \leq R^2 \leq 0.58$ ) by all the models.

In order to extend the potential of the CROPSCAN™ sensor and to determine temporal variations, it was further evaluated by including the datasets of different seasons (autumn, spring and summer) and the spectral data evaluated by PLSR (Chapter 5). In this study, PLSR used the information from all wavelengths to explain maximum variation and hence, accurate results were obtained. The global model successfully predicted ( $0.60 \leq R^2 \leq 0.67$ ) pasture quality parameters (CP, ADF, NDF, lignin, ME and OMD). More accurate results were achieved when PLSR models were developed separately for each season. The prediction results varied with season and quality parameter. This was partly due to the seasonal variations of pasture caused by various proportions of green and dead vegetation.



The level of accuracy of the seasonal models was close to the values of the hyperspectral results in Chapter 3. Therefore, the methods of study used in Chapters 4 and 5 could be used to determine pasture quality information and to extrapolate to the space and airborne sensors for regional scale mapping, which have similar wavebands.

Despite the CROPSCAN sensor having the ability to predict pasture quality information with moderate accuracy, this sensor relies on natural illumination for its light source. However, the illumination conditions were inconsistent, due to the unstable New Zealand weather conditions, such as high cloud cover and changing sun angle. Alternatively, active sensors (Crop Circle™) with a consistent artificial light source, may? could?become available for vegetation studies. With a similar sampling environment to Chapters 3, 4 and 5, a Crop Circle™ Model-ACS470 was used to estimate pasture biomass and standing crude protein. This sensor had three wavebands (two visible and one near infrared) for study. Various vegetation indices were used to establish the relationship between reflectance data and measured data. The results show that the new index, PI, has a high correlation with pasture biomass ( $R^2 = 0.69$ ;  $RMSE = 518 \text{ kg ha}^{-1}$ ) and standing crude protein ( $R^2 = 0.77$ ;  $RMSE = 110 \text{ kg ha}^{-1}$ ), compared to other indices. Spatial analysis was also undertaken from pasture biomass on ten randomly selected fields. From these results, it can be noted that the spatial dependency of the ten fields is moderate to strong: and it varies greatly between fields.

The achieved results of this dissertation demonstrated as follows:

- Proximal hyperspectral and multispectral sensor can be used to predict *in situ* pasture quality under diverse environmental conditions.
- Season-specific calibration models are recommended to quantify pasture quality, which improved the results as compared to global models.
- Pasture biomass and standing crude protein can be quantified using pasture index (derived from the reflectance of Crop Circle™)
- Spatial maps of pasture biomass and standing crude protein can be produced using Crop Circle™.

This quantitative description and assessment of pasture quality and quantity could enable farmers to optimise decisions as follows:

- Accurate feed quality information can be provided to improve animal performance whilst feed or pasture wastage can be minimised.
- The real-time information of pasture quality and quantity helps to monitor the feed status and identify where supplementary feed needs to be provided if inadequate pasture is available.
- Manipulation of stocking rates according to the pasture availability in paddock can be possible in order to fulfil the demand of every animal.
- Fertilisers can be applied when there is an exact demand for nutrients as it improves the fertiliser use efficiency and reduces nitrate leaching.
- Spatial variation of pasture characteristics can be measured when the sensor is integrated with global positioning system (GPS), as described in chapter 6. This provides precise information on pasture availability.
- Setting of break or virtual fences can be possible according to the spatial variation of pasture.
- Prescription maps can be developed based on the spatial information of pasture for applying variable rate fertilisers.
- Overall, uncertainty in decision making can be minimised.

## **7.2. Recommendations for future work**

- Even though the prediction of results of pasture quality parameters using PLSR was satisfactory, the other computational approaches (SVM, ANN and physically based approaches), listed in Chapter 2, need to be investigated as they may improve the prediction accuracy.

- Although proximal sensors provided satisfactory results for estimating pasture quality parameters, the study methods need to be extended for space and air borne sensing for regional scale mapping.
- The Chapter 4 clearly stated the impact of seasonal differences on prediction model accuracy. However, the reasons were not completely clear. As per the evidence of other published research reports the differences could be due to variation in botanical composition, vegetation fraction, plant structure and proportion of green and dead biomass. For this, further study should include the detail characteristics of pasture samples with a wide range of yield, percentage of botanics, green and dead vegetation, and water content. Moreover, significant effort will be required to collect enough samples in each season to provide a sufficient number of samples for developing robust models in future studies.
- The CROPSCAN™ instrument allowed the pasture quality parameters to be predicted with reasonable accuracy. In fact, this instrument may be affordable for consultants to use in the field to identify the quality of pasture in near real time. For this, further validation would require to develop robust calibrations.
- Experimental evidence of Fulkerson *et al.* (2005) suggests that accurate real-time measurement of pasture biomass can lead to improvements in pasture productivity and utilisation. Likewise, it was estimated that a 10% increase in pasture production was achieved using a C-Dax Pasture Meter (valued NZD \$ 5000) (Yule *et al.*, 2005). A key part of the process is to measure present performance in the field, this is only now starting to be completed for pasture mass. It is not yet clear what additional financial and productive benefits would be achieved by being able to measure pasture quality as part of pasture management system.

## **REFERENCES**



- Aiken, L. S., & West, S. G. (1991). *Multiple regression: Testing and interpreting interactions*. Newbury Park, CA.: Sage Publications, Inc.
- Albayrak, S. (2008). Use of Reflectance Measurements for the Detection of N, P, K, ADF and NDF Contents in Sainfoin Pasture. *Sensors*, 8(11), 7275-7286. doi: 10.3390/s8117275
- AOAC. (2005). *Official methods of analysis of AOAC International* (18th ed. Vol. 1). Gaithersburg, Md.: Association of Official Analytical Chemists Inc., AOAC International.
- ASD. (2010). FieldSpec<sup>®</sup> 3 User Manual. Boulder, CO 80301, USA: Analytical Spectral Devices Inc.
- Ausseil, A. G., Dymond, J. R., Dynes, R., Shepherd, J. D., DeVantier, B., & Sutherland, A. (2011). *Estimating pasture quality using Landsat ETM+: application for the greenhouse gas inventory of New Zealand*. Paper presented at the International Symposium on Remote Sensing for the Environment, Sydney, Australia.
- Baret, F., Guyot, G., & Major, D. (1989, 10-14th July). *TSAVI- A vegetation index which minimizes soil brightness effects on LAI and APAR estimation*. Paper presented at the Quantitative remote sensing: An economic tool for the Nineties; Proceedings of IGARSS '89 and Canadian Symposium on Remote Sensing, Vancouver, Canada.
- Beeri, O., Phillips, R., Hendrickson, J., Frank, A. B., & Kronberg, S. (2007). Estimating forage quantity and quality using aerial hyperspectral imagery for northern mixed-grass prairie. *Remote sensing of environment*, 110(2), 216-225.
- Berntsen, J., Thomsen, A., Schelde, K., Hansen, O., Knudsen, L., Broge, N., Hougaard, H., & Hørfarter, R. (2006). Algorithms for sensor-based redistribution of nitrogen fertilizer in winter wheat. *Precision Agriculture*, 7(2), 65-83. doi: 10.1007/s11119-006-9000-2
- Biewer, S., Erasmi, S., Fricke, T., & Wachendorf, M. (2009a). Prediction of yield and the contribution of legumes in legume-grass mixtures using field spectrometry. *Precision Agriculture*, 10(2), 128-144. doi: 10.1007/s11119-008-9078-9
- Biewer, S., Fricke, T., & Wachendorf, M. (2009b). Development of Canopy Reflectance Models to Predict Forage Quality of Legume-Grass Mixtures. *Crop Science*, 49(5), 1917-1926. doi: 10.2135/cropsci2008.11.0653

- Bonham-Carter, G. F. (1988). Numerical procedures and computer program for fitting an inverted gaussian model to vegetation reflectance data. *Computers & Geosciences*, 14(3), 339-356. doi: 10.1016/0098-3004(88)90065-9
- Broge, N. H., & Leblanc, E. (2000). Comparing prediction power and stability of broadband and hyperspectral vegetation indices for estimation of green leaf area index and canopy chlorophyll density. *Remote Sensing of Environment*, 76, 156-172. doi: 10.1016/S0034-4257(00)00197-8
- Bronson, K. F., Booker, J. D., Keeling, J. W., Boman, R. K., Wheeler, T. A., Lascano, R. J., & Nichols, R. L. (2005). Cotton Canopy Reflectance at Landscape Scale as Affected by Nitrogen Fertilization. *Agronomy Journal*, 97(3), 654-660. doi: 10.2134/agronj2004.0093
- Brown, M. E., Lary, D. J., Vrieling, A., Stathakis, D., & Mussa, H. (2008). Neural networks as a tool for constructing continuous NDVI time series from AVHRR and MODIS. *International Journal of Remote Sensing*, 29(24), 7141-7158.
- Cambardella, C. A., Moorman, T. B., Novak, J. M., Parkin, T. B., Karlen, D. L., Turco, R. F., & Konopka, A. E. (1994). Field-scale variability of soil properties in central Iowa soils. *Soil Science Society of America journal*, 58(5), 1501-1511.
- CCRS. (2011a, 15 July ). Fundamentals of Remote Sensing. A Canada Centre for Remote Sensing Remote Sensing Tutorial Retrieved 5 January, 2011, from <http://www.nrcan.gc.ca/earth-sciences/geography-boundary/remote-sensing/fundamentals/1430> [Accessed 5 January 2011].
- CCRS. (2011b). Glossary of remote sensing terms Retrieved 13 June, 2011, from [http://www.ccrs.nrcan.gc.ca/glossary/index\\_e.php?id=1602](http://www.ccrs.nrcan.gc.ca/glossary/index_e.php?id=1602)[Accesses 13 June 2011].
- Chappelle, E. W., Kim, M. S., & McMurtrey Iii, J. E. (1992). Ratio analysis of reflectance spectra (RARS): An algorithm for the remote estimation of the concentrations of chlorophyll A, chlorophyll B, and carotenoids in soybean leaves. *Remote Sensing of Environment*, 39(3), 239-247. doi: 10.1016/0034-4257(92)90089-3
- Chen, J. (1996). Evaluation of vegetation indices and a modified simple ratio for boreal applications. *Canadian Journal of Remote Sensing*, 22(3), 229-242.
- Cho, M. A. (2007). *Hyperspectral remote sensing of biochemical and biophysical parameters*. PhD thesis, Wageningen University, Enschede, the Netherlands.

- Retrieved from [http://www.itc.nl/library/papers\\_2007/phd/cho.pdf](http://www.itc.nl/library/papers_2007/phd/cho.pdf) [Accessed 26 April 2010].
- Cho, M. A., & Skidmore, A. K. (2006). A new technique for extracting the red edge position from hyperspectral data: The linear extrapolation method. *Remote Sensing of Environment*, 101(2), 181-193. doi: 10.1016/j.rse.2005.12.011
- Clevers, J. G. P. W., De Jong, S. M., Epema, G. F., Van Der Meer, F. D., Bakker, W. H., Skidmore, A. K., & Scholte, K. H. (2002). Derivation of the red edge index using the MERIS standard band setting. *International Journal of Remote Sensing*, 23(16), 3169-3184. doi: 10.1080/01431160110104647
- Colombo, R., Bellingeri, D., Fasolini, D., & Marino, C. (2003). Retrieval of leaf area index in different vegetation types using high resolution satellite data. *Remote Sensing of Environment*, 86(1), 120-131.
- Correll, O., Isselstein, J., & Pavlu, V. (2003). Studying spatial and temporal dynamics of sward structure at low stocking densities: the use of an extended rising-plate-meter method. *Grass and Forage Science*, 58(4), 450-454. doi: 10.1111/j.1365-2494.2003.00387.x
- Corson, D., Waghorn, G., Ulyatt, M., & Lee, J. (1999). NIRS: forage analysis and livestock feeding. *Proceedings of the New Zealand Grassland Association*, 61, 127-132.
- Cosgrove, G., Betteridge, K., Thomas, V., & Corson, D. (1998). *Sampling strategy for estimating dairy-pasture quality*. Paper presented at the Proceedings of the New Zealand Society of Animal Production, New Zealand.
- Cropscan<sup>TM</sup>. (2001). Multi Spectral Radiometer (MSR) User's Manual: CROPSCAN Inc., Rochester, MN 55906 USA.
- Curran, P. J. (1989). Remote sensing of foliar chemistry. *Remote Sensing of Environment*, 30(3), 271-278. doi: 10.1016/0034-4257(89)90069-2
- Curran, P. J., & Atkinson, P. M. (1998). Geostatistics and remote sensing. *Progress in Physical Geography*, 22(1), 61-78. doi: 10.1177/030913339802200103
- Curran, P. J., Dungan, J. L., & Peterson, D. L. (2001). Estimating the foliar biochemical concentration of leaves with reflectance spectrometry: Testing the Kokaly and Clark methodologies. *Remote Sensing of Environment*, 76(3), 349-359.



- Darvishzadeh, R., Skidmore, A., Schlerf, M., Atzberger, C., Corsi, F., & Cho, M. (2008). LAI and chlorophyll estimation for a heterogeneous grassland using hyperspectral measurements. *ISPRS Journal of Photogrammetry and Remote Sensing*, *63*(4), 409-426. doi: 10.1016/j.isprsjprs.2008.01.001
- Daughtry, C. S. T., Walthall, C. L., Kim, M. S., de Colstoun, E. B., & McMurtrey Iii, J. E. (2000). Estimating corn leaf chlorophyll concentration from leaf and canopy reflectance. *Remote Sensing of Environment*, *74*(2), 229-239.
- Davies, A. M. C., & Fearn, T. (2006). Back to basics: calibration statistics. *Spectroscopy Europe*, *18*(2), 31-32.
- Dawson, T. P., & Curran, P. (1998). Technical note. A new technique for interpolating the reflectance red edge position. *International Journal of Remote Sensing*, *19*(11), 2133-2140.
- Dawson, T. P., Curran, P. J., & Plummer, S. E. (1998). LIBERTY--Modeling the Effects of Leaf Biochemical Concentration on Reflectance Spectra. *Remote Sensing of Environment*, *65*(1), 50-60. doi: 10.1016/s0034-4257(98)00007-8
- Donald, G., Gherardi, S., Edirisinghe, A., Gittins, S., Henry, D., & Mata, G. (2010). Using MODIS imagery, climate and soil data to estimate pasture growth rates on farms in the south-west of Western Australia. *Animal Production Science*, *50*(6), 611-615.
- Duncan, J., Stow, D., Franklin, J., & Hope, A. (1993). Assessing the relationship between spectral vegetation indices and shrub cover in the Jornada Basin, New Mexico. *International Journal of Remote Sensing*, *14*(18), 3395-3416.
- Durbha, S. S., King, R. L., & Younan, N. H. (2007). Support vector machines regression for retrieval of leaf area index from multiangle imaging spectroradiometer. *Remote Sensing of Environment*, *107*(1-2), 348-361. doi: 10.1016/j.rse.2006.09.031
- Edirisinghe, A., Donald, G. E., Hill, M. J., & Henry, D. (2002, April 8-12, 2002). *Precision management of feed supply through timely delivery of biomass and growth rate estimates of western Australian annual pastures*. Paper presented at the 29th International Symposium on Remote Sensing of Environment, Buenos Aires, Argentina. CD-Rom.

- Eitel, J., Keefe, R., Long, D., Davis, A., & Vierling, L. (2010). Active Ground Optical Remote Sensing for Improved Monitoring of Seedling Stress in Nurseries. *Sensors*, 10(4), 2843-2850.
- Esbensen, K. H., Guyot, D., Westad, F., & Houmoller, L. P. (2009). *Multivariate data analysis - In Practice: An introduction to multivariate data analysis and experimental design* (5 ed.): CAMO: Oslo, Norway.
- FAO. (2010). Greenhouse Gas Emissions from the Dairy Sector: A Life Cycle Assessment (A. P. a. Health, Trans.). Rome, Italy: Food and Agriculture Organization.
- Feret, J.-B., François, C., Asner, G. P., Gitelson, A. A., Martin, R. E., Bidel, L. P. R., Ustin, S. L., le Maire, G., & Jacquemoud, S. (2008). PROSPECT-4 and 5: Advances in the leaf optical properties model separating photosynthetic pigments. *Remote Sensing of Environment*, 112(6), 3030-3043.
- FertResearch. (2009). New Zealand's fertiliser industry 2008–2009, Annual Update. PO Box 11519 , Manners Street Central , Wellington 6142.
- Flynn, E. S. (2006). *Using NDVI as a Pasture Management Tool*. M.Sc. thesis, University of Kentucky, Lexington, Kentucky. Retrieved from <http://hdl.handle.net/10225/533> [Accessed 12 Spetember 2009].
- Flynn, E. S., Dougherty, C. T., & Wendroth, O. (2008). Assessment of Pasture Biomass with the Normalized Difference Vegetation Index from Active Ground-Based Sensors. *Agronomy Journal*, 100(1), 114-121. doi: 10.2134/agrojn12006.0363
- Fonterra. (2010). Dairy's role in sustaining New Zealand. Wellington, New Zealand: New Zealand Institute of Economic Research Inc.
- Frame, J. (1993). Herbage mass. In A. Davies (Ed.), *Sward measurement handbook* (pp. 59-63). Reading, United Kingdom: British Grassland Society.
- Fulkerson, W., McKean, K., Nandra, K., & Barchia, I. (2005). Benefits of accurately allocating feed on a daily basis to dairy cows grazing pasture. *Australian Journal of Experimental Agriculture*, 45(4), 331-336.
- Gamon, J. A., Field, C. B., Goulden, M. L., Griffin, K. L., Hartley, A. E., Joel, G., Penuelas, J., & Valentini, R. (1995). Relationships Between NDVI, Canopy Structure, and Photosynthesis in Three Californian Vegetation Types. *Ecological Applications*, 5(1), 28-41.

- Gamon, J. A., & Surfus, J. S. (1999). Assessing leaf pigment content and activity with a reflectometer. *New Phytologist*, 143(1), 105-117.
- Gao, B. C. (1996). NDWI--A normalized difference water index for remote sensing of vegetation liquid water from space. *Remote Sensing of Environment*, 58(3), 257-266.
- Gao, J. (2006). Quantification of grassland properties: how it can benefit from geoinformatic technologies? *International Journal of Remote Sensing*, 27(7), 1351-1366.
- Gausman, H. W. (1974). Leaf reflectance of near-infrared. *Photogrammetric Engineering*, 40(2), 183-191.
- Gebbers, R., & Adamchuk, V. I. (2010). Precision Agriculture and Food Security. *Science*, 327(5967), 828-831. doi: 10.1126/science.1183899
- Gitelson, A. A., Merzlyak, M. N., & Chivkunova, O. B. (2001). Optical Properties and Nondestructive Estimation of Anthocyanin Content in Plant Leaves. *Photochemistry and Photobiology*, 74(1), 38-45. doi: 10.1562/0031-8655(2001)0740038opaneo2.0.co2
- Gitelson, A. A., Vina, A., Ciganda, V., Rundquist, D. C., & Arkebauer, T. J. (2005). Remote estimation of canopy chlorophyll content in crops. *Geophysical Research Letters*, 32, L08403.
- Gitelson, A. A., Zur, Y., Chivkunova, O. B., & Merzlyak, M. N. (2002). Assessing Carotenoid Content in Plant Leaves with Reflectance Spectroscopy. *Photochemistry and Photobiology*, 75(3), 272-281. doi: 10.1562/0031-8655(2002)0750272accipl2.0.co2
- Grossman, Y. L., Ustin, S. L., Jacquemoud, S., Sanderson, E. W., Schmuck, G., & Verdebout, J. (1996). Critique of stepwise multiple linear regression for the extraction of leaf biochemistry information from leaf reflectance data. *Remote Sensing of Environment*, 56(3), 182-193.
- Guyot, G., & Baret, F. (1988, 18-22 January). *Utilisation de la haute resolution spectrale pour suivre l'etat des couverts vegetaux*. Paper presented at the Proceedings of the 4th International colloquium on spectral signatures of objects in remote sensing, Assois, France.

- Haboudane, D., Miller, J. R., Pattey, E., Zarco-Tejada, P. J., & Strachan, I. B. (2004). Hyperspectral vegetation indices and novel algorithms for predicting green LAI of crop canopies: Modeling and validation in the context of precision agriculture. *Remote Sensing of Environment*, *90*(3), 337-352. doi: 10.1016/j.rse.2003.12.013
- Haboudane, D., Miller, J. R., Tremblay, N., Zarco-Tejada, P. J., & Dextraze, L. (2002). Integrated narrow-band vegetation indices for prediction of crop chlorophyll content for application to precision agriculture. *Remote Sensing of Environment*, *81*(2), 416-426.
- Hansen, P. M., & Schjoerring, J. K. (2003). Reflectance measurement of canopy biomass and nitrogen status in wheat crops using normalized difference vegetation indices and partial least squares regression. *Remote Sensing of Environment*, *86*(4), 542-553. doi: 10.1016/s0034-4257(03)00131-7
- He, Y., Guo, X., & Wilmshurst, J. F. (2009). Reflectance measures of grassland biophysical structure. *International Journal of Remote Sensing*, *30*(10), 2509 - 2521.
- Hedley, C. B., & Yule, I. J. (2009). Soil water status mapping and two variable-rate irrigation scenarios. *Precision Agriculture*, *10*(4), 342-355.
- Hill, M. J., Vickery, P. J., Furnival, E. P., & Donald, G. E. (1999). Pasture Land Cover in Eastern Australia from NOAA-AVHRR NDVI and Classified Landsat TM. *Remote Sensing of Environment*, *67*(1), 32-50. doi: 10.1016/s0034-4257(98)00075-3
- Hodgson, J., & Brookes, I. M. (1999). Nutrition of grazing animals. In J. White & J. Hodgson (Eds.), *New Zealand pasture and crop science* (pp. 117-132). Auckland, N.Z: Oxford University Press.
- Hodgson, J., Matthews, P. N. P., Matthew, C., & Lucas, R. J. (2000). Pasture measurement. In J. White & J. Hodgson (Eds.), *New Zealand pasture and crop science* (pp. 59-65): Oxford University Press.
- Holmes, C. W., Wilson, G. F., Mackenzie, D. D. S., Flux, D. S., Brookes, I. M., & Davey, A. W. F. (2007). *Milk production from pasture*. Palmerston North, New Zealand: Massey University.
- Horler, D., Dockray, M., & Barber, J. (1983). The red edge of plant leaf reflectance. *International Journal of Remote Sensing*, *4*, 273-288.

- Huemmrich, K. F., & Goward, S. N. (1997). Vegetation canopy PAR absorptance and NDVI: An assessment for ten tree species with the SAIL model. *Remote Sensing of Environment*, 61(2), 254-269. doi: 10.1016/s0034-4257(97)00042-4
- Huete, A. R. (1988). A soil-adjusted vegetation index (SAVI). *Remote Sensing of Environment*, 25(3), 295-309.
- Huete, A. R., Jackson, R. D., & Post, D. F. (1985). Spectral response of a plant canopy with different soil backgrounds. *Remote Sensing of Environment*, 17(1), 37-53.
- Irisarri, J. G. N., Oesterheld, M., Verón, S. R., & Paruelo, J. M. (2009). Grass species differentiation through canopy hyperspectral reflectance. *International Journal of Remote Sensing*, 30(22), 5959 - 5975.
- Jacquemoud, S., & Baret, F. (1990). PROSPECT: A model of leaf optical properties spectra. *Remote Sensing of Environment*, 34(2), 75-91.
- Jacquemoud, S., Baret, F., Andrieu, B., Danson, F. M., & Jaggard, K. (1995). Extraction of vegetation biophysical parameters by inversion of the PROSPECT + SAIL models on sugar beet canopy reflectance data. Application to TM and AVIRIS sensors. *Remote Sensing of Environment*, 52(3), 163-172. doi: 10.1016/0034-4257(95)00018-v
- Jago, R. A., Cutler, M. E. J., & Curran, P. J. (1999). Estimating Canopy Chlorophyll Concentration from Field and Airborne Spectra. *Remote Sensing of Environment*, 68(3), 217-224. doi: 10.1016/S0034-4257(98)00113-8
- Jiang, Y., & Carrow, R. N. (2007). Broadband Spectral Reflectance Models of Turfgrass Species and Cultivars to Drought Stress. *Crop Science*, 47(4), 1611-1618. doi: 10.2135/cropsci2006.09.0617
- Jongschaap, R. E. E. (2006). Run-time calibration of simulation models by integrating remote sensing estimates of leaf area index and canopy nitrogen. *European Journal of Agronomy*, 24(4), 316-324. doi: 10.1016/j.eja.2005.10.009
- Jordan, C. F. (1969). Derivation of Leaf-Area Index from Quality of Light on the Forest Floor. *Ecology*, 50(4), 663-666.
- Jungho Im, J. R. J. (2008). Hyperspectral Remote Sensing of Vegetation. *Geography Compass*, 2(6), 1943-1961. doi: 10.1111/j.1749-8198.2008.00182.x

- Kaufman, Y., & Tanre, D. (1992). Atmospherically resistant vegetation index (ARVI) for EOS-MODIS. *IEEE Transactions on Geoscience and Remote Sensing*, 30(2), 261-270.
- Kawamura, K., Akiyama, T., Yokota, H., Tsutsumi, M., Yasuda, T., Watanabe, O., Wang, G., & Wang, S. (2005). Monitoring of forage conditions with MODIS imagery in the Xilingol steppe, Inner Mongolia. *International Journal of Remote Sensing*, 26(7), 1423-1436. doi: 10.1080/01431160512331326783
- Kawamura, K., Betteridge, K., Sanches, I. D., Tuohy, M. P., Costall, D., & Inoue, Y. (2009). Field radiometer with canopy pasture probe as a potential tool to estimate and map pasture biomass and mineral components: a case study in the Lake Taupo catchment, New Zealand. *New Zealand Journal of Agricultural Research*, 52, 417-434.
- Kawamura, K., Watanabe, N., Sakanoue, S., & Inoue, Y. (2008). Estimating forage biomass and quality in a mixed sown pasture based on partial least squares regression with waveband selection. *Grassland Science*, 54(3), 131-145.
- Kimes, D. S., Nelson, R. F., Manry, M. T., & Fung, A. K. (1998). Review article: Attributes of neural networks for extracting continuous vegetation variables from optical and radar measurements. *International Journal of Remote Sensing*, 19(14), 2639 - 2663.
- Kokaly, R. F. (2001). Investigating a Physical Basis for Spectroscopic Estimates of Leaf Nitrogen Concentration. *Remote Sensing of Environment*, 75(2), 153-161. doi: 10.1016/S0034-4257(00)00163-2
- Kokaly, R. F., & Clark, R. N. (1999). Spectroscopic Determination of Leaf Biochemistry Using Band-Depth Analysis of Absorption Features and Stepwise Multiple Linear Regression. *Remote Sensing of Environment*, 67(3), 267-287. doi: 10.1016/S0034-4257(98)00084-4
- Kumar, L., Schmidt, K., Dury, S., & Skidmore, A. (2002). Imaging spectrometry and vegetation science. In F. D. van der Meer & S. M. de Jong (Eds.), *Imaging spectrometry -Basic Principles and Prospective Applications* (1 ed., Vol. 4, pp. 111-156): Kluwer Academic Publishers. (Reprinted from: 3).

- Kusumo, B. H. (2009). *Development of field techniques to predict soil carbon, soil nitrogen and root density from soil spectral reflectance*. PhD thesis, Massey University, Palmerston North, New Zealand. Retrieved from <http://hdl.handle.net/10179/1015> [Accessed 15 March 2011].
- Kusumo, B. H., Hedley, C., Hedley, M., Hueni, A., Tuohy, M., & Arnold, G. (2008). The use of diffuse reflectance spectroscopy for in situ carbon and nitrogen analysis of pastoral soils. *Australian Journal of Soil Research*, 46(6-7), 623-635. doi: 10.1071/SR08118
- Kusumo, B. H., Hedley, M. J., Hedley, C. B., Arnold, G. C., & Tuohy, M. P. (2009a). Predicting pasture root density from soil spectral reflectance: field measurement. *European Journal of Soil Science*, 61(1), 1-13. doi: 10.1111/j.1365-2389.2009.01199.x
- Kusumo, B. H., Hedley, M. J., Hedley, C. B., Hueni, A., Arnold, G. C., & Tuohy, M. P. (2009b). The use of Vis-NIR spectral reflectance for determining root density: evaluation of ryegrass roots in a glasshouse trial. *European Journal of Soil Science*, 60(1), 22-32. doi: 10.1111/j.1365-2389.2008.01093.x
- Large, E. C. (1954). Growth stages in cereals illustration of the Feekes scale. *Plant Pathology*, 3(4), 128-129. doi: 10.1111/j.1365-3059.1954.tb00716.x
- Lary, D. J. (2010). Artificial Intelligence in Geoscience and Remote Sensing In P. Imperatore & D. Riccio (Eds.), *Geoscience and Remote Sensing, New Achievements* (pp. 508): InTech.
- Lebot, V., Champagne, A., Malapa, R., & Shiley, D. (2009). NIR Determination of Major Constituents in Tropical Root and Tuber Crop Flours. *Journal of Agricultural and Food Chemistry*, 57(22), 10539-10547. doi: 10.1021/jf902675n
- Legates, D. R., & McCabe, G. J. J. (1999). Evaluating the use of “goodness-of-fit” Measures in hydrologic and hydroclimatic model validation. *Water Resource Research*, 35(1), 233-241. doi: 10.1029/1998wr900018
- Li, F., Miao, Y., Hennig, S., Gnyp, M., Chen, X., Jia, L., & Bareth, G. (2010). Evaluating hyperspectral vegetation indices for estimating nitrogen concentration of winter wheat at different growth stages. *Precision Agriculture*, 11(4), 335-357. doi: 10.1007/s11119-010-9165-6

- Lillesand, T. M., Kiefer, R. W., & Chipman, J. W. (2004). *Remote sensing and image interpretation*: John Wiley & Sons Ltd.
- Liu, H. Q., & Huete, A. (1995). A feedback based modification of the NDVI to minimize canopy background and atmospheric noise. *IEEE Transactions on Geoscience and Remote Sensing*, 33(2), 457-465.
- Liu, J., Miller, J. R., Pattey, E., Haboudane, D., Strachan, I. B., & Hinthner, M. (2004, 20-24 Sep, 2004). *Monitoring crop biomass accumulation using multi-temporal hyperspectral remote sensing data*. Paper presented at the Geoscience and Remote Sensing Symposium, IGARSS '04. Proceedings.
- López-Granados, F., Jurado-Expósito, M., Álamo, S., & García-Torres, L. (2004). Leaf nutrient spatial variability and site-specific fertilization maps within olive (*Olea europaea* L.) orchards. *European Journal of Agronomy*, 21(2), 209-222. doi: 10.1016/j.eja.2003.08.005
- Marten, G. C., Halgerson, J. L., & Cherney, J. H. (1983). Quality Prediction of Small Grain Forages by Near Infrared Reflectance Spectroscopy. *Crop Science*, 23(1), 94-96.
- Marten, G. C., Shenk, J. S., & Barton, F. E. I. (1985). Near Infrared Reflectance Spectroscopy (NIRS): Analysis of forage quality *Agriculture handbook : No.643* (pp. 96): United States Dept. of Agriculture, Agricultural Research Service.
- Martin, M. E., & Aber, J. D. (1997). High spectral resolution remote sensing of forest canopy lignin, nitrogen, and ecosystem processes. *Ecological Applications*, 7(2), 431-443.
- Matson, P., Johnson, L., Billow, C., Miller, J., & Pu, R. (1994). Seasonal Patterns and Remote Spectral Estimation of Canopy Chemistry Across the Oregon Transect. *Ecological Applications*, 4(2), 280-298.
- Melgani, F., & Bruzzone, L. (2004). Classification of hyperspectral remote sensing images with support vector machines. *IEEE Transactions on Geoscience and Remote Sensing* 42(8), 1778-1790.
- Melyukhina, O. (2011). Risk Management in Agriculture in New Zealand *OECD Food, Agriculture and Fisheries Working Papers* (Vol. 42): OECD.
- MfE. (2008). Fact sheet-21 Agriculture in the emissions trading scheme. PO Box 10362, Wellington, New Zealand.



- Miehle, P., Livesley, S., Li, C., Feikema, P., Adams, M., & Arndt, S. (2006). Quantifying uncertainty from large-scale model predictions of forest carbon dynamics. *Global Change Biology*, 12(8), 1421-1434. doi: 10.1111/j.1365-2486.2006.01176.x
- Miller, J. N., & Miller, J. C. (2005). *Statistics and chemometrics for analytical chemistry*: Pearson Prentice Hall, Harlow.
- Miller, J. R., Hare, E. W., & Wu, J. (1990). Quantitative characterization of the vegetation red edge reflectance. I, An inverted-Gaussian reflectance model. *International Journal of Remote Sensing*, 11(10), 1755-1773.
- Minasny, B., McBratney, A. B., & Whelan, B. M. (2005). VESPER (Variogram Estimation and Spatial Prediction plus Error) (Version 1.62). McMillan, Building A05, New South Wales: Australian Centre for Precision Agriculture, The University of Sydney. Retrieved from <http://www.usyd.edu.au/agriculture/acpa/software/vesper.shtml> [Accessed 10 April 2010].
- MINITAB. (2007). MINITAB Statistical Software (Version 15): Minitab Inc., State College, PA.
- Montandon, L. M., & Small, E. E. (2008). The impact of soil reflectance on the quantification of the green vegetation fraction from NDVI. *Remote Sensing of Environment*, 112(4), 1835-1845. doi: 10.1016/j.rse.2007.09.007
- Moriasi, D. N., Arnold, J. G., Van Liew, M. W., Bingner, R. L., Harmel, R. D., & Veith, T. L. (2007). Model evaluation guidelines for systematic quantification of accuracy in watershed simulations. *Transactions of the ASABE*, 50(3), 885-900.
- Mosali, J. (2007). Use of In-Season Reflectance for Predicting Yield Potential in Bermudagrass. *Communications in Soil Science and Plant Analysis*, 38(11), 1519-1531.
- Mullen, R. W., Freeman, K. W., Raun, W. R., Johnson, G. V., Stone, M. L., & Solie, J. B. (2003). Identifying an In-Season Response Index and the Potential to Increase Wheat Yield with Nitrogen *Agronomy Journal*, 95(2), 347-351.
- Murray, R. I., & Yule, I. J. (2007). Developing variable rate application technology: Economic impact for farm owners and topdressing operators. *New Zealand Journal of Agricultural Research*, 50(1), 65-72. doi: 10.1080/00288230709510283

- Mutanga, O. (2004). *Hyperspectral remote sensing of tropical grass quality and quantity*. PhD thesis, Wageningen University, Wageningen, The Netherlands.
- Mutanga, O., & Skidmore, A. (2003). *Continuum-removed absorption features estimate tropical savanna grass quality in situ*. Paper presented at the Proceedings of the 3rd EARSeL workshop on imaging spectroscopy, Herrsching, Germany.
- Mutanga, O., & Skidmore, A. K. (2004a). Integrating imaging spectroscopy and neural networks to map grass quality in the Kruger National Park, South Africa. *Remote Sensing of Environment*, 90(1), 104-115. doi: 10.1016/j.rse.2003.12.004
- Mutanga, O., & Skidmore, A. K. (2004b). Narrow band vegetation indices overcome the saturation problem in biomass estimation. *International Journal of Remote Sensing*, 25(19), 3999-4014. doi: 10.1080/01431160310001654923
- Mutanga, O., & Skidmore, A. K. (2007). Red edge shift and biochemical content in grass canopies. *ISPRS Journal of Photogrammetry and Remote Sensing*, 62(1), 34-42. doi: 10.1016/j.isprsjprs.2007.02.001
- Mutanga, O., Skidmore, A. K., Kumar, L., & Ferwerda, J. (2005). Estimating tropical pasture quality at canopy level using band depth analysis with continuum removal in the visible domain. *International Journal of Remote Sensing*, 26(6), 1093 - 1108.
- NASA. (1994). Accelerated Canopy Chemistry Program. In J. Aber (Ed.), *Final Report to NASA-EOS-IWG*. Washington, DC: National Aeronautics and Space Administration.
- NASA. (1998). The remote sensing tutorial Retrieved from <http://rst.gsfc.nasa.gov/> [Accessed 28 April 2010].
- Nash, J. E., & Sutcliffe, J. V. (1970). River flow forecasting through conceptual models part I - A discussion of principles. *Journal of hydrology*, 10(3), 282-290. doi: 10.1016/0022-1694(70)90255-6
- Nguyen, H., Kim, J., Nguyen, A., Nguyen, L., Shin, J., & Lee, B.-W. (2006). Using canopy reflectance and partial least squares regression to calculate within-field statistical variation in crop growth and nitrogen status of rice. *Precision Agriculture*, 7(4), 249-264. doi: 10.1007/s11119-006-9010-0
- Ollinger, S. V., Smith, M. L., Martin, M. E., Hallett, R. A., Goodale, C. L., & Aber, J. D. (2002). Regional variation in foliar chemistry and N cycling among forests of

- diverse history and composition. *Ecology*, 83(2), 339-355. doi: 10.1890/0012-9658(2002)083[0339:rvifca]2.0.co;2
- Ozaki, Y., McClure, W., & Christy, A. (2005). Spectral analysis. In Y. Ozaki, W. McClure & A. Christy (Eds.), *Near infrared spectroscopy in food science and technology*. New Jersey: Wiley-Interscience, John Wiley & Sons, Inc. Hoboken
- Peñuelas, J., Gamon, J. A., Fredeen, A. L., Merino, J., & Field, C. B. (1994). Reflectance indices associated with physiological changes in nitrogen- and water-limited sunflower leaves. *Remote Sensing of Environment*, 48(2), 135-146. doi: 10.1016/0034-4257(94)90136-8
- Penuelas, J., Pinol, J., Ogaya, R., & Filella, I. (1997). Estimation of plant water concentration by the reflectance Water Index WI (R900/R970). *International Journal of Remote Sensing*, 18(13), 2869-2875. doi: 10.1080/014311697217396
- Prieto, N., Andrés, S., Giráldez, F. J., Mantecón, A. R., & Lavín, P. (2006). Potential use of near infrared reflectance spectroscopy (NIRS) for the estimation of chemical composition of oxen meat samples. *Meat Science*, 74(3), 487-496. doi: 10.1016/j.meatsci.2006.04.030
- Pullanagari, R. R., Yule, I., Tuohy, M., Hedley, M., Dynes, R., & King, W. (2012a). In-field hyperspectral proximal sensing for estimating quality parameters of mixed pasture. *Precision Agriculture*, 13(3), 351-369. doi: 10.1007/s11119-011-9251-4
- Pullanagari, R. R., Yule, I. J., Hedley, M. J., Tuohy, M. P., Dynes, R. A., & King, W. M. (2012b). Multispectral Radiometry to Estimate Pasture Quality Components. *Precision Agriculture*, (Accepted).
- Pullanagari, R. R., Yule, I. J., King, W., Dalley, D., & Dynes, R. (2011a). The use of optical sensors to estimate pasture quality. *International Journal on Smart Sensing and Intelligent Systems*, 4(1), 125-137.
- Qi, J., Chehbouni, A., Huete, A. R., Kerr, Y. H., & Sorooshian, S. (1994). A modified soil adjusted vegetation index. *Remote Sensing of Environment*, 48(2), 119-126.
- Raun, W., Solie, J., Johnson, G., Stone, M., Mullen, R., Freeman, K., Thomason, W., & Lukina, E. (2002). Improving Nitrogen Use Efficiency in Cereal Grain Production with Optical Sensing and Variable Rate Application *Agronomy Journal*, 94(4), 815-820.

- Raun, W. R., Solie, J. B., Johnson, G. V., Stone, M. L., Lukina, E. V., Thomason, W. E., & Schepers, J. S. (2001). In-Season Prediction of Potential Grain Yield in Winter Wheat Using Canopy Reflectance. *Agronomy Journal*, 93(1), 131-138.
- Reyniers, M., & Vrindts, E. (2006). Measuring wheat nitrogen status from space and ground-based platform. *International Journal of Remote Sensing*, 27(3), 549 - 567.
- Richardson, A. J., & Wiegand, C. (1977). Distinguishing vegetation from soil background information. *Photogrammetric Engineering and Remote Sensing* 43(12), 1541-1552.
- Roberts, D. F. (2009). *A soil and Crop based Strategy for Sensor-Based Variable-Rate Nitrogen Management in Corn*. PhD thesis, University of Nebraska, Lincoln, Nebraska, USA. Retrieved from <http://proquest.umi.com/pqdlink?Ver=1&Exp=10-15-2016&FMT=7&DID=1824846861&RQT=309&attempt=1&cfc=1> [Accessed 28 November 2010].
- Rondeaux, G., Steven, M., & Baret, F. (1996). Optimization of soil-adjusted vegetation indices. *Remote Sensing of Environment*, 55(2), 95-107.
- Roujean, J. L., & Breon, F. M. (1995). Estimating PAR absorbed by vegetation from bidirectional reflectance measurements. *Remote Sensing of Environment*, 51(3), 375-384.
- Rouse, J., Haas, R., Schell, J., Deering, D., & Harlan, J. (1973). Monitoring the vernal advancement and retrogradation (green wave effect) of natural vegetation. *NASA/GSFC, Type II, Final Report*. Greenbelt, Maryland, USA.
- Ruiliang, P., Peng, G., Biging, G. S., & Larrieu, M. R. (2003). Extraction of red edge optical parameters from Hyperion data for estimation of forest leaf area index. *IEEE Transactions on Geoscience and Remote Sensing*, 41(4), 916-921.
- Sanches, I. D. (2009). *Hyperspectral proximal sensing of the botanical composition and nutrient content of New Zealand pastures*. Unpublished PhD thesis, Massey University, Palmerston North, New Zealand.
- Sanches, I. D., Tuohy, M. P., Hedley, M. J., & Bretherton, M. R. (2009). Large, durable and low-cost reflectance standard for field remote sensing applications. *International Journal of Remote Sensing*, 30(9), 2309-2319. doi: 10.1080/01431160802549377

- Sanderson, M. A., Rotz, C. A., Fultz, S. W., & Rayburn, E. B. (2001). Estimating forage mass with a commercial capacitance meter, rising plate meter, and pasture ruler. *Agronomy Journal*, *93*(6), 1281-1286.
- Satellite-Imaging-Corporation. (2011). WorldView-2 Satellite Sensor Characteristics Retrieved from <http://www.satimagingcorp.com/> [Accessed 15 July 2011].
- Savitzky, A., & Golay, M. J. E. (1964). Smoothing and Differentiation of Data by Simplified Least Squares Procedures. *Analytical Chemistry*, *36*(8), 1627-1639. doi: 10.1021/ac60214a047
- Schellberg, J., Hill, M. J., Gerhards, R., Rothmund, M., & Braun, M. (2008). Precision agriculture on grassland: Applications, perspectives and constraints. *European Journal of Agronomy*, *29*(2-3), 59-71. doi: 10.1016/j.eja.2008.05.005
- Schlerf, M., & Atzberger, C. (2006). Inversion of a forest reflectance model to estimate structural canopy variables from hyperspectral remote sensing data. *Remote Sensing of Environment*, *100*(3), 281-294. doi: 10.1016/j.rse.2005.10.006
- Schröder, J. J., Neeteson, J. J., Oenema, O., & Struik, P. C. (2000). Does the crop or the soil indicate how to save nitrogen in maize production?: Reviewing the state of the art. *Field Crops Research*, *66*(2), 151-164. doi: 10.1016/S0378-4290(00)00072-1
- Schut, A. G. T., Lokhorst, C., Hendriks, M. M. W. B., Kornet, J. G., & Kasper, G. (2005). Potential of imaging spectroscopy as tool for pasture management. *Grass and Forage Science*, *60*(1), 34-45. doi: 10.1111/j.1365-2494.2005.00449.x
- Schut, A. G. T., van der Heijden, G. W. A. M., Hoving, I., Stienezen, M. W. J., van Evert, F. K., & Meuleman, J. (2006). Imaging Spectroscopy for On-Farm Measurement of Grassland Yield and Quality. *Agronomy Journal*, *98*(5), 1318-1325. doi: 10.2134/agronj2005.0225
- Solari, F., Shanahan, J., Ferguson, R., Schepers, J., & Gitelson, A. (2008). Active Sensor Reflectance Measurements of Corn Nitrogen Status and Yield Potential. *Agronomy Journal*, *100*(3), 571.
- Stagakis, S., Markos, N., Sykioti, O., & Kyparissis, A. (2010). Monitoring canopy biophysical and biochemical parameters in ecosystem scale using satellite hyperspectral imagery: An application on a *Phlomis fruticosa* Mediterranean

- ecosystem using multiangular CHRIS/PROBA observations. *Remote Sensing of Environment*, 114(5), 977-994. doi: 10.1016/j.rse.2009.12.006
- Stamatiadis, S., Taskos, D., Tsadila, E., Christofides, C., Tsadilas, C., & Schepers, J. (2009). Comparison of passive and active canopy sensors for the estimation of vine biomass production. *Precision Agriculture*, 11(3), 306-315. doi: 10.1007/s11119-009-9131-3
- Starks, P. J., Zhao, D., & Brown, M. A. (2008). Estimation of nitrogen concentration and in vitro dry matter digestibility of herbage of warm-season grass pastures from canopy hyperspectral reflectance measurements. *Grass and Forage Science*, 63(2), 168-178.
- Starks, P. J., Zhao, D., Phillips, W. A., Brown, M. A., & Coleman, S. W. (2005, 4–6 Oct.). *Productivity and forage quality of warm season grass pastures in relation to canopy reflectance in ASTER wavebands*. Paper presented at the 20th Biennial Workshop on Aerial Photography, Videography, and High Resolution Digital Imagery for Resource Assessment, Weslaco, TX.
- Starks, P. J., Zhao, D., Phillips, W. A., & Coleman, S. W. (2006a). Development of canopy reflectance algorithms for real-time prediction of bermudagrass pasture biomass and nutritive values. *Crop Science*, 46(2), 927. doi: 10.2135/cropsci2005.0258
- Starks, P. J., Zhao, D., Phillips, W. A., & Coleman, S. W. (2006b). Herbage mass, nutritive value and canopy spectral reflectance of bermudagrass pastures. *Grass and Forage Science*, 61(2), 101-111.
- Stubbs, T. L., Kennedy, A. C., & Fortuna, A.-M. (2009). Using NIRS To Predict Fiber and Nutrient Content of Dryland Cereal Cultivars. *Journal of Agricultural and Food Chemistry*, 58(1), 398-403. doi: 10.1021/jf9025844
- Thenkabail, P., Smith, R., & De Pauw, E. (2000). Hyperspectral vegetation indices and their relationships with agricultural crop characteristics. *Remote Sensing of Environment*, 71(2), 158-182.
- Thomson, N., Upsdell, M., Hooper, R., Henderson, H., Blackwell, M., McCallum, D., Hainsworth, R., Macdonald, K., Wildermoth, D., & Bishop-Hurley, G. (2001). *Development and evaluation of a standardised means for estimating herbage mass of dairy pastures using the rising plate meter*. Paper presented at the Proceedings of the New Zealand Grassland Association.

- Thulin, S. M. (2008). *Hyperspectral Remote Sensing of Temperate Pasture Quality*. PhD thesis, RMIT University, Melbourne, Australia. Retrieved from <http://adt.lib.rmit.edu.au/adt/public/adt-VIT20090507.163006> [Accessed 21 June 2010].
- Tremblay, N., Wang, Z., Ma, B.-L., Belec, C., & Vigneault, P. (2009). A comparison of crop data measured by two commercial sensors for variable-rate nitrogen application. *Precision Agriculture*, *10*(2), 145-161. doi: 10.1007/s11119-008-9080-2
- Trenholm, L. E., Carrow, R. N., & Duncan, R. R. (1999). Relationship of Multispectral Radiometry Data to Qualitative Data in Turfgrass Research. *Crop Science*, *39*(3), 763-769. doi: 10.2135/cropsci1999.0011183X003900030025x
- Trotter, M., Lamb, D., Donald, G., & Schneider, D. (2010). Evaluating an active optical sensor for quantifying and mapping green herbage mass and growth in a perennial grass pasture. *Crop and Pasture Science*, *61*(5), 389-398.
- Tsai, F., & Philpot, W. (1998). Derivative Analysis of Hyperspectral Data. *Remote Sensing of Environment*, *66*(1), 41-51. doi: 10.1016/S0034-4257(98)00032-7
- Tucker, C. J. (1977). Asymptotic nature of grass canopy spectral reflectance. *Applied Optics*, *16*(5), 1151-1156.
- Tucker, C. J. (1979). Red and photographic infrared linear combinations for monitoring vegetation. *Remote Sensing of Environment*, *8*(2), 127-150. doi: 10.1016/0034-4257(79)90013-0
- Vapnik, V. N. (2000). *The nature of statistical learning theory* (2 nd ed.): Springer Verlag.
- Verhoef, W. (1984). Light scattering by leaf layers with application to canopy reflectance modeling: the SAIL model. *Remote Sensing of Environment*, *16*(2), 125-141.
- Villarreal, M., Cochran, R. C., Johnson, D. E., Towne, E. G., Wilson, G. W. T., Hartnett, D. C., & Goodin, D. G. (2006). The use of pasture reflectance characteristics and arbuscular mycorrhizal root colonization to predict pasture characteristics of tallgrass prairie grazed by cattle and bison. *Grass & Forage Science*, *61*(1), 32-41. doi: 10.1111/j.1365-2494.2006.00505.x

- Viña, A., & Gitelson, A. A. (2005). New developments in the remote estimation of the fraction of absorbed photosynthetically active radiation in crops. *Geophysical Research Letters*, 32, L17403.
- Viscarra Rossel, R. A. (2008). ParLeS: Software for chemometric analysis of spectroscopic data. *Chemometrics and Intelligent Laboratory Systems*, 90(1), 72-83. doi: 10.1016/j.chemolab.2007.06.006.
- Volkers, K. C., Wachendorf, M., Loges, R., Jovanovic, N. J., & Taube, F. (2003). Prediction of the quality of forage maize by near-infrared reflectance spectroscopy. *Animal Feed Science and Technology*, 109(1-4), 183-194. doi: Doi: 10.1016/s0377-8401(03)00173-1
- Wang, F.-m., Huang, J.-f., & Lou, Z.-h. (2010). A comparison of three methods for estimating leaf area index of paddy rice from optimal hyperspectral bands. *Precision Agriculture*, 12(3), 439-447. doi: 10.1007/s11119-010-9185-2
- White, J. D., Trotter, C. M., Brown, L. J., & Scott, N. (2000). Nitrogen concentration in New Zealand vegetation foliage derived from laboratory and field spectrometry. *International Journal of Remote Sensing*, 21(12), 2525 - 2531.
- Williams, P., & Norris, K. (1987). *Near-infrared technology in the agricultural and food industries*. MN 55121, USA: American Association of Cereal Chemists, Inc.
- Wold, S., Sjöström, M., & Eriksson, L. (2001). PLS-regression: a basic tool of chemometrics. *Chemometrics and Intelligent Laboratory Systems*, 58(2), 109-130. doi: 10.1016/S0169-7439(01)00155-1
- Xue, L., Cao, W., Luo, W., Dai, T., & Zhu, Y. (2004). Monitoring Leaf Nitrogen Status in Rice with Canopy Spectral Reflectance. *Agronomy Journal*, 96(1), 135-142.
- Yoder, B. J., & Waring, R. H. (1994). The normalized difference vegetation index of small Douglas-fir canopies with varying chlorophyll concentrations. *Remote Sensing of Environment*, 49(1), 81-91. doi: 10.1016/0034-4257(94)90061-2
- Yule, I., & Pullanagari, R. (2009, 11-12 February ). *Use of Reflectance Sensors to Optimise Nutrient Management*. Paper presented at the Nutrient Management in a Rapidly Changing World, Massey University, Palmerston North, New Zealand.
- Yule, I. J., Lawrence, H. G., Hedley, C., Pullanagari, R., Draganova, I., Betteridge, K., & Dynes, R. (2010, 3 & 4 September). *Technologies to improve productivity and*



- reduce environmental impact of dairy systems*. Paper presented at the EcoTechs Conference: International workshop:Eco-design Methods and Tools for Agricultural Technologies, Clermont-Ferrand, France.
- Yule, I. J., Lawrence, H. G., & Murray, R. I. (2005). Yield mapping to improve dairy farm production. *Transactions of the ASABE, Paper No. 051074*, 30.
- Zarco-Tejada, P. J. (2000). *Hyperspectral remote sensing of closed forest canopies: Estimation of chlorophyll fluorescence and pigment content*. PhD thesis, York University, Toronto, Ontario, Canada.
- Zarco-Tejada, P. J., & Miller, J. R. (1999). Land cover mapping at BOREAS using red edge spectral parameters from CASI imagery. *Journal of Geophysical Research*, 104(D22), 27921-27933.
- Zarco-Tejada, P. J., Miller, J. R., Noland, T. L., Mohammed, G. H., & Sampson, P. H. (2001). Scaling-up and model inversion methods with narrowband optical indices for chlorophyll content estimation in closed forest canopies with hyperspectral data. *IEEE Transactions on Geoscience and Remote Sensing*, 39(7), 1491-1507.
- Zarco-Tejada, P. J., Rueda, C., & Ustin, S. (2003). Water content estimation in vegetation with MODIS reflectance data and model inversion methods. *Remote Sensing of Environment*, 85(1), 109-124.
- Zhao, D., Huang, L., Li, J., & Qi, J. (2007a). A comparative analysis of broadband and narrowband derived vegetation indices in predicting LAI and CCD of a cotton canopy. *ISPRS Journal of Photogrammetry and Remote Sensing*, 62(1), 25-33. doi: 10.1016/j.isprsjprs.2007.01.003
- Zhao, D., Starks, P. J., Brown, M. A., Phillips, W. A., & Coleman, S. W. (2007b). Assessment of forage biomass and quality parameters of bermudagrass using proximal sensing of pasture canopy reflectance. *Grassland Science*, 53, 39-49.
- Zhao, D. H., Li, J. L., & Qi, J. G. (2005). Identification of red and NIR spectral regions and vegetative indices for discrimination of cotton nitrogen stress and growth stage. *Computers and Electronics in Agriculture*, 48(2), 155-169.

## Author's publications

### Journal Publications

Pullanagari, R. R., Yule, I. J., King, W., Dalley, D., & Dynes, R. (2011) The use of optical sensors to estimate pasture quality. *International Journal on Smart Sensing and Intelligent Systems*, 4(1), 125-137.

Pullanagari, R. R., Yule, I., Tuohy, M., Hedley, M., Dynes, R., & King, W. (2011) In-field hyperspectral proximal sensing for estimating quality parameters of mixed pasture. *Precision Agriculture*. 13(3), 351-369. doi: 10.1007/s11119-011-9251-4

Pullanagari, R. R., Yule, I., Hedley, M. J., Tuohy, M. P., Dynes, R., & King, W. (2012). Multispectral Radiometry to Estimate Pasture Quality Components. *Precision Agriculture* (Accepted).

Pullanagari, R. R., Yule, I. J., Tuohy, M. P., Hedley, M. J., Dynes, R. A., & King, W. M. (2011). Proximal sensing of the seasonal variability of pasture nutritive value using multispectral radiometry. *Grass & Forage Science* (Accepted).

Pullanagari, R.R., Yule, I. J., Tuohy, M. P., Hedley, M. J., Dynes, R. A. and King, W. M. (2011). Estimation of pasture biomass, standing crude protein and spatial analysis of herbage biomass using an active optical sensor. *Agronomy Journal* (Under review).

### Conference Presentations and Proceedings

Yule, I., & Pullanagari, R. (2009). Use of Reflectance Sensors to Optimise Nutrient Management. In: *Nutrient Management in a Rapidly Changing World*, (Eds L. D. Currie & C. L. Lindsay) Occasional Report No. 22. Fertilizer and Lime Research Centre, Massey University, Palmerston North, New Zealand, 70-79.

- Pullanagari, R.R., I. Yule., 2009, Reflectance sensors to optimise nutrient management. Landwise Workshop 2009. Havelock North, New Zealand. May 14<sup>th</sup> 2009.
- Pullanagari, R. R., Yule, I., Dalley, D., King, W., & Dynes, R. (2009). *Issues around pasture quality and production measurement systems*. In: *Proceedings of the 13th Symposium on Precision Agriculture in Australasia*, (Eds M. G. Trotter, E. B. Garraway & D. W. Lamb) University of New England, Armidale, NSW, Australia, 103.
- Pullanagari, R. R., & Yule, I. J. (2010). In-field methods of collecting crop reflectance data. In: *Farming's Future: Minimising Footprints and Maximising Margins*, (Eds L. D. Currie & C. L. Christensen) Occasional Report No.23, Fertiliser and Lime Research centre, Palmerston North, New Zealand, 429-433.
- Pullanagari, R.R. and Ian Yule. Sensing options for New Zealand Growers, LandWISE Crop Sensor Workshop, 14th May 2010, Hastings New Zealand.
- Yule, I. J., Lawrence, H. G., Hedley, C., Pullanagari, R., Draganova, I., Betteridge and Dynes, R. (2010) Technologies to improve productivity and reduce environmental impact of dairy systems. Paper presented at the EcoTechs Conference: International workshop: *Eco-design Methods and Tools for Agricultural Technologies*, Clermont-Ferrand, France. <http://www.ecotechs2010.org>.
- Pullanagari, R. R., Yule, I. J., Tuohy, M., Dynes, R., & King, W. (2011). Pasture quality measurement tools for decision making. In: *Adding to the Knowledge Base for the Nutrient Manager*, (Eds L. D. Currie & C. L. Christensen) Occasional Report No.24. Fertiliser and Lime Research centre, Massey University, Palmerston North, New Zealand.
- Pullanagari, R. R., Yule, I. J., Tuohy, M., Dynes, R., & King, W. (2012). Sensors for assessing pasture quality. In: *Advanced Nutrient Management: Gains from the Past - Goals for the Future*, (Eds L. D. Currie & C. L. Christensen) Occasional Report No.25. Fertiliser and Lime Research centre, Massey University, Palmerston North, New Zealand.